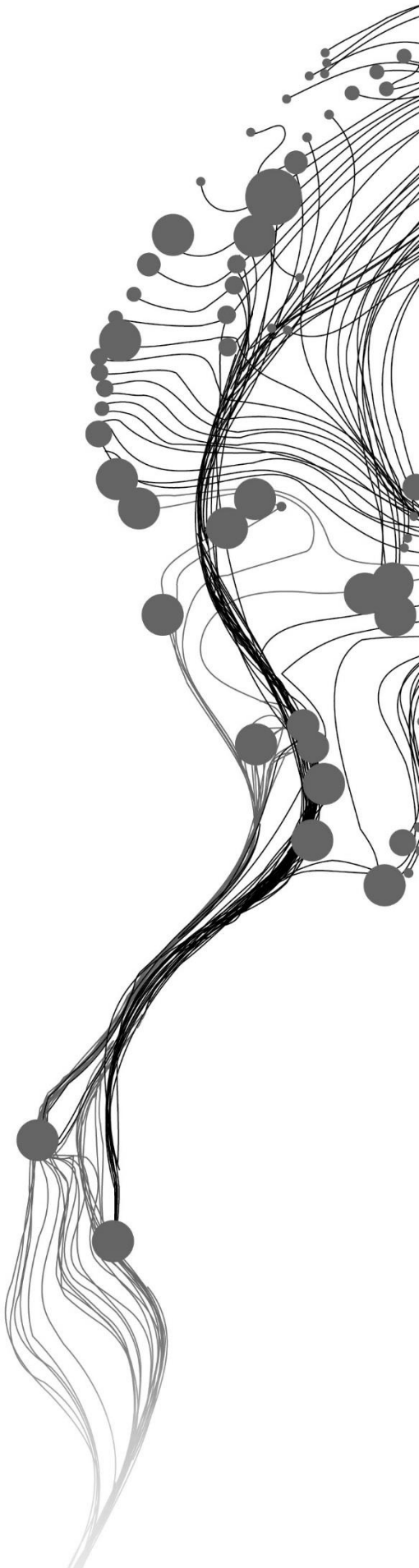


# **MODELING OF GROUNDWATER SYSTEMS IN A WETLAND: A CASE STUDY OF THE AAMSVEEN, THE NETHERLANDS**

**STEPHEN GEORGE EMMANUEL  
FEBRUARY 2019**

**SUPERVISORS:  
Dr. Zoltan Vekerdy  
Dr. M.W. Lubczynski**





# **MODELING OF GROUNDWATER SYSTEMS IN A WETLAND: A CASE STUDY OF THE AAMSVEEN, THE NETHERLANDS**

**STEPHEN GEORGE EMMANUEL**

**Enschede, The Netherlands, February 2019**

Thesis submitted to the Faculty of Geo-Information Science and Earth Observation of the University of Twente in partial fulfilment of the requirements for the degree of Master of Science in Geo-information Science and Earth Observation.

Specialization: Water Resources and Environmental Management

**SUPERVISORS:**

Dr. Zoltan Vekerdy

Dr. M.W. Lubczynski

**THESIS ASSESSMENT BOARD:**

Dr. Ir. C. Van Der Tol (Chair, ITC)

Dr. P. Gurwin (External Examiner, University of Wraclow, Poland)

#### DISCLAIMER

This document describes work undertaken as part of a programme of study at the Faculty of Geo-Information Science and Earth Observation of the University of Twente. All views and opinions expressed therein remain the sole responsibility of the author, and do not necessarily represent those of the Faculty.

## ABSTRACT

Aamsveen, which is located in the Dutch-German border, is a wetland and is preserved by the European Union under Natura 2000. The wetland has a thick vegetation all around it and consists of deciduous and evergreen trees, shrubs and heath. The area outside the wetland consists mainly of grass as the vegetation apart from the trees and a small area is covered by the agricultural crops like maize, rapeseed etc. The water table is generally high throughout the year around the wetland and ponding occurs in the main wetland throughout the year. The stratigraphy of the study area consists of peat and sand. Aamsveen receives rainfall throughout the year which makes the dynamics of the groundwater-surface water to be high. The aim of this research was to analyse the surface-groundwater interactions and to quantify the fluxes. Since, the wetland occupied a large area, it was also an aim to decipher the major outflow component of the system and to decide if a large amount of groundwater is lost through the streams or through evapotranspiration.

The approach used in this model was to simulate the surface-groundwater interactions in Aamsveen under transient conditions using an integrated hydrological model, MODFLOW-NWT in Modelmuse coupled with UZF1, SFR2, FHB, drain and reservoir packages that are able to describe the temporal and spatial variability of the water balance components. Integration of earth observation was also an integral part of the research and this was done by classifying sentinel-2 image of the study area into various land cover classes and mapping their changes. The model was built by assigning 2 layers with peat having an even thickness of 3.4 metres and sand having variable thicknesses at different locations, the data for which was obtained by the bore hole log profiles. The simulation was run in transient mode for a period of 4 years from 1<sup>st</sup> January 2012 to 31<sup>st</sup> December 2015.

This analysis provides the following results: a) The major outflow component from the system was evapotranspiration which accounted for 63.2 % of the entire precipitation and 37.8% from the groundwater including the unsaturated zone. This was higher than the baseflow which shows that more water is lost through evapotranspiration than the streams b) The stream flow into the groundwater was measured to be lower than the flow from groundwater to stream which implies that the streams gain water from the groundwater through the system c) The area has high exfiltration of 55.7% d) the baseflow was measured to be 13.4 % e) a high reservoir leakage was obtained which was around 34.6% which is greater than the groundwater entering the reservoir which means that the groundwater receives a lot of water from the reservoir f) The model can provide better results with the use of LAK package in MODFLOW.

Keywords: integrated hydrological model, MODFLOW-NWT, evapotranspiration, baseflow, Aamsveen.

## ACKNOWLEDGEMENTS

First and foremost, I would like to thank the Lord Jesus Christ for his grace and for this gift of life and for miraculously making it possible for me to pursue Master of Science in this prestigious institution by providing the financial means through the Netherlands Fellowship Programme (NFP). I also thank him for providing good health throughout my studies and his presence especially during the time when I had a bad internal pain and swelling in my right eye, which according to the doctors could have led to blindness. I owe my life and everything I have to him alone who is the creator of life and the author of my salvation. May his peace and eternal love reach everyone who happens to read this thesis. I would like to thank my parents for being flexible and encouraging and supporting me to pursue my studies even after a break of few years. I owe a lot to them for all the love and good things they have provided to me since my childhood. I hope I make them proud of all my achievements in this life until now. You will forever have my love and respect.

I sincerely thank Dr. Zoltan Vekerdy, my first supervisor, for his patience, guidance and support throughout my research duration. At the time when all the topics for integrated hydrological modelling were exhausted, he came up with this proposed topic and helped me to pursue what I had desired to do after coming to ITC, i.e. integrated hydrological modelling. I know that he has had high expectations and whatever I have achieved, it is only because of his guidance, critical approach and “out of the box” thinking patterns which helped me develop a critical thinking attitude. I can confidently say, that I have already picked the basics of my interests and I will definitely propel forward and make valuable contributions in my field. I thank him for his humility, friendliness and ease of access which are the most important aspects for a student’s development.

I would like to thank Dr. Maciek Lubczynski, my second supervisor, for his timely help regarding numerous decisions that I had to take during my thesis. I thank him for his patience, for explaining to me the same things multiple times due to my lack of understanding of those things. I can truly say, that many aspects of my work have been made better through his consultations and contributions. His readiness and willingness to engage in active discussions have helped me to understand many important aspects of integrated groundwater modelling. I would like to thank Ir. Arno Van Lieshout, for agreeing to read the final document and providing his valuable suggestions and corrections in the final report. I thank ITC’s administration for providing and arranging all the things required for a good and comfortable stay and education. I want to thank the Kingdom of The Netherlands for being so open and providing opportunities to international students thereby helping to build a better future for this world. I thank NFP for providing financial assistance which made everything possible.

From Vechtstromen, I want to thank Ir. Bas Worm for his timely help and guidance for acquiring the required data and for being approachable and for providing the right sources regarding data availability. I also would like to thank Mr. Wouter ten Harkel for his support in providing data, I also thank Mr. Tobias Renner and Miss Greda Boertin for providing information and data that I needed.

I also thank Mrs. Kathrin Zweers, Dr. Caroline Lievens and Dr. Dhruva Shreshta for their help with the lab work in the Geo-science laboratory.

I thank the ‘De Deur’ church for their constant prayers and fellowship. I thank Rita for her constant help and assistance throughout my master’s thesis. I don’t know how I would have done without her. Looking forward to many more years ahead.

## TABLE OF CONTENTS

---

<b>1. INTRODUCTION</b>	1
1.1. Background	1
1.2. Previous studies in Aamsveen	2
1.3. Problem statement	4
1.4. Research objectives	4
1.5. Research novelty	5
<b>2. STUDY AREA</b>	6
2.1. Study Area	6
2.2. Location	6
2.3. Climate	7
2.4. Topography and land cover	7
2.5. Soil and Lithology	9
2.6. Hydrogeology	11
2.7. Data availability and monitoring networks	11
<b>3. METHODOLOGY</b>	14
3.1. Data Processing	15
3.2. The conceptual model	21
3.3. Numerical Model	22
3.4. Model Parameterization	31
3.5. State variables	32
3.6. Transient simulation	34
3.7. Sensitivity analysis	36
3.8. Water balance	36
<b>4. RESULTS AND DISCUSSION</b>	38
4.1. Model driving forces	38
4.2. Interception and infiltration rates	39
4.3. Crop coefficients	40
4.4. Extinction depth	42
4.5. Hydraulic conductivity	42
4.6. Sensitivity analysis on groundwater heads	52
4.7. Sensitivity analyses of the groundwater fluxes	52
4.8. Volumetric Water budget	55
4.9. Water balance	56
4.10. Yearly variations in the water balance components	57
4.11. Temporal variability of the water fluxes	58
<b>5. CONCLUSION AND RECOMMENDATIONS</b>	60
5.1. Conclusion	60
5.2. Model failures	62
5.3. Recommendations	62

## LIST OF FIGURES

---

Figure 1: Layout of Aamsveen (Source ArcGIS base map) .....	6
Figure 2: Percentage of different types of land covers in Aamsveen .....	7
Figure 3: Classified Land cover Map of 25 <sup>th</sup> September 2016 of Aamsveen .....	8
Figure 4: Spatial representation of the five soil parent material districts in the Netherlands. The pre-Quaternary formations are not included within these parent material districts due to their very restricted occurrence. Adopted from Veer (2006). .....	10
Figure 5: Aamsveen wetland showing the cross section of the different layers (Bell et al. 2015).....	11
Figure 6: Monitoring network of the study area .....	13
Figure 7: Flow chart of the study .....	14
Figure 8: Thickness Maps of Peat (on the left) and Sand (on the right) in metres. ....	16
Figure 9: Locations of the soil samples .....	17
Figure 10: Grain-size distribution curves of samples from D1 .....	19
Figure 11: Grain-size distribution curves of samples from D2 .....	20
Figure 12: Grain-size distribution curves of samples from G1 .....	20
Figure 13: Grain-size distribution curves of samples from G2 .....	20
Figure 14: Grain-size distribution curves of samples from G3 .....	21
Figure 15: Grain-size distribution curves of samples from G4 .....	21
Figure 16: The conceptual model of Aamsveen .....	22
Figure 17: Boundary conditions of the study area.....	26
Figure 18: Measured heads of the piezometers during the simulation period .....	33
Figure 19: Measured discharges of the streams in Aamsveen .....	34
Figure 20: Rainfall and temperature of Aamsveen .....	38
Figure 21: Daily reference evapotranspiration of the study area.....	38
Figure 22: Interception maps for Summer and Winter in Aamsveen .....	39
Figure 23: Yearly crop coefficient maps of Aamsveen .....	41
Figure 24: Extinction depth map of Aamsveen.....	42
Figure 25: Hydraulic conductivities [m day <sup>-1</sup> ] of the first layer and second layers.....	43
Figure 26: Discharge at Melodiestraat stream gauge .....	43
Figure 27: Discharge at Aamsveen stream gauge.....	44
Figure 28: Observed vs simulated stream flow at Aamsveen’s camping area.....	45
Figure 29: Location of the Aamsven Camping area stream gauge downstream from the lake.....	47
Figure 30: Water Management in progress at Aamsveen’s Camping area .....	48
Figure 31: Observed vs simulated heads for B35A0836 (A).....	49
Figure 32: Observed vs simulated heads for B35A0837(B).....	49
Figure 33: Observed vs simulated heads for B35A0890 (C).....	49
Figure 34: Observed vs simulated heads for B35A0835 (D) .....	50
Figure 35: Sensitivity analysis of the groundwater heads.....	52
Figure 36: Sensitivity analysis of Extinction depth on groundwater fluxes.....	53
Figure 37: Sensitivity analysis of Hydraulic conductivity on groundwater fluxes.....	53
Figure 38: Sensitivity analysis of Maximum Unsaturated Vertical Conductivity on groundwater fluxes ....	54
Figure 39: Sensitivity analysis of specific yield on groundwater fluxes .....	55
Figure 40: Daily variability of groundwater fluxes for the whole simulation period starting 1st January 2012 to 31st December 2015 .....	58
Figure 41: Yearly variations in the water fluxes .....	59
Figure 42: Schematic of the distribution of fluxes in the study area from 2012-2015 in [mm] .....	59



## LIST OF TABLES

---

Table 1: Summary of the human interventions in Aamsveen done for its management (Bakhtiyari 2017)..	2
Table 2: Description of major lithological units in the Netherlands and the different formations discerned (P = Pleistocene, H = Holocene). Adopted from Veer (2006).	9
Table 3: Overview of five soil parent material districts in the Netherlands and the Holocene formations and members commonly occurring in the topsoil layer. Adopted from Veer (2006).	10
Table 4: Acquired datasets for Aamsveen.	12
Table 5: Hydraulic conductivities of the soil samples.	18
Table 6: Results of the CHN analyser.	19
Table 7: Interception rate of the various land covers for summer.	28
Table 8: Interception rate of the various land covers for winter.	28
Table 9: Rooting depth of various land covers in [m].	28
Table 10: Crop coefficient values for the various land covers.	29
Table 11: Error Analysis of Heads after Transient Calibration.	50
Table 12: Final Calibrated Transient state model parameters: EXTDP-extinction depth; EXTWC-extinction water content; THTS- saturated volumetric water content; KVuz- unsaturated vertical hydraulic conductivity; STRHC1- stream bed vertical hydraulic conductivity; STRTOP- stream bed top; STRTHICK- stream bed thickness; Sy- specific yield; Ss- specific storage; Rbthck- reservoir bed thickness; Kx-horizontal hydraulic conductivity. C indicates all those parameters that have been adjusted during calibration. N indicates all the parameters that were not adjusted but were assumed to be true.	51
Table 13: Unsaturated zone package volumetric budget (2012 – 2015).	55
Table 14: Volumetric budget of the entire model for the entire simulation.	56
Table 15: Yearly water balances of the entire simulation period starting from 1 <sup>st</sup> January 2012 to 31 <sup>st</sup> December 2015 in [mm year <sup>-1</sup> ].	57



# 1. INTRODUCTION

## 1.1. Background

A wetland is a place where water saturation dominates, and which has an influence on the development of soil and the various communities of plants and animals. This generally results in bogs and marshes etc. Like the coral reefs and rainforests, wetlands are also considered to be highly productive ecosystems. Though there are places that can occasionally be saturated with water, mainly after a storm, they are not considered as wetlands since wetlands are saturated with water either permanently or seasonally. Wetlands may be covered with either fresh, brackish or salty water. The wetland development takes place in areas which are topographically low, where the exfiltration of the groundwater takes place or also in places where surface runoff can accumulate.

Despite the fact that wetlands cover only around 1.5% of the surface of the earth, they are able to provide high 40% of global ecosystem services and have an important role in global and local water cycles and also connect water, food and energy which is a challenge in the society in the area of sustainable management (Clarkson et al. 2013). In their natural state, they provide hydrological benefits like maintenance of water quality, groundwater recharge and flood control apart from providing habitat for wildlife (Brown, 1976). Since the microbes and plant life along with wildlife, are a part of the global cycle of among others, water, sulphur and nitrogen, according to scientists, an additional function of the wetlands may be included for atmospheric maintenance. The influence of the wetlands on hydrological cycle is now widely accepted and hence they are important elements in water management policies at various regional, national and international scales (Bullock and Acreman 2003). Wetlands are able to absorb water during the rainy seasons and hence reduce the risk of flooding and during dry periods, they can also release water gradually, thereby ensuring the availability of water during these periods of no rain (Jafari 2009). Expectations are that, by using the wetlands wisely, it would contribute to the integrity of ecology and secure livelihoods especially for those communities that are dependent on the service of the ecosystem for sustenance (Kumar et al. 2011)

Aamsveen is one of the wetland sites under Natura 2000. The surface geology of Aamsveen consists of the deposits of Aeolian sand of the Weichselian age (Kuhry 1985). The lowest parts of the wetland are covered with peat. The cover sand's surface is almost flat but forms local ridges around a height of 2 metres. Due to the excavation of large pieces of high moor, currently, the nature has been reserved. Heathlands, wet trunks, pits where peat has been excavated and barren grasslands are found in Aamsveen.

The ecosystem of peatlands is complex and fragile since they are driven by many processes that are biological, chemical or physical. Since peatlands may also serve as sinks or sources or even transformers of contaminants and also nutrients, they significantly impact the water quality, ecosystem productivity and also emissions of greenhouse gases. The peatlands have started to decrease in their extent because of activities like groundwater extraction from underlying aquifers. Predicted changes in precipitation and temperature in the future are likely to add to the pressure in the peatlands (Landes et al. 2014). In the case of Aamsveen, the major cause for decrease in peat is the excessive peat mining. Since the demand for water is ever increasing, there is also an increase in the need for mitigation of the impacts of ground water developments on the environment.

In planning of water resources and for its development and management, groundwater holds fundamental importance. Tools like numerical modelling of groundwater can increase the understanding of the groundwater systems by aiding in the study of the groundwater systems (Kumar & Singh 2015)

## 1.2. Previous studies in Aamsveen

Throughout time, many human interventions have been done for improving the wetland since Aamsveen originally was a peat mining area and was exploited. The interventions have been done with the aim to make Aamsveen a self-regulatory system (Lianghui 2015). Table 1 summarizes the interventions and the objectives/purpose of these interventions done with time in Aamsveen (Bakhtiyari 2017). The last major intervention was done by blocking the drain tube which drained water from the reservoirs in the wetland and by constructing a new channel that goes around the wetland. This was done to restore the original stream and the catchment area of the Glanerbeek. Few MSc theses were conducted for assessing the change after the blockage of the drain pipe and construction of the new channel. Their summary, results and conclusions are described later in this chapter.

Table 1: Summary of the human interventions in Aamsveen done for its management (Bakhtiyari 2017)

Year	Action	Reason/purpose
1969	❖ End of peat extraction ❖ Channel dig along the lowest part of the wetland	The channel was dug to make drainage of upstream agriculture lands possible, since the altitude influence the former flow direction directly towards the Glanerbeek; this caused a lot of water logging problems for the German farmers
1983	❖ Replace the open channel with tubes	To avoid dehydration of the nature conservation area, but still drain the upstream agriculture lands through the channel replaced by tube to the Flörbach <sup>1</sup> and then to the Glanerbeek
1993-1995	❖ Split area into smaller compartments with dams	Raise the groundwater level by holding more rainwater and reduce the infiltration of nutrient rich waters coming from the surrounding farmlands
2005-2006	❖ Minor raises were done on the bottom level of the Glanerbeek	To reduce the amount of water that was drained from the wetland
2011	❖ Block the drain tube and reconstruct the new channel that goes around the wetland	Restore the original stream and catchment area of the Glanerbeek

### 1.2.1. The Regional model

A large-scale regional model has been developed which also includes Aamsveen. It has been modelled using MODFLOW, in the iMOD environment with 25\*25 m spatial resolution. This steady state model does not consider peat in its layers, although it happens to be important in the current study area of Aamsveen. The first layer of this model represents boulder clay but does not consider a thin layer of sand which exists in Aamsveen. Some drains and streams in Aamsveen are not represented in this model hence, it does not cover enough details of the surface hydrology (Bakhtiyari 2017). Hence, the model cannot aptly describe the dynamics of the groundwater system that take place in Aamsveen.

### 1.2.2. Study conducted by Xing Lianghui

Lianghui (2015) had studied the changes in vegetation and nutrients due to the wetland reconstruction by controlling of water level within the time frame of 2002-2014. She concluded that the vegetation had increased by comparing the NDVI maps of 2004 and 2011 since a significant change was introduced to the drainage of Aamsveen in 2011. She concluded that the groundwater level change before and after 2011 was very small and was smaller than the mapping accuracy. Hence, there was no significant change proved in the groundwater levels. Due to this, her results also couldn't quantify the relation between the groundwater level and the changes in the vegetation. Her conclusion was that it takes several years for the natural reaction of the vegetation to take place due to small changes in groundwater levels, hence a longer period is required for studying the relationship between them after the diversion of the canal had been done. Hence, her study could not describe the groundwater systems.

### 1.2.3. Nyarugwe's model.

Nyarugwe (2016) divided the entire simulation period into 2 parts since, in 2011, alterations had been done in the drains of the wetland. He developed two separate steady state models, one for the pre-2011 phase and the other for the post-2011 phase. Nyarugwe had concluded that the wetland had become wetter after the alterations in 2011. He also concluded that evapotranspiration was more before the 2011 changes in Aamsveen. He analysed that Aamsveen receives around 8.5% recharge but is responsible for 43% of the catchment evapotranspiration losses. Since there were 2 independent calibrations of these models, they resulted in having different hydraulic conductivities of the same area which is unrealistic. Also, he considered only 2 classes of the land cover. Hence, this study also lacks the details necessary for understanding the groundwater systems in Aamsveen. Land cover classes used in the assessment were not adequate enough to represent the entire catchment. More land cover classes would provide better simulation and would be able to show the changes in vegetation with the changes in groundwater. Since it was a steady state model, it could only provide the overview of the change but could not quantify the daily fluxes.

### 1.2.4. Bakhtiyari's model.

Bakhtiyari (2017) developed a model which was comparatively more detailed. She had considered 7 land cover classes for a better simulation of the evapotranspiration. Her model was also a steady state model for the pre-2011 and post-2011 phases. In both the pre-2011 and post-2011 scenarios, Bakhtiyari concluded that the groundwater leakage to stream was the highest which was around 73.67% with the drain outflow and evapotranspiration being only around 12.86% and 13.47% respectively. Hence, this study concluded the outflow of groundwater through the streams to be the highest. Since Aamsveen is an area where the dynamics of fluxes are high, a steady-state model cannot really provide details or quantify the fluxes acting in the area. Moreover, this model had a grid-size of 100 metres, which can be said to be too large in relation to the catchment area since a smaller grid size can capture more details like more precise land cover classes and better spatial distribution of the fluxes. Hence, her model also could not provide a strong case for quantifying the fluxes.

### 1.3. Problem statement

Since the wetlands provide eco-hydrological services which are of utmost importance, they have been exploited to meet the needs of humans. These anthropogenic activities are quickly degrading the wetlands presently and are having a negative impact on the environment. Wetlands are quickly disappearing and there is a need for their preservation. Preservation and restoration of wetlands are now parts of sustainability goals. Nowadays, wetlands pose environmental questions that are politically sensitive due to information deficiencies, economic structures that are inappropriate, planning concept deficiencies, conflicts in governmental policies and overall institutional weaknesses. A wise use of the wetland should be based on ecosystem functioning's sound understanding (Maltby 1991). Activities of humans over several past decades have impacted wetlands globally (Lin et al. 2007). Many projects have been undertaken to stabilize and improve the wetlands for their sustenance. The real question is whether the hydraulic interventions applied in the wetlands is bringing a positive change and thereby providing expected results.

Since the results from the previous theses done on Aamsveen, did not consider the dynamics of the fluxes in different stress periods in the distribution of fluxes, the questions about the distribution of fluxes in the surface-groundwater interactions still remain unanswered. One of the major questions is whether the groundwater loss through leakage to stream is higher or the evapotranspiration. Understanding this will provide more insights for planning and management of Aamsveen. The steady-state models of Nyarugwe and Bhaktiyari have limitations in terms of land cover classes and also their models could not describe the processes and quantify the fluxes in the unsaturated zone. Being steady-state models, they can never explain the dynamics of the water balance in various seasons which again does not become helpful in assessing the changes caused by human interventions.

Since, Aamsveen is a wetland with fluxes which vary temporally and spatially, the temporal fluctuations of fluxes have not yet been assessed in these models. The incorporation of these aspects will increase the accuracy in characterizing the area and moreover, a transient model is needed to quantify and assess the distribution of the fluxes that would explain the dynamics of the water balance in different stress periods. This will be helpful in making interventions in a controlled manner for a positive development of Aamsveen.

### 1.4. Research objectives

The main objective is to assess the dynamics of surface-groundwater interactions in the Aamsveen by an integrated model that includes the simulation of the hydraulic interventions in 2011.

The specific objectives are:

- i. To update the conceptual model of the wetland
- ii. To map the land cover changes in the modelled period
- iii. To describe the surface-groundwater interactions of the wetland
- iv. To assess the results of the present model and old models

### **1.4.1. Research questions**

#### **1.4.1.1. Main research question**

What are the main fluxes of the surface-groundwater interactions in the Aamsveen wetland?

#### **1.4.1.2. Specific research questions.**

- i. Can the boundaries be better conceptualized compared to the previous models?
- ii. What is the model's sensitivity to the land cover classes of the study area?
- iii. What are the variations in SW-GW interactions in the study area?
- iv. What are the effects of the hydraulic interventions in Aamsveen?

### **1.5. Research novelty**

Since the Aamsveen comes under Natura 2000, extensive research was carried out into the origin and operation of Aamsveen by commissioning of specialized research agencies by the Natura project team. They came up with the conclusion that the surface water system is losing water in both Dutch and German areas and that the level of groundwater is very low which is not enough to form active peat (Bell et al. 2018). This means that the behaviour of the fluxes in Aamsveen need to be studied and also quantified for a proper assessment of the wetland. Some models have been developed to describe the surface-groundwater interactions in Aamsveen, yet they lack many details which can be incorporated into the model to provide better simulation of the interaction of fluxes in Aamsveen. Some of these details that can be incorporated into the model for better simulated results are a more detailed land cover map, variable thicknesses of the layers, a dynamic simulation of the fluxes and a proper description of the fluxes in the saturated and unsaturated zones.

The previous steady state model of Bakhtiyari (2017) integrated few land cover classes, which were not able to aptly describe the complete land cover since there were still room for more details in the land cover map which would provide better representation of the study area and hence provide better results. Hence, this research aims to incorporate more land cover classes which would aptly be able to describe the land cover/land use of Aamsveen and also be able to describe the temporal variations in the land cover changes, which was initially not considered, which would affect the water balance of the study area. Also, in the other models, an even and continuous thickness of the peat and sand layers have been used which is not really a good representation of the aquifer thicknesses. In this research, borehole log profile data has been used to create the variable thicknesses of the sand layer to closely resemble the stratigraphy and finally, the aim of this research is to develop a transient numerical model which would not only quantify the surface water-groundwater interactions but also be able to describe their variations in space and time. This would be the first dynamic model since the old models are steady state models. The methodology also consists of incorporation of a more detailed Earth Observation based land cover mapping in the modelling of the area.

## 2. STUDY AREA

### 2.1. Study Area

The study area covers Glanerbrug and Aamsveen, in which the majority of the area is a wetland. This is part of the Natura 2000, so it is protected under European Union's programme.

### 2.2. Location

Aamsveen is located on the border of Netherlands and Germany, around 5 km southeast of the city of Enschede. With the central coordinates of 52° 10' 56" N, 6° 57' 7" E, most of the wetland is located in Germany. While the Dutch portion of the wetland is around 175 hectares, the German side is around 700 hectares. The entire catchment is around 23 km<sup>2</sup>, but the wetland is only around 4 km<sup>2</sup>. The study area has bog in its centre with a stream located on the west side. This bog also extends across the border to the German side. Due to the digging of peat, certain undulations have been caused in the groundwater (Bell et al. 2015). The main stream in the basin flows from Southwest to Northeast. This stream which starts from the weir, was reconstructed in 2011 when certain modifications were done in drainage plans of the area. The major stream is called Glanerbeek.



Figure 1: Layout of Aamsveen (Source ArcGIS base map)



### 2.3. Climate

The Koppen climate category of Aamsveen like the rest of Netherlands, is the Marine West Coast climate and it is influenced by the Atlantic Ocean and the North Sea. Since, it is located inland, the winters are a little more severe as compared to rest of the Netherlands. Due to the small expanse of the country, there is hardly a big difference in the climate between the rest of the Netherlands. The average yearly rainfall received by Aamsveen is around 785 mm and 9.6°C is the average temperature of the area

### 2.4. Topography and land cover

Different types of vegetations cover the Aamsveen such as bog, woodland, grassland, swamp forests etc. Located almost at the centre of the area of study, it is covered by wetland, vegetation and forests. Also, peat is found here. Primary land cover is grass around the peat land. The surface geology here consists of a combination of sand and peat layers. The topography is flat and has the elevation ranges between 38-54 metres. In the previous modelling studies, simple and over generalized land cover map was used. For the present study, a new land cover map was made to cover also the temporal variability of the land cover. The present map contains 9 classes as compared to 7 classes by Bakhtiyari (2017) and 2 classes by Nyarugwe (2016). The major change in the map is the further categorization of the trees into evergreen and deciduous trees. Deciduous trees shed their leaves in the winter that affects the infiltration and the evapotranspiration applied to the model. Since, there are no leaves during the winter months, infiltration is higher due to throughfall and stem flow and the evapotranspiration is very low. Bare soil has also been added as a class which again has a big effect on infiltration and evapotranspiration. The land cover map was made by classifying Sentinel-2A MSI image from 25<sup>th</sup> September 2016. The topography is flat in the study area. Higher areas are on the western side which gradually start to taper towards the eastern boundary, but most of the wetland has a very flat topography.

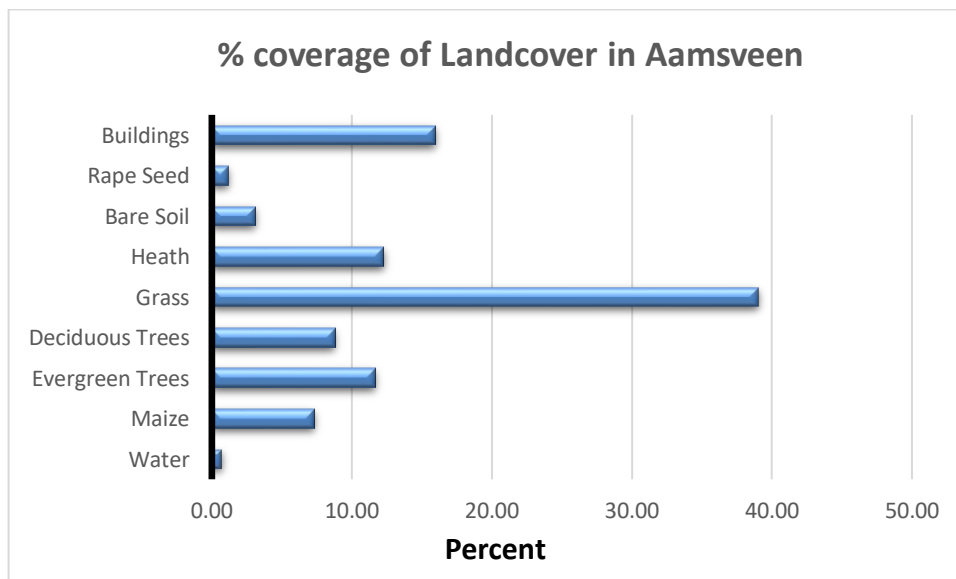


Figure 2: Percentage of different types of land covers in Aamsveen

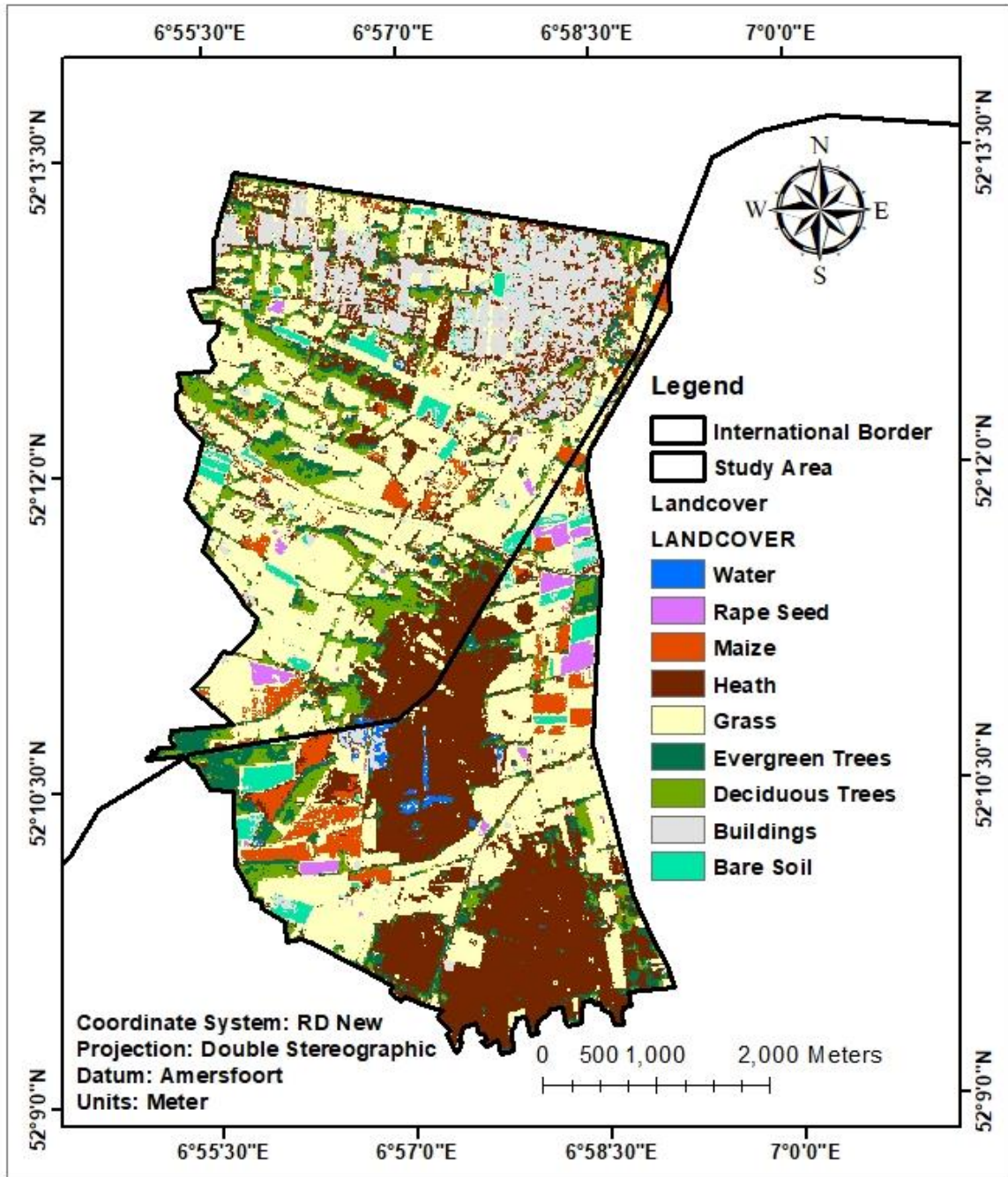


Figure 3: Classified Land cover Map of 25<sup>th</sup> September 2016 of Aamsveen

## 2.5. Soil and Lithology

Due to the North Sea basin's subsidence and sedimentary infill which happened extensively, as a result, a thick layer of unconsolidated sediments form the subsurface of the Netherlands. The deposition of the sediments happened extensively during the Quaternary period. The sediments are either fluvial, glaciogenic or marine. Also, the local geogenesis of the sediments are more of peat and aeolian deposits. This is also the case of the Aamsveen wetland area (Veer 2006).

Table 2: Description of major lithological units in the Netherlands and the different formations discerned (P = Pleistocene, H = Holocene). Adopted from Veer (2006).

<b>Geogenesis</b>	<b>Lithology</b>	<b>Formations</b>
Marine deposits	Often calcareous, silty and clayey deposits, interlayered with (fine) sandy deposits	Maassluis(P), Eem(P), Naaldwijk (H)
Fluvial deposits	Pleistocene formations have fine to coarse sands, including gravel, locally some clay and peat layers. Holocene formations are more clayey.	Waalre (P), Sterksel (P), Urk (P), Kreftenheye (P), Peize (P), Appelscha (P), Echteld (H), Beegden (H+P)
Glaciogenic deposits	Various glacial deposits: glacial till and boulder clay, fluvio- and lacustro-glacial deposits (clay to coarse sand)	Peelo (P), Drenthe (P)
Local deposits	Either fine to medium, sometimes loamy, sandy deposits (aeolian and local fluvial), loess deposits and peat (various types).	Sand: Stamproy (P), Boxtel (H) Peat: Woudenberg (P), Nieuwkoop (H)

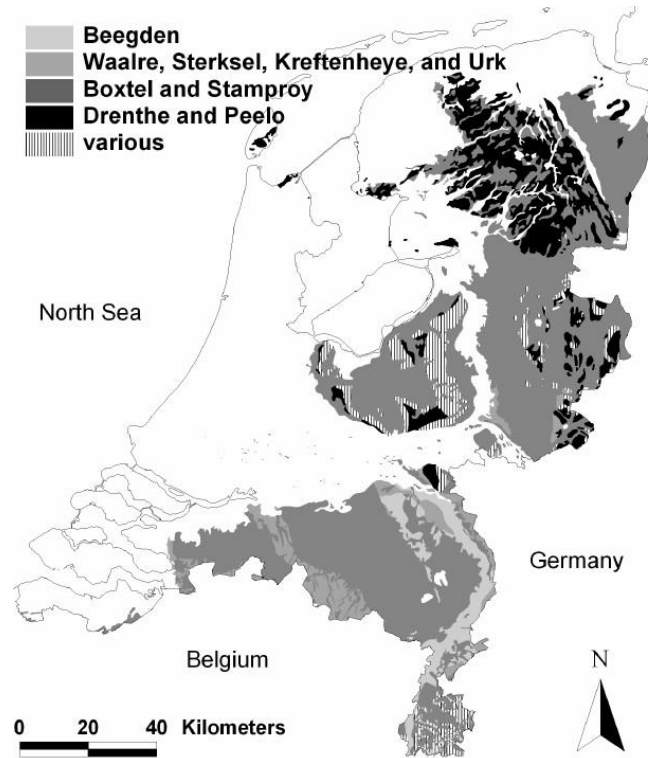


Figure 4: Spatial representation of the five soil parent material districts in the Netherlands. The pre-Quaternary formations are not included within these parent material districts due to their very restricted occurrence. Adopted from Veer (2006).

Table 3: Overview of five soil parent material districts in the Netherlands and the Holocene formations and members commonly occurring in the topsoil layer. Adopted from Veer (2006).

Formation	District	Member	Geogenesis and lithology
Sand	Boxtel (Naaldwijk)	Kootwijk Schoorl	Aeolian sand (fine Sand to medium sand) Eolian dunes (fine to medium sand)
Peat	Nieuwkoop	Griendtsveen Singraven Hollandveen Basisveen	Oligotrophic sphagnum-mosses peat (high moor) Mesotrophic wood peat formed in local streams (brook deposits) Meso- to eutrophic reed, sedge and wood peat Meso- to eutrophic reed, sedge and wood peat
Fluviatile	Echteld Beegden	Rosmalen Wijchen	Fluviatile deposits of Rhine and Meuse (mainly clay and silt to fine and coarse sand, locally some peat) Fluviatile deposits, upper Meuse only (mainly silt to clay) Fluviatile deposits, upper Meuse only (fine to coarse sand, some gravel)
Marine	Naaldwijk	Walcheren Wormer Zandvoort	Marine and peri marine deposits (mainly fine sand to clay) Marine and peri marine deposits (mainly silty clay to clay) Coastal bars, beaches (fine to medium sand)

According to Table 3, Aamsveen area, which is very close to the Singraven near the Village Dene kamp, is a wetland that highly consists of Oligotrophic sphagnum-mosses peat and Mesotrophic wood peat formed in local streams underlain by sandy layer (Veer 2006).

## 2.6. Hydrogeology

The hydro stratigraphy of the study area consists of 2 layers, peat and sand with boulder clay as the base layer (Wong et al. 2007). They mention that this is observed in the eastern part of the Netherlands, where the study area is located. The groundwater table varies with the annual variations in the rainfall. Peat was present in large quantities until it was removed by human activities in a large area of the wetland. The area in-between the bog and the Glanerbeek, remains wet during the winter season, and the groundwater is generally between 0-20 cms below the surface

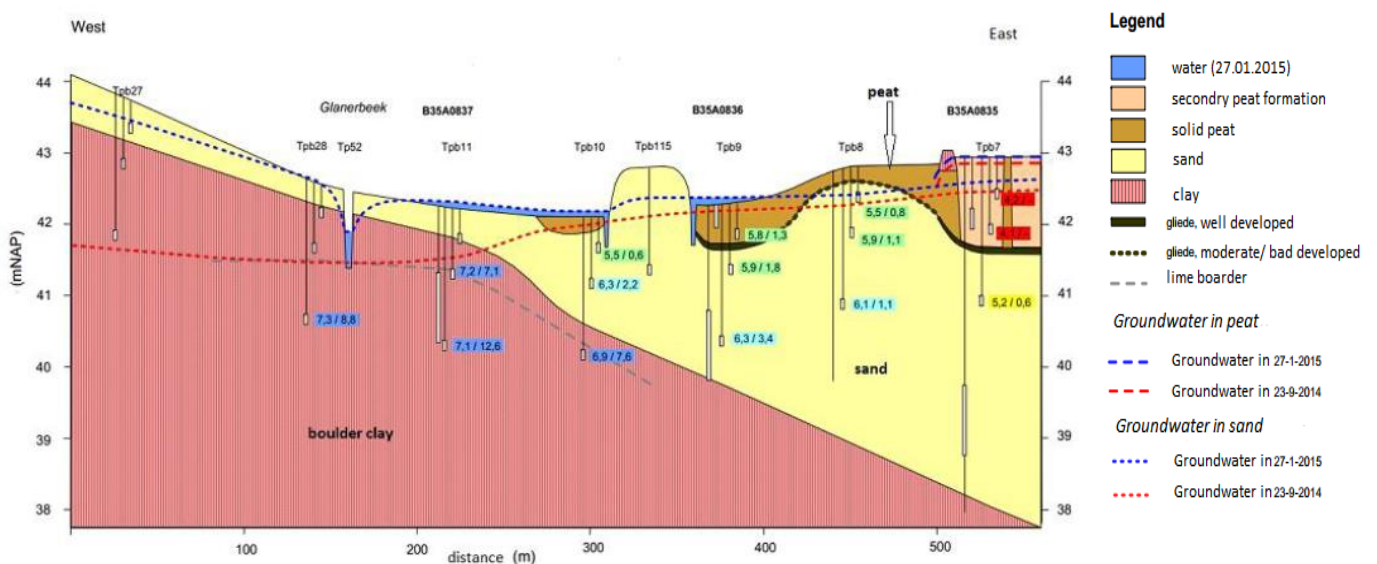


Figure 5: Aamsveen wetland showing the cross section of the different layers (Bell et al. 2015)

## 2.7. Data availability and monitoring networks

There is 1 weather station, located close to Aamsveen, which provides the data for precipitation and evapotranspiration. Due to this, the precipitation data obtained from this station is considered for the entire region. There are two stream gauges in the study area. The data of these were provided by the water board, Vechtstromen, responsible for maintenance of the wetland. A few groundwater monitoring bore holes are also located inside the study area, but more are concentrated around the wetland region. They provide the data of the groundwater heads during the entire simulation period.

### 2.7.1. Datasets

The acquired datasets are listed in Table 4. The different archives that were used to obtain the data are <https://www.knmi.nl>, which provided the forcing data and <https://www.dinoloket.nl> which provided the data for the groundwater levels. Vechtstromen provided the gauge discharges and Sentinel 2A was used to obtain the images for classification of the land cover of Aamsveen. The field work consisted of measuring the saturated hydraulic conductivities of the site and the sampling was done for laboratory analysis to analyse the grain-size distribution of the samples at ITC, University of Twente

Table 4: Acquired datasets for Aamsveen

<b>Acquired Data</b>	<b>Data Type</b>	<b>Source</b>	<b>Temporal/spatial resolution</b>
<b>Hydrological Data</b>	Groundwater level	DINOloket	(2012-2015)
	Gauge data (discharge)	DINOloket	(2012-2015)
	K	Field sampling	-----
<b>Meteorological Data</b>	Precipitation	KNMI	Daily (2012-2015)
	PET	KNMI	Daily (2012-2015)
<b>MAPS</b>	DEM	Water Board	30 m
	Potentiometric map	KNMI, LANUV	
	Land cover	Classified from Sentinel 2A	10 m, 60 m
	Sand Depth	DINOloket	-----
	Peat Depth	DINOloket	-----

### 2.7.2. Monitoring network

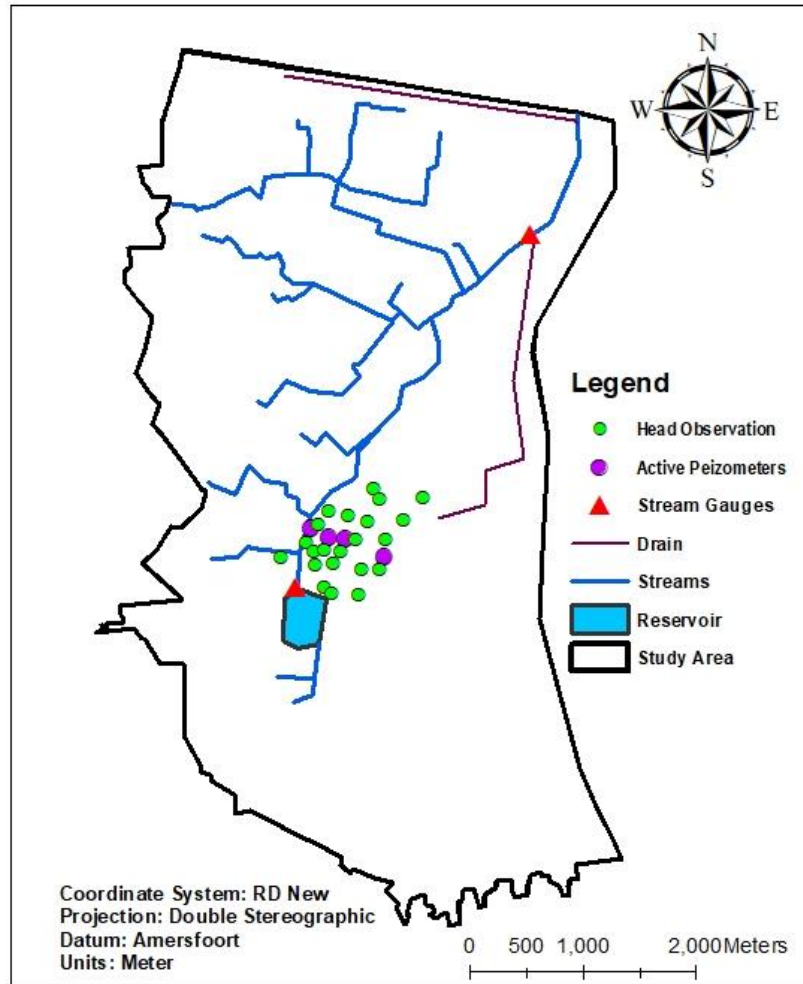


Figure 6: Monitoring network of the study area

Figure 6 shows the monitoring network of the study area. The location of 2 stream gauges are shown by red triangles. For the entire simulation period from 1<sup>st</sup> January 2012 to 31<sup>st</sup> December 2015, only 4 piezometers were active whose locations are shown by the purple dots. The rest of the boreholes had observations that were outside the simulation period.

### 3. METHODOLOGY

Figure 7 shows the flow progress of the study. The first step was to classify a Sentinel 2A image to make a land cover map of the study area. This land cover map was used to assign the potential evapotranspiration to the various land covers using crop coefficients (Kc) at various growth stages. After the pre-processing of the data which included the interception map, extinction depth map, using precipitation to calculate infiltration etc, the conceptual model was prepared after which, using the required data, the numerical model was prepared. The numerical model was calibrated and once the calibration was attained, the water budget was prepared after which the sensitive analysis was done.

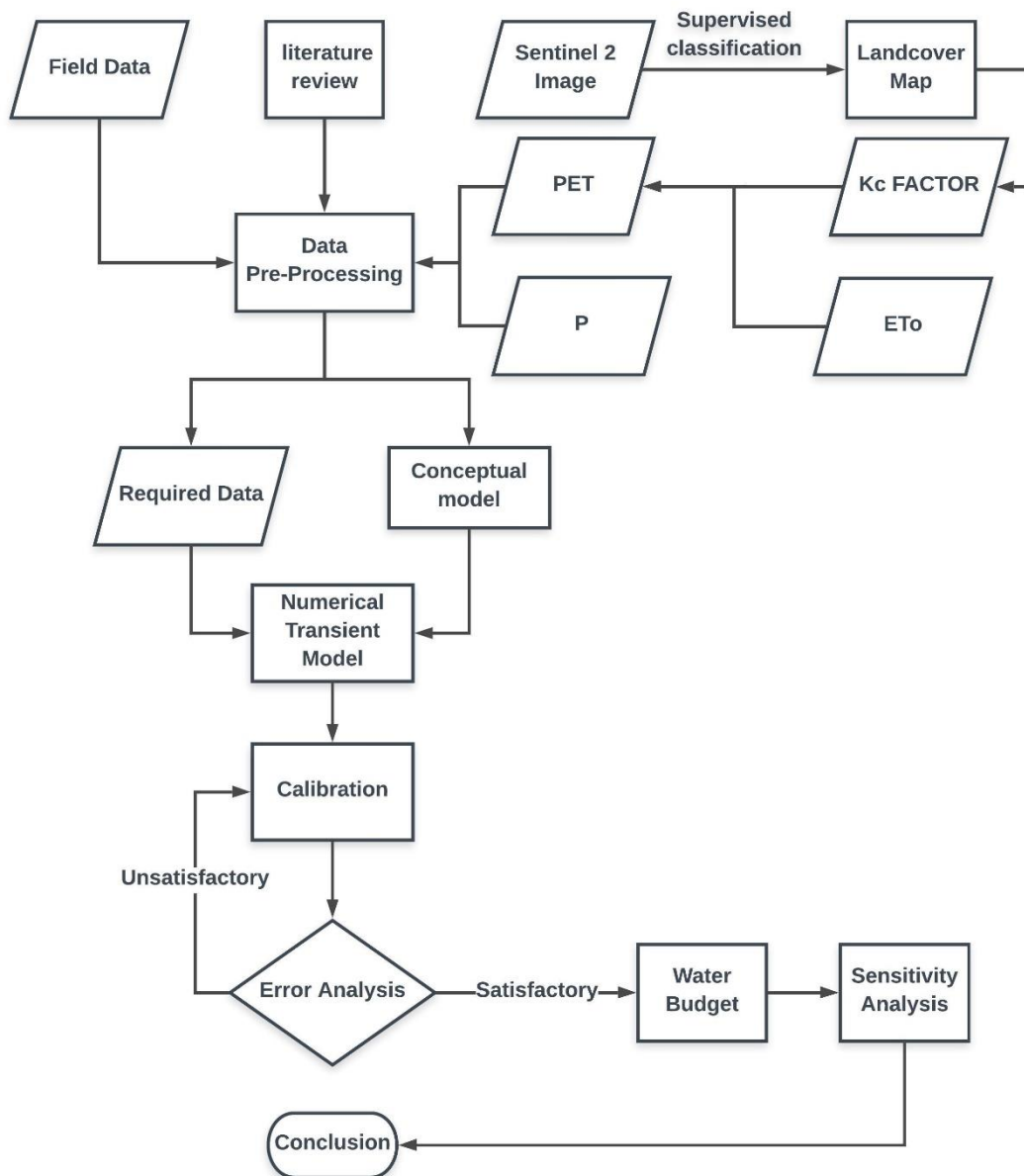


Figure 7: Flow chart of the study



A model is a simplified representation of a complex natural world. Numerical methods in groundwater modelling make use of governing equations that are able to calculate heads at certain locations. They are not continuous in space or time and the heads are usually calculated at certain discrete points, yet they are capable of solving full transient 3D governing equations that are anisotropic and heterogenous under complex initial and boundary conditions (Anderson et. al. 2015). Finite element and finite difference methods are the most common groundwater numerical methods (Tanner and Hughes 2015).

### **3.1. Data Processing**

The driving forces used in the study area were homogenous, hence no processing was required for them. Since, the study area is relatively small, the weather station is close by and it is considered to provide sufficient spatial coverage of the data for the driving forces. Other data that were required by the model are described in this chapter.

#### **3.1.1. Hydro-stratigraphic units**

In the present study, field work was done to analyse the hydro-stratigraphy of the area. In the main wetland, a layer of peat was found which was underlain by sand, below which an impermeable layer of clay exists. Hence, in this model, 2 layers have been included to represent the medium of the groundwater flow.

##### **3.1.1.1. Peat**

The first layer included sand and peat, of which peat was found to be in range of 0.1 to 3 meters as seen in Figure 8. This data was obtained by analysing the profiles of the boreholes present in the wetland where peat is formed. Using this information, the thickness of peat was extrapolated, and a thickness map of peat was made. However, even though there were a large number of boreholes, they were concentrated only around the Dutch side of the wetland, which actually covered less than half of the actual peat area of the entire wetland. During the field work, it was also noticed that the peat layers was thicker in the German side as compared to the Dutch side which could not be represented by the thickness map of peat since there were no bore hole data in the German side. Hence, this map was not sufficient enough to aptly indicate the peat depth in the German side of the wetland. The peat layer's thickness used in the present model was taken as 3.4 metres overall for a better model response.

##### **3.1.1.2. Sand**

The second layer, sand, forms the top layer in areas outside the main wetland where there is no peat formed. The thickness of sand is also variable, and the thickness map of the sand was interpolated by using the profiles of the boreholes present in the entire study area. Since, these boreholes covered the entire study area, they were considered adequate to distil a thickness map of the sand layer which can be seen in Figure 8. The borehole data was provided by <https://www.dinoloket.nl/en/subsurface-data>. The data were taken from 53 boreholes that were present inside and outside the entire study area and this map was imported as an ASCII raster file and was used as the thickness of the sand layer in the model.

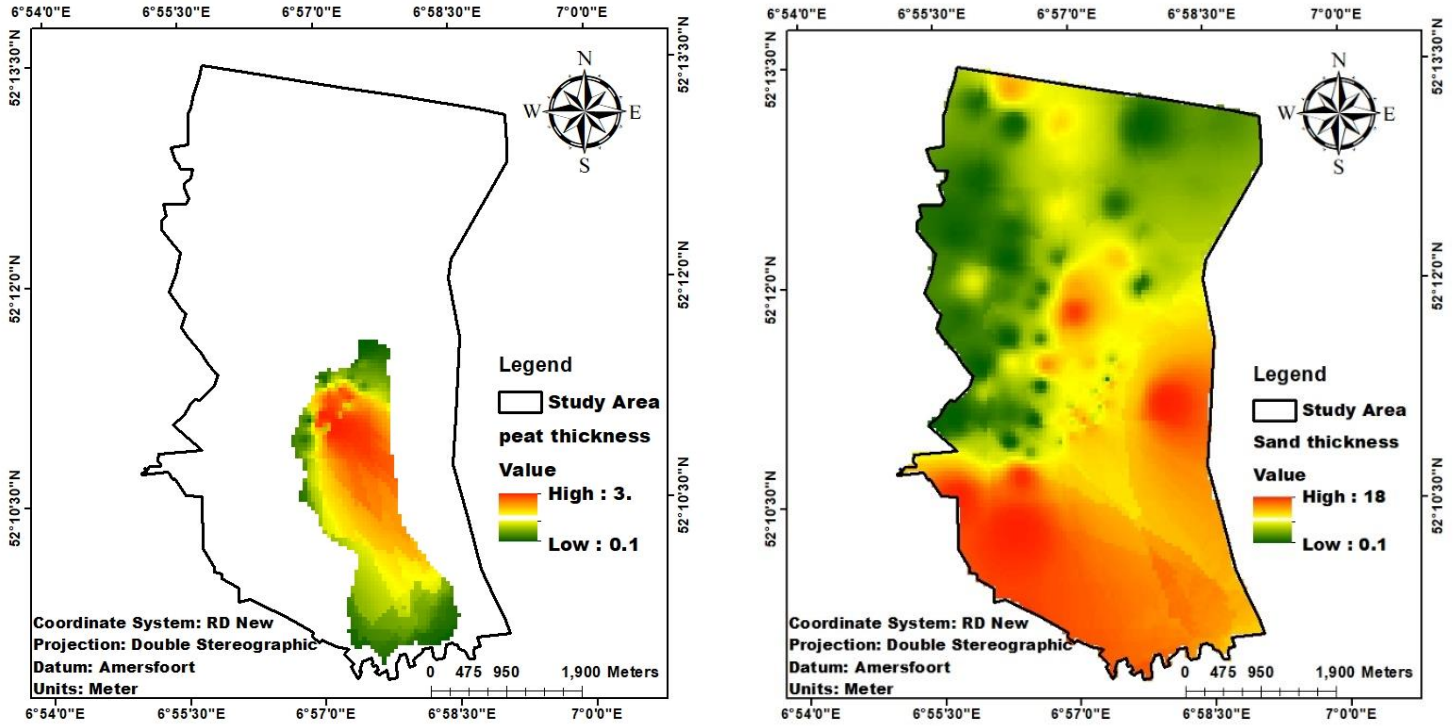


Figure 8: Thickness Maps of Peat (on the left) and Sand (on the right) in metres.

### 3.1.2. Hydraulic conductivity

The hydraulic conductivity of the study areas was defined by collecting soil samples from the field. Since, in the previous studies, soil samples had been exclusively taken from the Dutch side of the study area and no samples were taken from the German side, main importance was given for the collection of samples from the German side. Due to the limitations in the lab capacity and the available time for sampling, it was not possible to take undisturbed samples using a ring sampler. Hence, the disturbed samples were taken by the help of auger at different depths. The samples were taken from 6 different locations, keeping the spatial variability of the samples. 2 samples were taken from the Dutch side and 4 samples were taken from the German side. Peat and sand samples were collected, and the hydraulic conductivity was calculated by the help of the Kozeny-Carman equation represented in equation 1. Figure 9 shows the locations from where the samples have been taken. The red dots show the location from where samples have been collected in the previous study by Bakhtiyari (2017). The green pentagons show the location of the sites from where the samples have been collected in the present study.

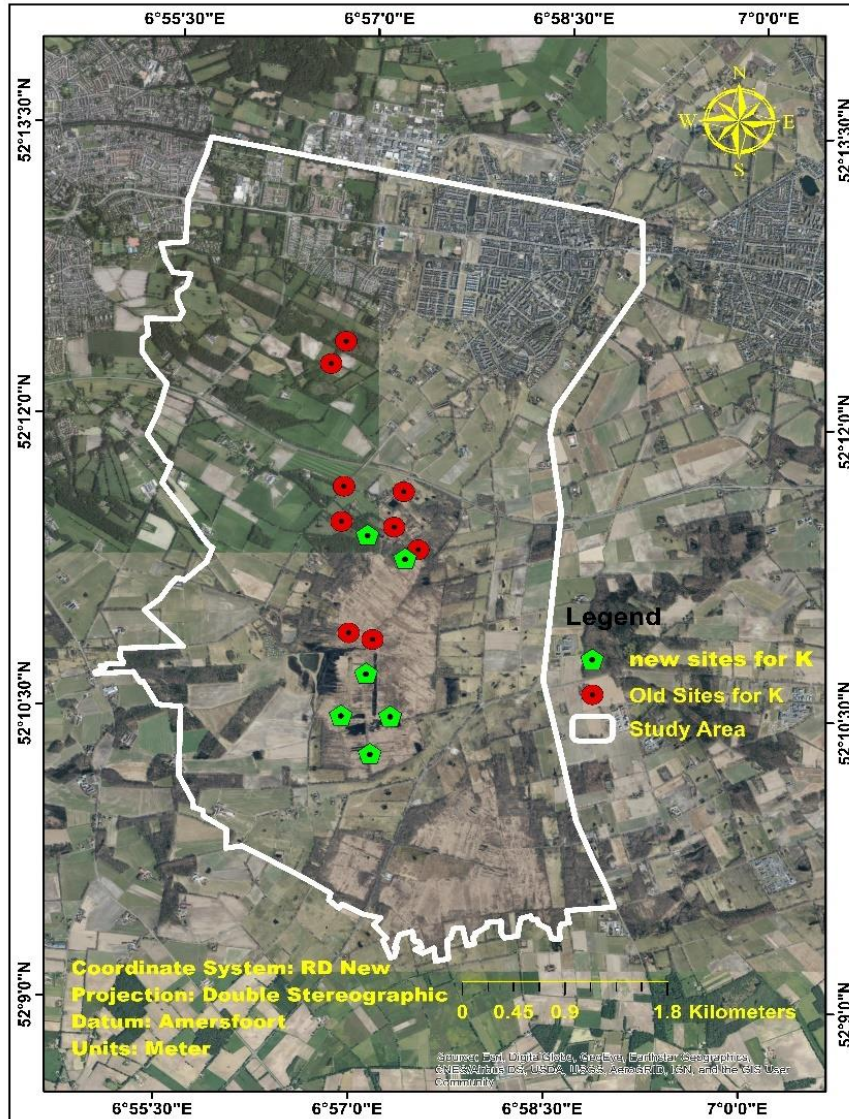


Figure 9: Locations of the soil samples

### 3.1.3. Kozeny-Carman equation

The Kozeny-Carman equation is used to find the saturated hydraulic conductivity of the soil whose particle size is larger than that of clay and smaller than 3 mm. Kozeny (1927) derived an equation for conduction of water in the voids and capillaries of the soil which was based on the equations of Darcy and Poiseuille. This equation was later modified by Carman (1937). The resultant equation is known as Kozeny-Carman equation which has excessively been used to calculate the saturated hydraulic conductivity of soil (sand). The Kozeny-Carman equation is given below by Hwang et al. (2017)

$$K_s = \frac{g}{\mu} * 8.3 * 10^{-3} * \left[ \frac{P^3}{1-P^2} \right] * d_{10}^2 \quad (1)$$

Where  $K_s$  is the saturated hydraulic conductivity [ $\text{m day}^{-1}$ ],  $P$  is the porosity in percentage,  $\mu$  is the viscosity of water [ $\text{NS m}^{-2}$ ],  $d$  is the effective grain size in [ $\text{mm}$ ] and  $g$  is the gravitational constant [ $\text{m s}^{-2}$ ]. Many authors have proposed different methods for calculation of the effective grain size which are arithmetic, geometric and harmonic mean respectively. Bear (1972) preferred the use of harmonic mean while Todd (1959) suggested the use of geometric mean, while Urumović (2016) suggested the use of either the arithmetic mean or harmonic mean, after overiewing various

literatures. Also, few authors have suggested the use of  $D_{10}$  as the referential size of the grain. This means that the size of the sieve at which only 10 % of the fines (particles smaller than this sieve size) passes and the rest 90 % are retained on the sieve. This effective grain size  $D_{10}$  was suggested by Allen Hazen after performing several experiments because this size was found to be the best to relate to most of the soil properties. Hence, for this study, the referential or the effective grain size was taken as  $D_{10}$ . The locations from where the samples have been collected are specified in Table 5. The samples were analysed in the laboratory. According to the demand of the Kozeny-Carman equation, the effective or referential grain size or diameter was needed to be specified. This was done by sieve analysis or the grain-size distribution. The organic matter like leaves and roots can have binding or cementing properties which can provide faulty grain-size distribution. Hence, it was necessary to remove these organic matters in order to get the best results. This consisted of preparing a known amount of the soil samples and weighing them in the weighing balance. A calculated amount of Hydrogen Peroxide was added to the samples at regular intervals by keeping the samples on a water bath until all the frothing was removed and a clear solution was obtained. This can also take more than one week depending on the amount of organic content. Hydrogen peroxide reduces the organic content to Carbon dioxide and water. Once the frothing was removed, the solution was boiled at  $105^{\circ}\text{C}$  with the stirrer to stir the solution until all the hydrogen peroxide was removed from the solution. A dispersing agent was added after the organic content was removed and left to shake in the shaker, which separated the particles for a better analysis, after this, the samples were passed through  $50\ \mu\text{m}$  sieve. The proportion of the sample that passed through the sieve was taken for the pipette analysis for separating the silt and clay fractions. The proportion of each sample that was retained on the  $50\ \mu\text{m}$  were taken for sieve analysis to find out the sand diameter sizes. The final hydraulic conductivity was obtained by taking the average of the conductivities of both the samples for every location.

Table 5: Hydraulic conductivities of the soil samples

Sample	Location	Sample Numbers	$K_s$ (mday <sup>-1</sup> )	Coordinates	
				Lat	Long
D1	Netherlands	Sample A	26.64	N 52° 11' 2 4.6"	6° 57' 01.5" E
		Sample B	10.5		
D2	Netherlands	Sample A	19.02	N 52° 11' 17.6"	6° 57' 19.3" E
		Sample B	13.99		
G1	Germany	Sample A	5.91	N 52° 10' 17.1"	6° 57' 05.7" E
		Sample B	5.89		
G2	Germany	Sample A	6.98	N 52° 10' 28.9"	6° 57' 14.6" E
		Sample B	7.30		
G3	Germany	Sample A	8.46	N 52° 10' 41.8"	6° 57' 02.8" E
		Sample B	8.39		
G4	Germany	Sample A	8.40	N 52° 10' 28.7"	6° 56' 51.8" E
		Sample B	7.62		

The carbon content in the peat samples were calculated by the help of CHN analyser. CHN analyser calculates the Carbon, Nitrogen and Hydrogen percentage of the soil sample. The samples were analysed to test for the percentage of Carbon and hydrogen content so that the organic content of the soil samples would be known.

Table 6: Results of the CHN analyser

Run	Weight (gm)	Run Date	Date	Mode	Result Carbon	Result Hydrogen	Result Nitrogen
G1	1.849	12-12-2018	2018-12-12	CHN	49.88%	5.44%	0.61%
G2	1.869	12-12-2018	2018-12-12	CHN	50.92%	5.41%	0.66%
G3	1.734	11-12-2018	2018-12-11	CHN	52.06%	5.81%	0.61%
G4	1.849	11-12-2018	2018-12-11	CHN	52.12%	5.84%	0.61%
G5	1.772	11-12-2018	2018-12-11	CHN	20.55%	2.13%	0.35%
G6	1.75	11-12-2018	2018-12-11	CHN	20.38%	2.20%	0.37%

According to the results in Table 6, the samples taken from the top of the surface had around 50% carbon content which is very high. The samples G5 and G6 had comparatively lower carbon content since they were not taken from the top layer of the study area. After the sieve analysis was done, the result was plotted on a logarithmic scale. The effective or the referential grain size was determined by the graph. The grain size in [mm] was plotted against percentage finer and the corresponding grain diameter or size was taken which coincided with 10% finer. This value was used in [mm] in the Kozeny-Carman equation for determining the  $K_s$ .

The porosity of the soil samples were calculated by using the equation given by Cosby et al. (1981) which was  $\Phi = 0.489 - 0.001268 * (\% \text{ sand})$  (2)

here,  $\Phi$  is the soil porosity (%) and  $(\% \text{ sand})$  is the percentage of sand in the soil sample. Figures 10-15 show the particle size distribution curves obtained from the sieve analysis of the soil samples.

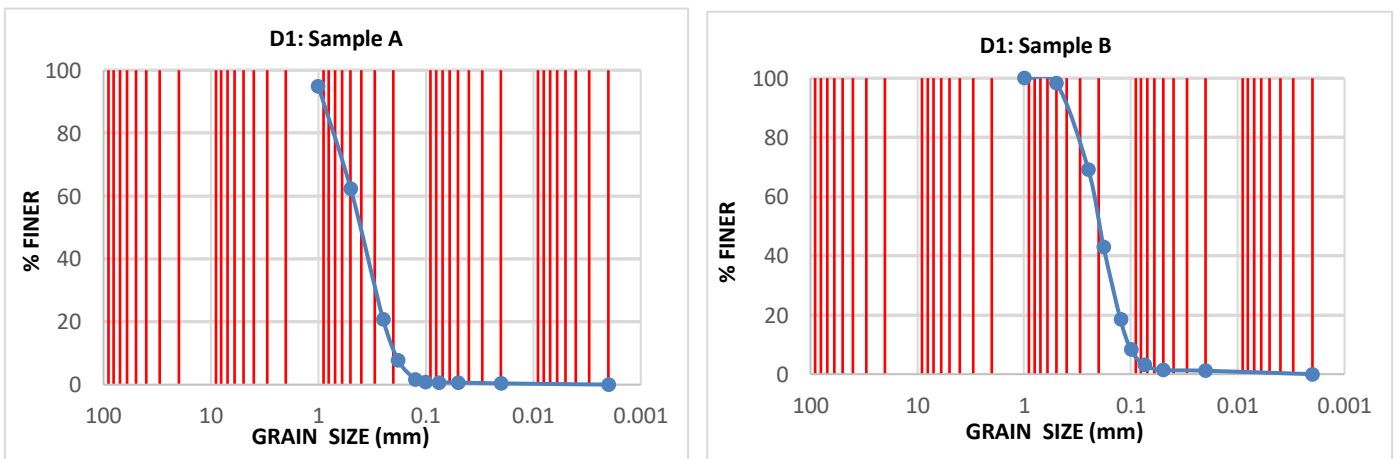


Figure 10: Grain-size distribution curves of samples from D1

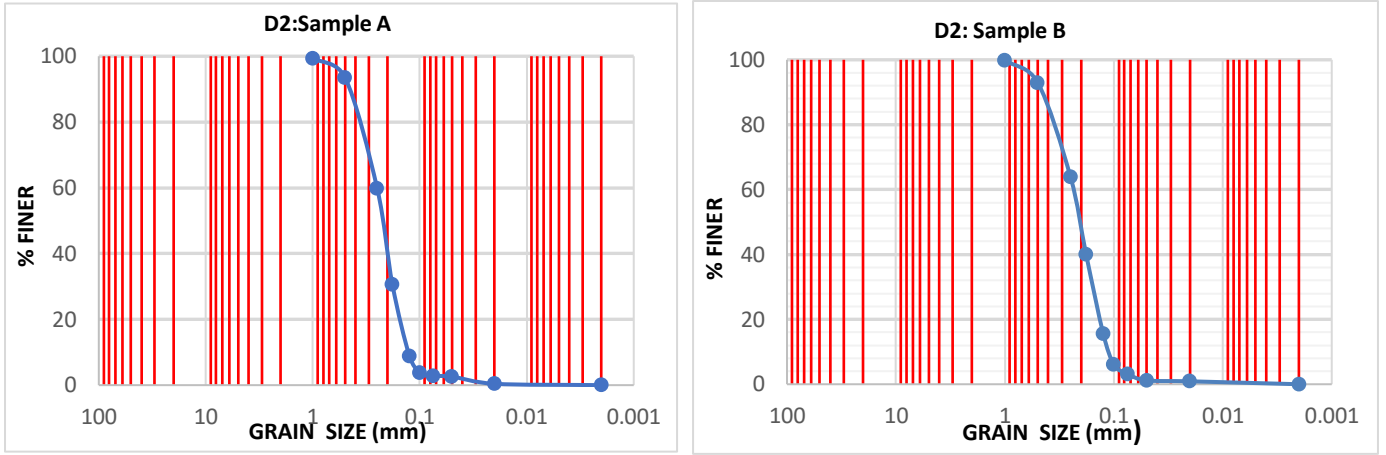


Figure 11: Grain-size distribution curves of samples from D2

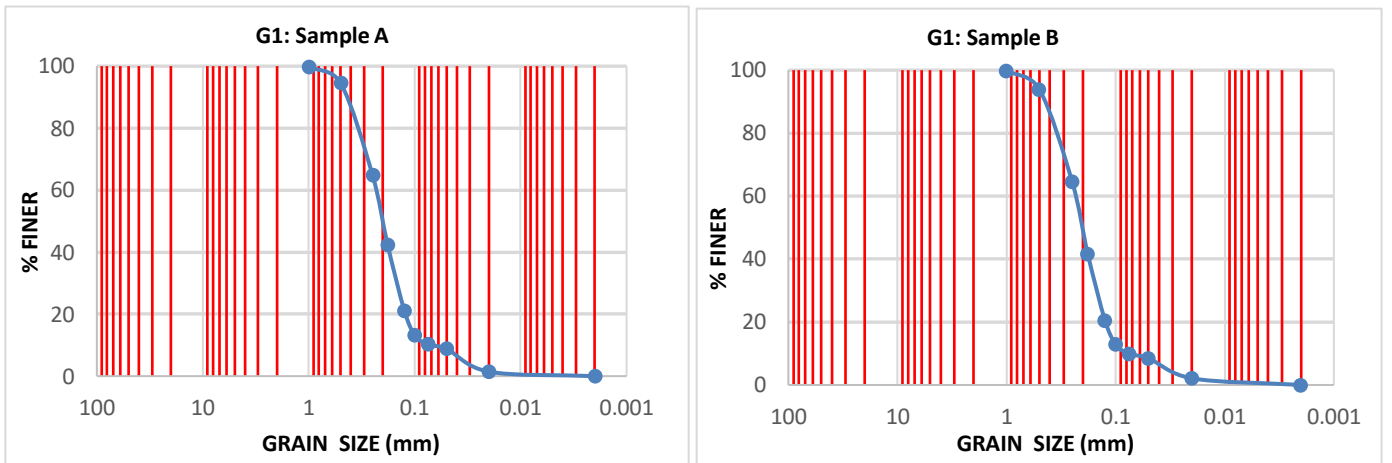


Figure 12: Grain-size distribution curves of samples from G1

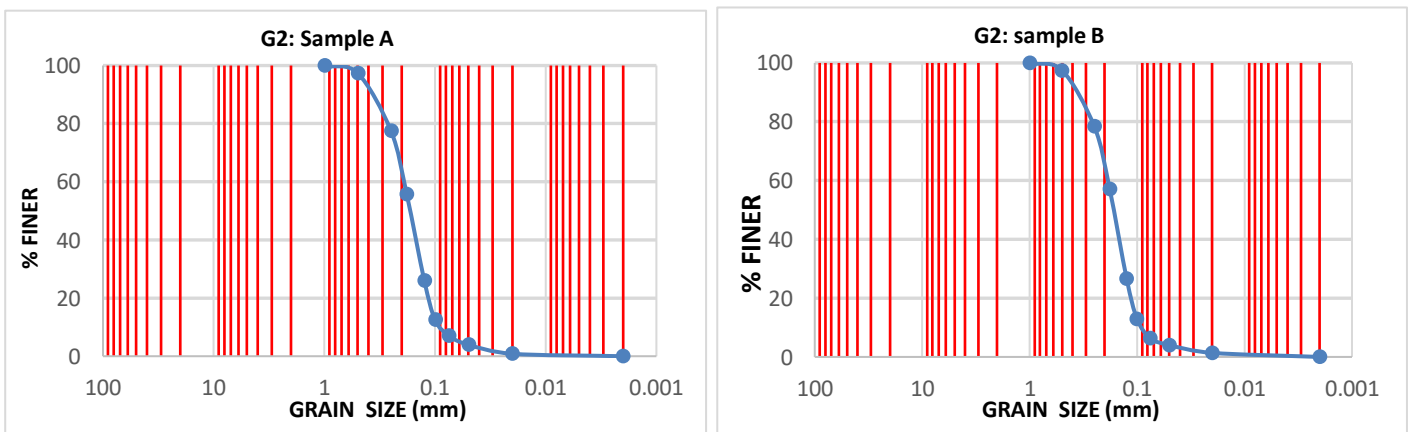


Figure 13: Grain-size distribution curves of samples from G2



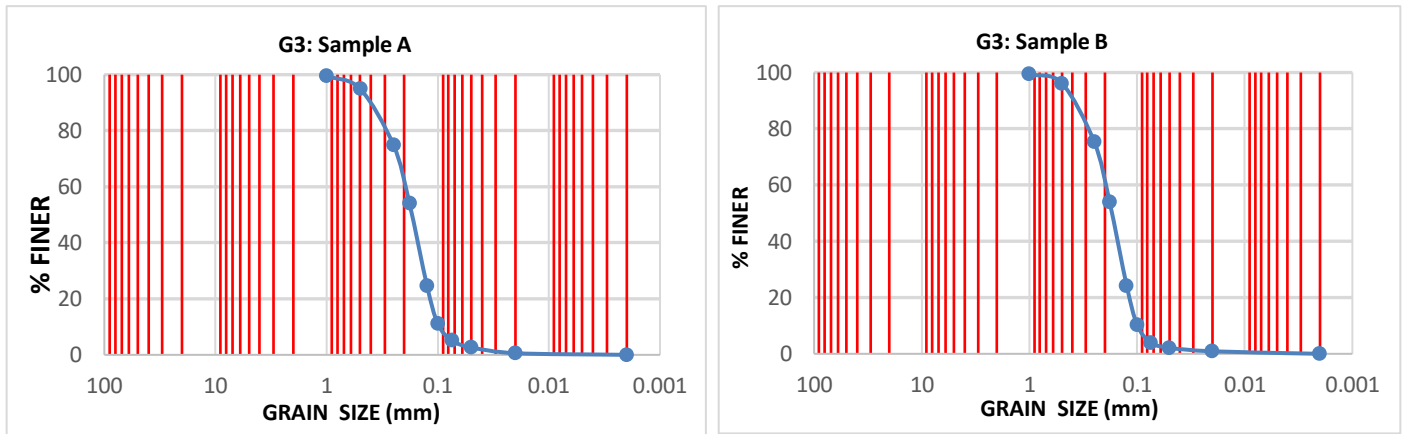


Figure 14: Grain-size distribution curves of samples from G3

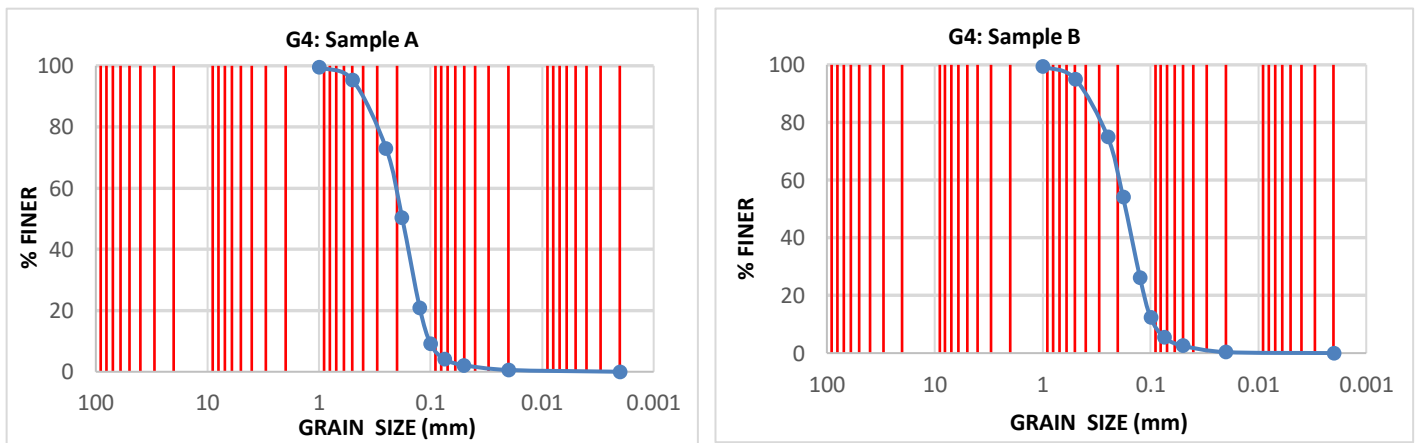


Figure 15: Grain-size distribution curves of samples from G4

The hydraulic conductivity zones were prepared based on the calculated  $K_s$  values from the field samples. These values were changed during calibration to produce better match between the simulated and the observed quantities. These  $K_s$  values obtained from the field worked well as initial values which gave a good convergence to the model. Also, the differences between the simulated and the observed were not high, which suggests that these  $K_s$  values of the calibrated model are close to the reality.

### 3.2. The conceptual model

A conceptual model is shown by Figure 16 which represents the boundary conditions and the hydro-stratigraphy of Aamsveen. After the identification of the objectives, a conceptual model is made, and this makes it the most important part. It requires a good geology, boundary conditions and hydrology hydraulic parameters (Franklin and Zhang 2003). The western side of Aamsveen has higher elevations which formed a water divide due to which water flows from west to east inside the study area as can be seen from Figure 16. The North-western side of the study area has thinner layer of sand as compared to the rest of the study area. Peat is found mainly in the wetland of the study area. Boulder clay is found below the sand layer. The rainfall is the main source of recharge for the entire study area. Low flux enters the study area from the eastern boundary. The study area

consists of surface drain and the streams which drain the wetland and reservoirs. There are also areas where peat was exploited before 1969, and now are filled with water and form ponds.

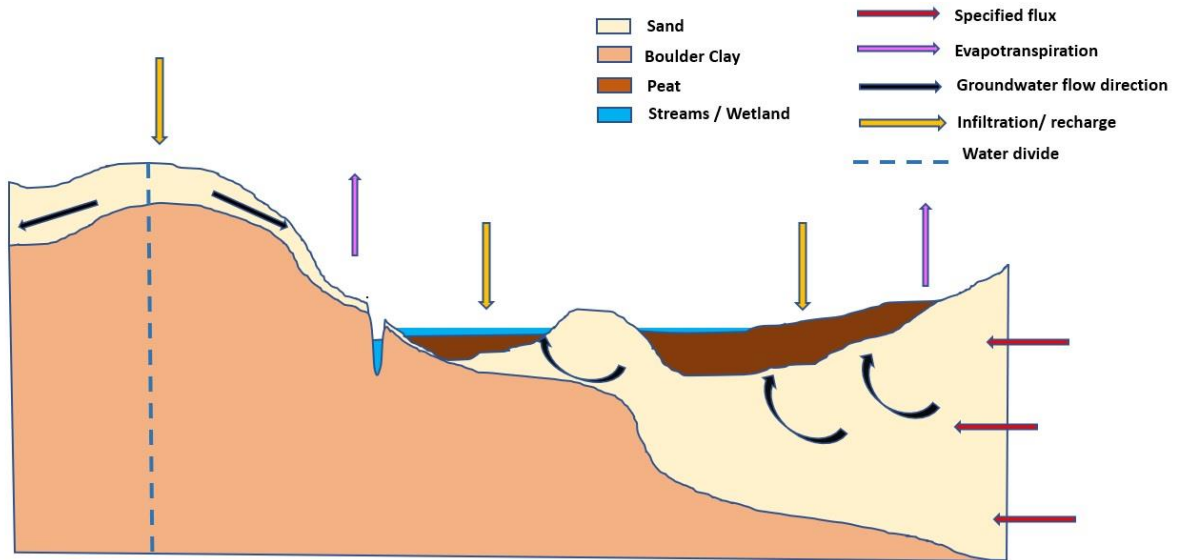


Figure 16: The conceptual model of Aamsveen

### 3.2.1. Sources and sinks

Precipitation is the main source of recharge in the area which is intercepted by the thick vegetation present especially in the wetland area. The vegetation here consists of heath, grass and trees (evergreen and deciduous). There are no wells which are used to pump out water for irrigation purposes in and around the region. The only outflow of the groundwater is through evapotranspiration and flow through channels and streams.

### 3.2.2. Flow direction

The study area has higher elevations on the west side and is lower on the east and the north side. The conceptualization of the flow system of the groundwater is from higher hydraulic heads in the west of the study area to lower north and east area.

## 3.3. Numerical Model

### 3.3.1. Literature review on surface-groundwater studies.

The groundwater is continually moving, with its volume continuously increasing with the surface water and rain water percolations and decreasing due to processes like evapotranspiration, exfiltration etc. It can be in a state of hydrological equilibrium over a long period of time when the average recharge is equal to the average discharge, but in many cases, this gets disturbed by human interference. Excessive interference of man in many ways like abstraction from wells create undesirable effects and ultimately cause the depletion of the groundwater reserve. The difficulty of developing analytical solutions to complex groundwater processes have been persisting for a long time. The answer lies in the form of mathematical or numerical models. Although not new, they are used widely due to the availability of high speed computers (Boonstra & Ridder 1981).



Surface-groundwater interactions are fundamentally important for ecosystem functioning and their understanding plays a crucial role in the management of the fluxes that are exchanged between groundwater and surface water in the areas of river basin management (Brenot et al. 2015). Local changes that occur at regional scales of  $10^3$  to  $10^5$  km<sup>2</sup> are globally linked due to the complete development of the interactions between the environment and the human system. Hence, practitioners and scientists agree upon the necessity of the management of integrated water resources and therefore, a lot of attention has been given to the surface and groundwater interactions (Barthel and Banzhaf 2016).

Integrated hydrological modelling accounts for the interactions between the systems of the surface water and groundwater. In some models, the basin parameters are disaggregated into landforms that are discrete and have similar hydrologic properties. The characteristics of the area may be impervious, have a variable clay or organic fractions, areas with variable water table depths or different land covers. Though, there is a requirement of a computational structure, discrete landforms can be incorporated within the basins, which significantly allow the analysis of distributed parameters (Zhang et al. 2012).

To examine the groundwater flow dynamics and for evaluating their management, the development of numerical models is done for selected watersheds. The simulations are able to reproduce the observed behaviours of the water table (Jiang et al. 2004). Due to the fact that the sub-surface is not seen, the most defensible description for quantitative analyses, forecasts of the proposed actions and their effect on the groundwater systems would be the model. Mostly, the preferred models are the processed based ones since they use processes that occur and also apply the rules of physics to aptly represent the groundwater dynamics and they are solved mathematically by numerical or analytical models. Analytical models are highly simplified, especially with respect to the spatial heterogeneity and this limits their application to the systems that are relatively very simple and are not appropriate as far as the groundwater systems and problems are concerned. The numerical models can be represented in steady state and transient conditions in 3 dimensions in media that is heterogenous with high complexity of the boundaries and the networks. Generally based on either finite element or finite difference methods and they are also capable in solving the groundwater problems (Anderson et al. 2015). Many groundwater models have been developed that enable a modeler to model the groundwater- surface water and their interactions and their system. Some examples are models like MIKE-SHE, FEFLOW, MODFLOW, GSFLOW, HYDROGEOSPHERE, FHM, CATHY, SWATMOD etc.

### **3.3.2. Software and code selection.**

Since a 3D simulation of the surface-groundwater is necessary for a good simulation of the processes and quantification of fluxes, MODFLOW-2005 was selected in order to model the Aamsveen area. The solver was chosen as MODFLOW-NWT since this is especially advantageous as far as drying and rewetting of a cell is concerned (Niswonger et al. 2011). The packages used in this model are UZF1 by Niswonger et al. (2006), SFR2 by Niswonger and Prudic (2010), Reservoir package explained by Fenske et al. (1996) and FHB package explained by Leake et al. (1997) for the boundary conditions. MODFLOW-NWT stands for the Newtonian formulation of the MODFLOW-2005 (Harbaugh 2005).

This software was selected because it was capable of solving the problems in non-linearities of drying and wetting of cells unlike Picard's method which was used in MODFLOW-2005. The other advantage was that this software is a free-source software which makes it easy and usable everywhere. The software was used under the environment of ModelMuse (Winston 2009).

ModelMuse also allows the user to define the spatial inputs by defining them as objects by using polygons, polylines and points etc. It has multiple ways to define the formulae, values etc and also provides the possibility of visualizing the selected input globally. Formulae can be assigned on individual objects or globally which provides an ease in working when the model is complex. This accounts for the solution of drying and rewetting nonlinearities. The partial differential equation that can describe in 3D, the movement of groundwater which has a constant density through the heterogenous aquifer which is anisotropic is presented below (Anderson et al. 2015).

$$\frac{\delta}{\delta x} \left( K_x \frac{\delta h}{\delta x} \right) + \frac{\delta}{\delta y} \left( K_y \frac{\delta h}{\delta y} \right) + \frac{\delta}{\delta z} \left( K_z \frac{\delta h}{\delta z} \right) = S_s \frac{\delta h}{\delta t} - W^* \quad (3)$$

Where,  $K_x, K_y, K_z$  are the hydraulic conductivities in the respective directions [ $\text{m day}^{-1}$ ],  $h$  is the potentiometric heads [ $\text{m}$ ],  $S_s$  is the specific storage of the aquifer [ $\text{m}^{-1}$ ],  $t$  is the time [ $\text{day}^{-1}$ ] and  $W^*$  is the volumetric flux of sink/source [ $\text{mday}^{-1}$ ]. Usually  $\frac{\delta h}{\delta t} = 0$  in steady-state.

The UPW package has been included with the MODFLOW-NWT (Newtonian formulation), since the non-linearities of the cell drying and rewetting are treated by this package as the continuous function of the heads of the groundwater. The BCF (Block Centred Flow), LPF (Layer Property Flow) and HUF (Hydrogeologic Unit Flow) packages use a discrete approach in solving the rewetting and drying of the cells. Due to this, the Newtonian formulation for the unconfined groundwater flow problems are enabled further since Newton method requires smooth conductance derivatives for a full range of heads for a model cell. During initialization, the average hydraulic conductivity between the cells is calculated by UPW package and then during iteration of the solution, it averages the conductance between cells using the upstream saturated thickness (Niswonger et al. 2011).

### 3.3.3. Spatial grid design and vertical discretisation

The study area was divided into 50 x 50 m grids. Compared to the larger grid sizes done in the previous studies, this size would be able to provide better simulation of the fluxes. The 2 layers were made into convertible layers since this would let the bottom layer to be unconfined and be able to rewet again in case the water level drops below the bottom of this aquifer.

### 3.3.4. Driving forces.

Precipitation and potential evapotranspiration were required as the driving forces. The evapotranspiration data provided by the weather station is based on Makkink's equation which already serves as the reference evapotranspiration. It is based on the incoming radiation and temperature (Rjtema 1959). Hence, no further processing of the driving forces was done. Makkink based his potential evapotranspiration [ $\text{mm day}^{-1}$ ] for grass which has been used as reference evapotranspiration in this study.

The equation that he had proposed according to Xu and Chen (2005) is :

$$ET_p = 0.61 * \frac{\Delta}{\Delta + \gamma} * \frac{R_s}{\lambda} - 0.12 \quad (4)$$

Where  $R_s$  = total solar radiation in [Cal cm<sup>-2</sup> day<sup>-1</sup>],  $\Delta$  is the slope of the saturation vapour pressure curve [mbar °C<sup>-1</sup>],  $\gamma$  is the psychrometric constant in [mbar °C<sup>-1</sup>],  $\lambda$  is the latent heat [cal g<sup>-1</sup>]

### 3.3.5. Boundary Conditions

#### 3.3.5.1. External boundary conditions

No-flow boundary was assigned to the entire boundary except the eastern boundary. The eastern side of the study area was analysed to have a gentle flow of flux from outside to inside of the study area which was estimated by the hydraulic heads inside and outside the study area and also by the presence of a groundwater divide which was indicated by the presence of a higher area outside this boundary and a river running parallel to the river inside the study area. This was analysed based on the groundwater heads available in the region. In the previous studies Bakhtiyari (2017) and Nyarugwe (2016) had assigned no-flow boundaries across the entire study area. Few data were made available by the German website <https://www.lanuv.nrw.de> which indicated a flow of flux at a very steady rate from across this eastern boundary. Hence, specified flow boundary was assigned to this boundary. The flux was calculated based on Darcy's law, which is given as the following (Brown 2002)

$$Q = KIA \quad (5)$$

Where Q is the volume flow rate [m<sup>3</sup> day<sup>-1</sup>], A is the area normal to the flow [m<sup>2</sup>], I, is change in the pressure head per length and K is the hydraulic conductivity [m day<sup>-1</sup>]. The boundary was assigned using the Flux and Head boundary package (FHB) package. The flux was calculated and applied as a constant throughout the boundary irrespective of the changes in stress periods.

The hydraulic conductivity used here was obtained from the lab after analysis of the sample of this area. The hydraulic conductivity was calculated to be 25 [m day<sup>-1</sup>]. The hydraulic gradient was calculated using [ $i = (h_2 - h_1) / L$ ], where  $h_2 - h_1$  is the difference in the heads between the isolines from the piezometers divided by the distance [m]. The values were calculated to be 1/1000 = 0.001. The area was taken as the thickness of the aquifer multiplied by the size of the grids. Since the thickness of sand was variable, an average of 10 metres was used which gave the area as 10 m \* 50 m which equals 500 m<sup>2</sup>. The total flux was calculated to be 25 \* 0.001 \* 500 = 12.5 [m<sup>3</sup> day<sup>-1</sup>]. This was further distributed throughout the entire boundary by dividing this to each cell as 12.5 / [50 m \* 50 m] = 0.005 m<sup>3</sup> day<sup>-1</sup>. This value of flux was distributed throughout the entire boundary inside the FHB package (Flow and Head Boundary Package).

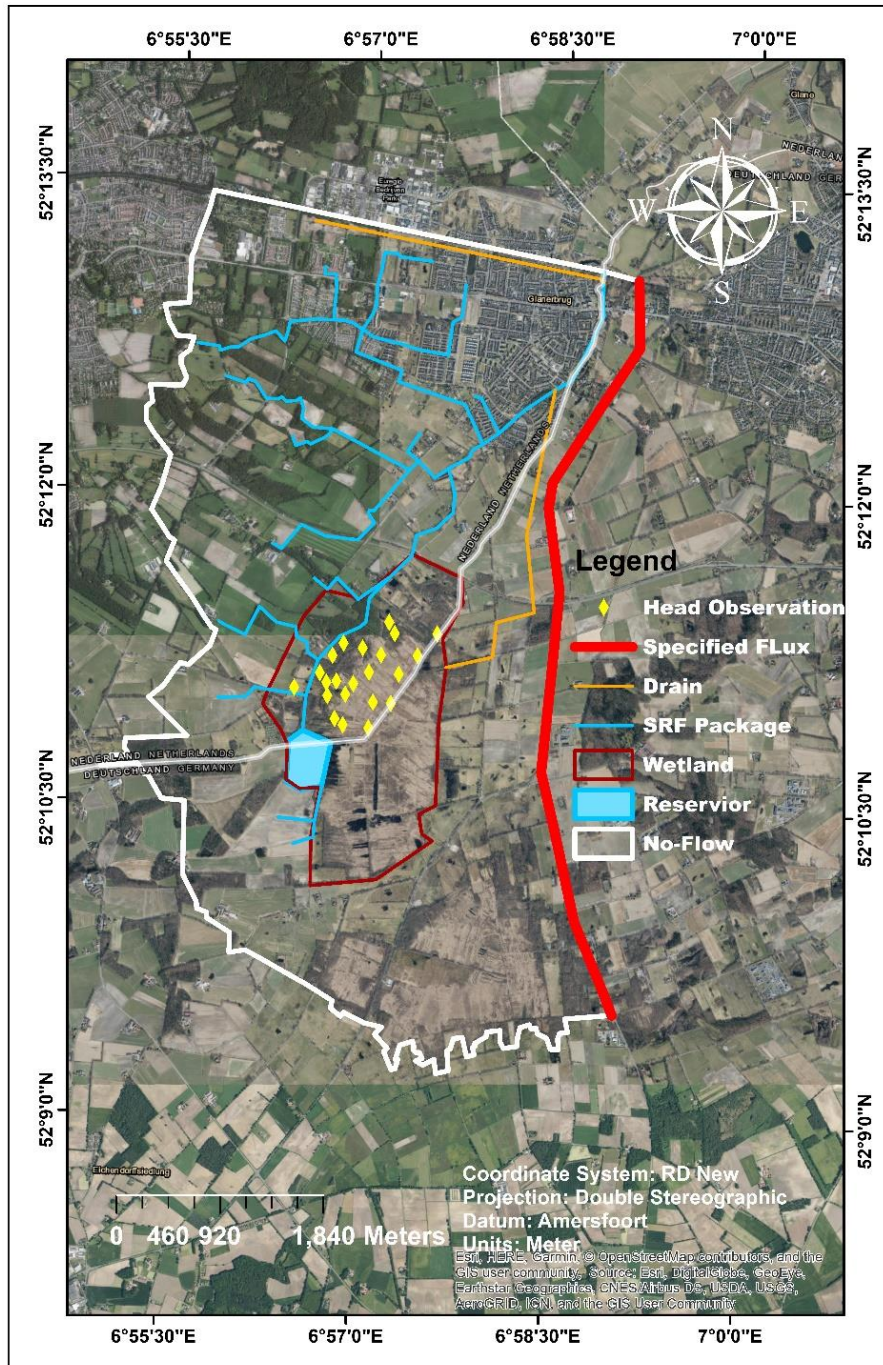


Figure 17: Boundary conditions of the study area

### 3.3.5.2. Internal boundary conditions

For simulating sources and sinks within the study area, the RES1 (Reservoir Package) was used to simulate the flows from surface water bodies present within the study area, SFR2 (Stream Flow Routing) package was used to simulate the stream flows and UZF1 (Unsaturated Zone Flow) package was used to simulate the flows in unsaturated zone. The DRN (Drain package) was used to simulate the flow carried by the surface drain and the HOB (Head Observation package) was used to input the observed groundwater heads.

Many models of the humid settings do not include the unsaturated zone processes and the water is instantaneously added as a recharge to the water table (Hunt et al. 2008). Since, the UZF1 package simulates vertical flow through the unsaturated zone, it combines groundwater flow package and a boundary condition package. The recharge to the groundwater is delayed by the UZF package, since the water which percolates through the unsaturated zone may even reach the groundwater table at the end of a stress period. For simulation of the vertical unsaturated flow, the method of characteristics is used in order to solve the kinetic wave approximation to Richard's equation. The assumptions are for the hydraulic properties to be uniform, it does not take into account the negative potential gradients since the unsaturated flow responds only to gravity potential gradients (Niswonger et al. 2006). The package requires the rate of infiltration, water content (initial, saturated and extinction), Brooke's Corey component, potential evapotranspiration and maximum unsaturated vertical hydraulic conductivity.

### 3.3.5.3. Unsaturated zone flow package (UZF1)

For the simulation of the unsaturated flow zone, Modflow offers UZF1 package (Niswonger et al. 2006). This package divides the infiltration into recharge, evapotranspiration and unsaturated storage. It applies the kinematic-wave approximation of Richards equation stated below (Niswonger et al. 2006).

$$\frac{\delta\theta}{\delta t} + \frac{\delta K(\theta)}{\delta z} + i = 0 \quad (6)$$

Where,  $\theta$  is the volumetric water content [ $\text{m}^3 \text{m}^{-3}$ ],  $K(\theta)$  is the unsaturated hydraulic conductivity as a function of the water content [ $\text{m day}^{-1}$ ],  $i$  is the evapotranspiration rate per depth [ $\text{day}^{-1}$ ], and  $t$  is the time [day]. For defining the unsaturated hydraulic conductivity, the Brooks Corey function has been introduced and is expressed in the equation

$$K(\theta) = K_S \left[ \frac{\theta - \theta_r}{\theta_s - \theta_r} \right]^\epsilon \quad (7)$$

Where,  $K_S$  is the saturated hydraulic conductivity,  $\theta_r$  is the residual water content,  $\theta_s$  is the saturated water content and  $\epsilon$  is the Brooks-Corey exponent.

### 3.3.6. Interception

Interception loss consists of the amount of rainfall which returns back to the atmosphere through evapotranspiration from the surface of the plants or is absorbed in the plant. Hence, this difference between the total precipitation and the amount which actually reaches the ground is the interception loss (Meriam 1960). The interception loss has been calculated based on the land cover of the study area. Various literatures were used to define the interception rate of the land cover. The interception rates that were adopted have been described in Tables 7 and 8. It is to be noted that the interception for rapeseed is not well defined hence it has been estimated by reviewing few reports including Drastig et al. (2019). To account for the temporal variability, interception maps were made separately for the summer and winter months since deciduous trees shed their leaves in winter months and the vegetation cover is generally thinner in the winter than in the summer.

$$I = P * (I_A * A_A + I_H * A_H + I_G * A_G + I_B * A_B + I_w * A_w) \quad (8)$$

Where  $I$  = interception of canopy per grid cell [ $\text{m day}^{-1}$ ],  $P$  is the precipitation [ $\text{m day}^{-1}$ ],  $I_A, I_S, I_G, I_w$  and  $I_B$  are interception losses by agriculture (Trees, agriculture), heath, grass and building [%].  $A_G, A_A, A_B, A_H$  and  $A_w$  are the spatial coverage (within the grid cell) of grasses, agriculture (crops, trees), buildings, heath and water respectively.

Table 7: Interception rate of the various land covers for summer

Land cover	Interception Rate (%)	Literature
Water	0	
Maize	16	(Jong & Jetten, 2007)
Evergreen Trees	17.3	(Jetten 1996)
Deciduous Trees	13	(Jong & Jetten, 2007)
Grass	7.9	(Corbett & Crouse 1968)
Heath	20	(Manning and Paterson-Jones 2007)
Bare Soil	0	
Rape Seed	14	(Drastig et al. 2019)
Buildings	76	(Linden 2010)

Table 8: Interception rate of the various land covers for winter

Land cover	Interception Rate (%)	Literature
Water	0	
Wheat	36	(Kozak et al. 2007)
Evergreen Trees	17.3	(Jetten 1996)
Deciduous Trees	0	
Grass	7.9	(Corbett & Crouse 1968)
Heath	20	(Manning and Paterson-Jones 2007)
Bare Soil	0	
Rape Seed	14	(Drastig et al. 2019)
Buildings	76	(Linden 2010)

### 3.3.7. Extinction depth

The UZF1 package required the extinction depth as one of the inputs since this is the depth at which evapotranspiration ceases to take place. A root map was developed from the original land cover map using various literatures and this map was used as the input for the extinction depth. Table 9 gives the various sources which were referred to obtain the root depth.

Table 9: Rooting depth of various land covers in [m].

LAND COVER	Rooting Depth (m)	Source
Water	0	
Maize	1.7	(Allen et al. 1998)
Evergreen Trees	3.36	(Foxx et al. 1984)
Deciduous Trees	3.32	(Foxx et al. 1984)
Grass	1.45	(Shah et al. 2007)
Heath	1.9	(Foxx et al. 1984)
Bare Soil	0.5	(Shah et al. 2007)
Rape Seed	1.5	(Allen et al. 1998)
Buildings	0	

### 3.3.8. Potential Evapotranspiration

For the calculation of potential evapotranspiration, crop coefficient ( $K_c$ ) maps were made. These maps were used as the model input and were multiplied by the reference evapotranspiration to obtain the potential evapotranspiration. Table 10 gives the details of the crop coefficients that were used in the model. The values of the coefficients were taken from Allen et al. (1998)

Table 10: Crop coefficient values for the various land covers.

Landcover	Jan	Feb	March	landcover	April	May	June	July	August	September	Landcover	October	November	December
Water	1.05	1.05	1.05	Water	1.05	1.05	1.05	1.05	1.05	1.05	Water	1.05	1.05	1.05
Grass	1	1	1	Grass	1	1	1	1	1	1	Grass	1	1	1
Heath	1.1	1.1	1.1	Heath	1.1	1.1	1.1	1.1	1.1	1.1	Heath	1.1	1.1	1.1
Wheat	1.5	0.25	0.25	Maize	1.2	1.2	1.2	0.6	0.6	0.6	Wheat	0.7	0.7	1.5
Evergreen Trees	1	1	1	Evergreen Trees	1	1	1	1	1	1	Evergreen Trees	1	1	1
Deciduous Trees	0.19	0.19	0.19	Deciduous Trees	0.8	0.8	0.8	0.8	0.8	0.8	Deciduous Trees	0.8	0.8	0.19
Bare Soil	1.2	1.2	1.2	Bare Soil	1.2	1.2	1.2	1.2	1.2	1.2	Bare Soil	1.2	1.2	1.2
Rape seed	1	1	1	Rape seed	1	1	1	0.35	0.35	0.35	Rape seed	1	1	1
Buildings	0	0	0	Buildings	0	0	0	0	0	0	Buildings	0	0	0

### 3.3.9. Infiltration

The UZF1 package requires the infiltration rate. The input in the UZF1 package for infiltration was provided as difference between the precipitation and the interception loss. This package also has the option to either route the excess water over the land surface to the stream or lake or else, this excess water is removed from the model. The water that is discharged to the land surface in this study area was routed directly towards the streams.

### 3.3.10. Streams

The interactions between streams and aquifers was simulated using the SFR package. This package is also able to simulate the interactions of the streams with the unsaturated zone. This is especially beneficial in the places where the water table is very low since it also considers the time delay which results due to the vertical flow of water to the water table. SFR is composed of a network of streams which have their individual segments and reaches. Similar to the UZF package, the method of characteristics is used to solve kinematic wave approximation to Richard's equation and hence simulates the flow in the unsaturated zone. Here, the seepage losses are usually restricted by the hydraulic conductivity of the unsaturated zone as compared to the SFR1 package which does not have this consideration. For each individual cell, whenever the water table becomes lower than the stream bed elevation, the unsaturated flow is simulated which is independent of the saturated flow. Similar to the river package, the exchange of the ( $Q$ ) volumetric flux is calculated using the equation (Brunner et al. 2010).

$$Q = \frac{KLw}{M} * (h_s - h_a) \quad (9)$$

where,  $Q$  is the volumetric flow which occurs between the aquifer and the respective stream section [ $\text{m}^3 \text{ day}^{-1}$ ],  $K$  is the hydraulic conductivity of the sediments of the streambed [ $\text{m day}^{-1}$ ],  $w$  is the stream width [ $\text{m}$ ]  $M$  is the thickness of the stream bed deposits, from the top to the bottom [ $\text{m}$ ],  $h_s$  is the stream head [ $\text{m}$ ] and  $h_a$  and is the aquifer head [ $\text{m}$ ].

### 3.3.11. Lakes/wetlands/reservoirs

Various packages are included in MODFLOW for simulating the surface water bodies. These include Reservoir package and Lake package. The reservoir package simulates the interactions of the surface water body with the vertical flow to the water table below it. Unlike the Lake package, the heads in the reservoir are not influenced by the interaction between the reservoir and the groundwater. The reservoir area expands and contracts with the fluctuations in the stage of the reservoir. The modelling of the areas surface water body was done by using the reservoir package which required certain inputs like the vertical hydraulic conductivity of the reservoir bed, starting stage and ending stage, reservoir bed elevation and also the thickness of the reservoir bed. The simulation of the vertical flow in the unsaturated zone is not done and this makes the flow to the water table instantaneous. This package also operates independently of the other packages.

### 3.3.12. Head Observation Package

This package is used to assign the head observations which are to be used in the process of calibration. The observation time is identified by the user by a stress period number, which is referred to as the reference stress period, IREFSP and a time offset (TOFFSET). This package allows the possibility of changing the number and length of the time steps and the stress periods without any change in the observation time definition (Harbaugh and Hill 2013).

### 3.3.13. Flow and head boundary package

The Flow and Head Boundary package (FHB1) is used for specifying the head cells and specified flow cells. These cells can vary their properties within a specified time. The FHB1 makes use of a function that is based on the values specified by the user to define the boundary conditions for the whole simulation period for each selected cell. The function calculates the values for each MODFLOW time-steps by linear interpolation. Since the package offers the input of both the specified heads or flows, if both the inputs are applied, the package overrides the specified flow function and the heads function is activated. These values can also be specified across the entire boundary instead of individual cells (Leake et al. 1997). It is similar to the WELL package and RECHARGE package of MODFLOW, but if all the 3 packages are active, FHB1 overrides the WELL and RECHARGE package.

### 3.3.14. Drain Package (DRN)

This package is designed for the simulation of the effects of certain features that remove water at a rate that is proportional to the differences between a fixed elevation and the head in the aquifer. This is called as the drain elevation. The drain functions based on the head of the aquifer and only removes water when the aquifer head is above the drain elevation. The equation of the functioning of the drain package is given by (Harbaugh 2005).

$$\begin{aligned} Q_{out} &= CD (h_{i,j,k} - HD), & h_{i,j,k} > HD \\ Q_{out} &= 0, & h_{i,j,k} \leq HD \end{aligned} \quad (10)$$



Where,  $Q_{out}$  is the flow from the aquifer into the drain [ $m^3 \text{ day}^{-1}$ ], CD is the drain conductance [ $m^2 \text{ day}^{-1}$ ], HD is the drain elevation and  $h_{i,j,k}$  is the head of the cell in which the drain is located.

### 3.4. Model Parameterization

#### 3.4.1. Newton-NWT solver

The criteria given for the solver in this model consists of: 'HEADTOL' which is the head tolerance [m] was set to 0.01 m. 'FLUXTOL' which is the flux tolerance, was set as 1 [ $m^3 \text{ day}^{-1}$ ]. 'MAXITEROUT' which is the maximum number of outer iterations was set as 5000. 'THICKFACT' which is the portion of cell thickness used for coefficient adjustment was set as 0.0001. The matrix solver called [LINMETH] gave a selection between 'GMRES' and 'CHI-MD' and the second option 'CHI-MD' was selected. 'IPRNWT', which is the option to print the solver convergence information was selected. NWT solver also provides an option for the user to correct the groundwater head which is relative to the altitude of the cell-bottom when dry cells surround a cell, called 'IBOTAV' and this was not selected. The model complexity denoted by 'OPTIONS' was selected as 'COMPLEX' among other options provided by NWT solver like 'SIMPLE', 'COMPLEX', 'SPECIFIED' etc. There is also another option called 'CONTINUE OPTION' which continues the model execution despite non-convergence. This option was also selected.

#### 3.4.2. UZF1

This package provides an option where the recharge and discharge can be simulated, which is called as 'NUZTOP'. The 'Top Active Cell' was selected for this option. 'IUZFTOP', which is the vertical hydraulic conductivity source, gave option to either use the vertical hydraulic conductivity from the flow package or to specify it. The 'specify vertical hydraulic conductivity (1)' option was selected. 'NTRAIL2' which is the number of trailing waves was selected as 15. 'NSETS2', which is the number of wave sets was selected as 20. Other options like 'IRUNFLG' (the route discharge to streams, lakes or SWR reaches, 'IETFLG' to simulate Evapotranspiration, 'SPECIFYTHTR', the option to specify the residual water content, 'SPECIFYTHTP', the option to specify initial unsaturated water content, the inverse of 'NOSURFLEAK' options were selected. 'SURFDEP', the average height of undulations in the land surface altitude was assigned as 0.01. The input parameters like the infiltration rate was assigned by subtracting the interception loss from the total precipitation and evapotranspiration demand was assigned by using multiplying the reference ET calculated in the station with the Kc map. The ET extinction depth was assigned using a root depth map created after making a land cover map of the study area. This was imported into the model as an ACSII Raster file. The ET extinction water content was assigned as 0.1 during the calibration for the entire simulation.

#### 3.4.3. SFR2

The option to adjust the seepage loss (LOSSFACT) was selected. 'ISFROPT' was selected which simulated unsaturated flow beneath the streams. The stream bed properties of 'ISFROPT' was selected as 'specify some stream bed properties by reach' which cannot inactivate the streams. The other option which was not selected was 'specify some stream bed properties using segment endpoints.' 'DLEAK' which is the tolerance, was assigned 0.0001 [ $m^3 \text{ day}^{-1}$ ]. 'NSTRAIL', the number of trailing waves was 15. 'NSFRSETS', which is the maximum number of trailing waves

was set to 20. 'ISUZN', the number of cells to define the unsaturated zone was set to 1. 'IRTF LG', which uses transient stream routing with kinematic-wave equation was activated. 'NUMTIM', the number of divisions per time step for kinematic waves as assigned as 1. 'WEIGHT', the time weighting factor for the kinematic wave solution was assigned as 1. 'FLOWTOL', the closure criterion for the kinematic wave solution was assigned as 0.01. The STRTOP, which is the stream bed top was assigned as 'Model Top'-1 to 'Model Top'-2 since the streams have different depth as the river flows around the study area. The stream slope which is 'SLOPE' was assigned as 0.2. Stream bed thickness (STRTHICK) was generally assigned as 0.1 m across the streams with 0.011m as the lowest value. The stream bed  $K_v$ , 'STRHC1' was assigned in the range of  $K_x * 0.3$  to  $K_x * 0.4$ . The saturated volumetric water content (THTS) was assigned 0.3 and THTI, the initial volumetric water content was assigned as 0.27. EPS, which is Brooke's Corey exponent was 3.5, which is the default value. UHC, which is the maximum unsaturated  $K_v$  was assigned 1 [m day<sup>-1</sup>]. For the stage calculation ('ICALC'), the option 'Rectangular channel (1)' for which 'ICALC'=1 was used which uses Manning's equation for the calculation of the depth, among the other option. Out of the other options, only the 'Rectangular channel (1)' and eight-point cross-section which again uses Manning's equation, allow the simulation of unsaturated flow beneath the streams.

#### **3.4.4. Reservoir package**

The thickness of the reservoir bed was set to 0.2 m. The reservoir hydraulic conductivity was assigned as 0.8 [m day<sup>-1</sup>]. The elevation of the reservoir was assigned as 'Model Top'.

#### **3.4.5. FHB boundary**

The Flow and Head boundary package was assigned in the eastern boundary. This package only required the fixed flow rate per unit length or area and was assigned as 0.0053 [m<sup>3</sup> day<sup>-1</sup>] as explained in the FHB boundary package.

#### **3.4.6. Drain package**

The elevation of the drain was set as the 'Model Top'-1'. The conductance of the drain was assigned as 0.5 per unit length of area.

### **3.5. State variables**

An integrated hydrological model is usually calibrated by the help of state variables which are usually the groundwater heads and the stream flows. These data are considered to represent the actual ground conditions. A model is assessed based on the discrepancies between the state variable and their simulated counterparts from the model. This model uses the groundwater heads and stream flows for calibration.

#### **3.5.1. Groundwater Heads**

The groundwater heads were made available from [www.dinoloket.nl](http://www.dinoloket.nl). Unfortunately, for the simulation period, the piezometers that were functioning were only present in the main wetland. Hence only these piezometers were made available and the calibration of the model was done by using these data. There were 4 piezometers that provided the data within the simulation period which were B35A0835, B35A0836, B35A0837 and B35A0890. The observations of these piezometers are given in Figure 18.

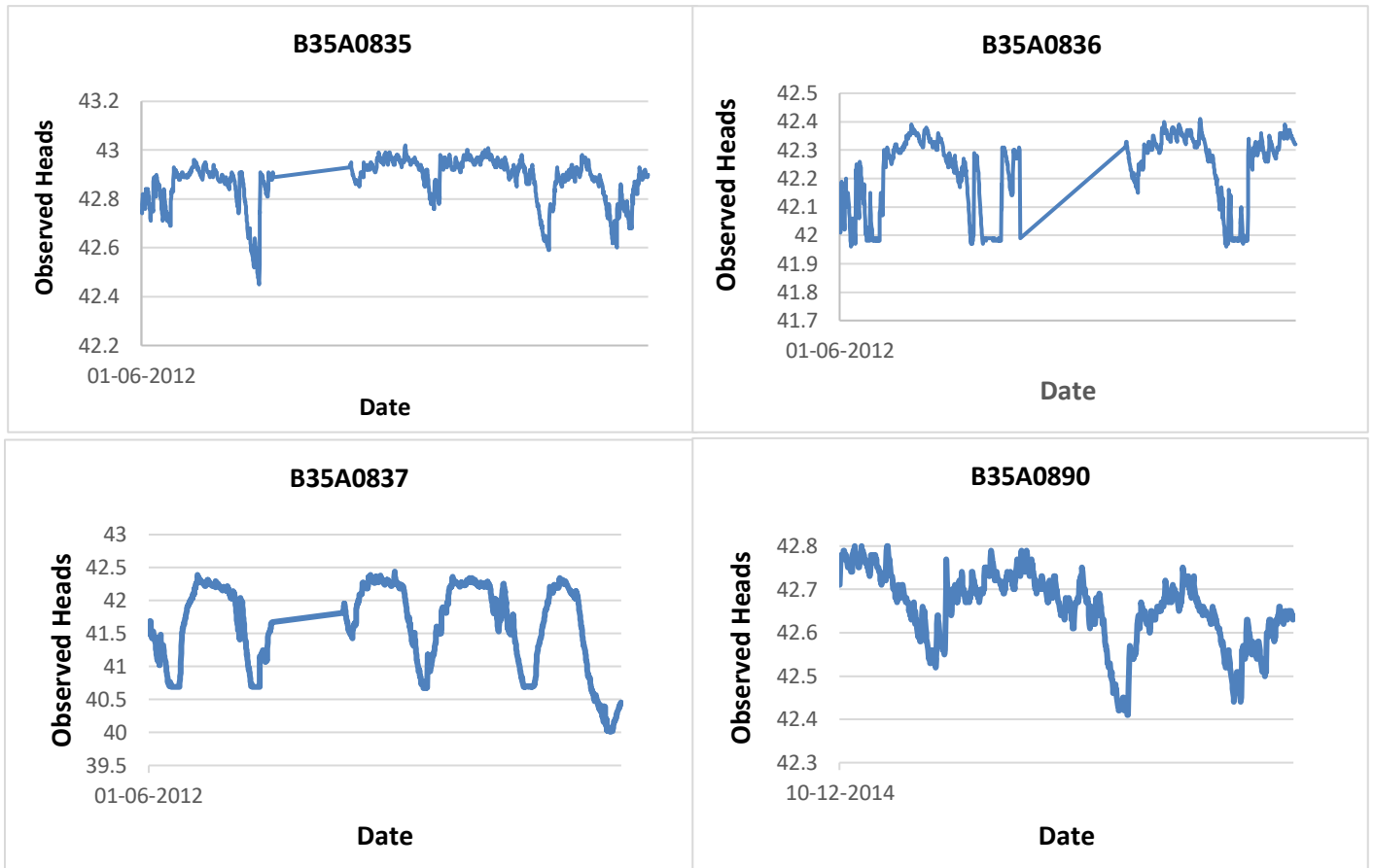


Figure 18: Measured heads of the piezometers during the simulation period

### 3.5.2. Stream Flows

The study area consists 2 stream gauges. The Glanerbeek which has its catchment in the study area is the main river that runs through the entire study area. The stream discharges are measured by weirs which record the discharge every hour. The measurements of the stream gauges that are located inside the study area which are located in Aamsveen camping site and Melodiestraat are shown in Figure 19. The daily discharge was calculated by taking the average of 24 hours every day.

The location of the stream gauges was assigned in the SFR package depending on the stream along which they were present. The output of the SFR package provides the simulated flows at those specific locations which were assigned in the SFR package. This flow is then calibrated with respect to the observed discharges at those particular locations.

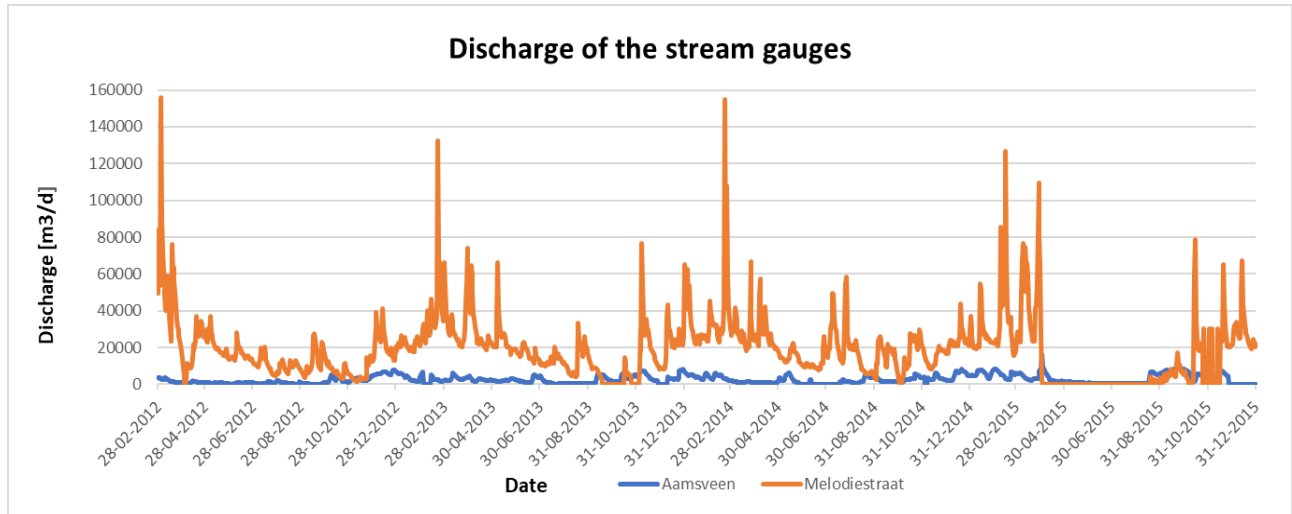


Figure 19: Measured discharges of the streams in Aamsveen

### 3.6. Transient simulation

Steady state models have already been developed in the past researches in the study area. The steady state models are not able to quantify the dynamics of the ground and surface water fluxes and hence there was a need to model the wetland in a transient mode for a better understanding of the distribution and the quantification of the fluxes. The transient modelling was done starting from January 1, 2012 till December 31, 2015. The discretization was done as daily stress periods and had total times steps of 1461 days. The units of length were in metres and the unit of time was assigned as days in the model.

#### 3.6.1. Initialization and Model warming

Initial time steps have a very strong influence in the warming of the model (Anderson et al. 2015). In some cases, the heads generated from a steady state models are used initially in the transient model. Generally easier to execute, steady state models can give important insights to the model behaviour and ultimately can provide useful information in the execution of complex transient models. In the present study, a steady state model was not developed since it was already done in the previous studies. Certain parameters like the initial hydraulic conductivity, SFR parameters from the previous models were used in the present transient model but the initial heads generated by those steady state could not be made use of due to the fact that the boundaries of the study area were changed. However, transient conditions are not very easy to simulate in Aamsveen since the place is generally saturated and the buffer capacity is usually low (high saturation) due to which there are delays in the peaks and magnitudes of the stream flows with respect to the rainfall, whereas, the steady state simulation does not consider this aspect. The initial heads were assigned by using the piezometric map that was made from the borehole data. As mentioned by Kinoti (2018), few researchers who have worked on groundwater models, have discarded the warming up data since their models performed better El-Zehairy et al (2018), Hassan et al. (2014) and Bakar (2015), but she did not discard the data and instead, she continued with the calibration after a warm-up period of 3 months. In this model, a warm period of 1 year was used but it was not discarded as done in few studies. The model was simulated ultimately for 4 years, including the 1-year warm-up period.

### 3.6.2. Model Calibration

Trial and error method was used to manually calibrate the model. The model was warmed up first for a 1-year period and then the whole model was run and calibrated. The hydraulic conductivity zones were adjusted along with the UZF parameters, SFR parameters and other parameters like the specific yield were adjusted in order to achieve a good calibration.

### 3.6.3. Evaluation of model performance

The evaluation of the performance of the model was done by the closure of the water balance and also based on the errors in the simulated versus observed groundwater heads and stream flows. The heads were evaluated by the ME (Mean Error), MAE (Mean Absolute Error) and RMSE (Root Mean Square Error). Modification of the model outputs for matching closely, the observation heads and flows maybe be the most limited meaning of a model's calibration. Calibration is also done keeping in mind, the model's capability to meet the required objectives which is influenced by flow system's conceptualization.

It is not necessary that some of the parameters which result in a better fit would always be reasonable based on our knowledge of their values which is also an indication of the problems in conceptualization of the model. Thus not only the closeness of fit between the observed and simulated values but also the extent of incorporation of certain simulation aspects are very necessary for the evaluation of a model's calibration (Reilly and Harbaugh 2004). Rientjes (2015) mentions the use of these equations mentioned below as means to quantify the average error of calibration and these are expressed by the average differences between the simulated and the observed values.

$$ME = \frac{1}{n} \sum_{i=1}^n (h_{obs} - h_{sim})_i \quad (11)$$

$$MAE = \frac{1}{n} \sum_{i=1}^n |(h_{obs} - h_{sim})_i| \quad (12)$$

$$RMSE = \sqrt{\left( \frac{1}{n} \sum_{i=1}^n (h_{obs} - h_{sim})_i^2 \right)} \quad (13)$$

Where  $n$  is the number of observations,  $h_{sim}$  is simulated head [m] and  $h_{obs}$  is the observed or measured head [m].

While calibrating a model, it is necessary to attain the right dynamics of the simulated values with the observed values since this would suggest that the model is sensitive to the hydrological changes in the area. Hence, for the comparison of the fitting of the hydrograph, Nash-Sutcliffe coefficient of efficiency given by Nash and Sutcliffe (1970) and RVE (Relative Volumetric Error) are also used for comparison of the simulated and the observed values of the flows. NS evaluates the fitness of the shapes of the model of the hydrograph and RVE evaluates the volume of the balance between observed and simulated flows. The equations for the evaluation are given as:

$$NS = 1 - \frac{\sum_{i=1}^n (Q_{obs} - Q_{sim})^2}{\sum_{i=1}^n (Q_{obs} - \overline{Q_{obs}})^2} \quad (14)$$

$$RVE = \left[ \frac{\sum_{i=1}^n Q_{sim}(i) - \sum_{i=1}^n Q_{obs}(i)}{\sum_{i=1}^n Q_{obs}(i)} \right] \quad (15)$$

Where NS= Nash Sutcliffe coefficient of efficiency, RVE is the relative volumetric error,  $Q_{obs}$  is the observed flows [ $\text{m}^3 \text{day}^{-1}$ ],  $Q_{sim}$  is the simulated flows [ $\text{m}^3 \text{day}^{-1}$ ] and  $\overline{Q_{obs}}$  is the mean runoff in time [ $\text{m}^3 \text{day}^{-1}$ ].

### 3.7. Sensitivity analysis

Analysing the sensitivity of the model helps to understand the uncertainties in the output of a numerical model. The parameters that the model is highly sensitive to and affect the model behaviour can be understood by doing the sensitivity analysis which also helps to understand the magnitude of the change a concerned parameter can have on the model's response.

The focus of the sensitivity analysis for this transient model was on the exfiltration of groundwater, groundwater evapotranspiration, net recharge and gross recharge and their response to hydraulic conductivities of the aquifer, the unsaturated zones maximum hydraulic conductivity, the extinction depth and the specific yield.

### 3.8. Water balance

The following equations were used to analyse the water balance of the entire domain. This was done for the surface, saturated and the unsaturated zones. The water balance is expressed as

$$P + SF = ET + Q_s \pm \Delta S + Q_D \quad (16)$$

where, P is the precipitation, ET is the total evapotranspiration,  $Q_s$  is the stream flow at the outlet,  $\Delta S$  is the change in storage, SF is the inflow of the flux across the eastern boundary of the study area and  $Q_D$  is the outflow through the drain. Further, the ET can be split up into:

$$ET = ET_g + ET_{uz} + I \quad (17)$$

where,  $ET_g$  is the evapotranspiration from the groundwater,  $ET_{uz}$  is the unsaturated zone evapotranspiration and I is the canopy interception.

The change in storage can also be expressed as:

$$\Delta S = \Delta S_g + \Delta S_{uz} \quad (18)$$

where,  $\Delta S_g$  is the change in the storage of groundwater and  $\Delta S_{uz}$  is the change of storage in the unsaturated zone.

The stream flow at the outlet of the catchment can be expressed as:

$$Q_s = Q_{H+D} + Q_B \quad (19)$$

where,  $Q_{H+D}$  is the Hortonian runoff (which occurs when precipitation is higher than infiltration rate) and the Dunnian runoff (occurs due to saturation) and  $Q_B$  is the baseflow which is calculated by measuring the difference between the leakage from the streams which reaches the groundwater  $Q_{s(in)}$  and the groundwater that reaches the streams  $Q_{s(out)}$ .

The land surface water balance can be expressed as:

$$P + Exf_{gw} = I + Q_H + Q_D + P_e \quad (20)$$

where  $Exf_{gw}$  is the groundwater exfiltration and  $P_e$  is the actual infiltration rate.

The water balance of the unsaturated zone can be expressed as:

$$P_e = R_g + ET_{uz} + \Delta s_{uz} \quad (21)$$

where  $R_g$  is the gross recharge.

The water balance of the saturated zone of the 2 aquifers can be expressed:

$$R_g + Q_{res(in)} + Q_{s(in)} + SF = ET_g + Exf + Q_{res(out)} + Q_{s(out)} \quad (22)$$

$Q_{res(in)}$  and  $Q_{res(out)}$  are the reservoir leakages into the groundwater and out from the groundwater respectively and  $Q_{s(in)}$  and  $Q_{s(out)}$  are the stream leakages into the groundwater and out of groundwater respectively.

The net recharge  $R_n$ , is defined as the actual amount of water that reaches the saturated zone  $R_g$  after considering the removal of the groundwater exfiltration  $Exf_{gw}$  and groundwater evapotranspiration  $ET_g$  and this can be expressed as:

$$R_n = R_g - Exf_{gw} - ET_g \quad (23)$$

## 4. RESULTS AND DISCUSSION.

### 4.1. Model driving forces

#### 4.1.1. Precipitation.

There is fairly a consistent rainfall throughout the year with more precipitation during the winter months. The data used for simulation was from January 01, 2012 until December 31, 2015.

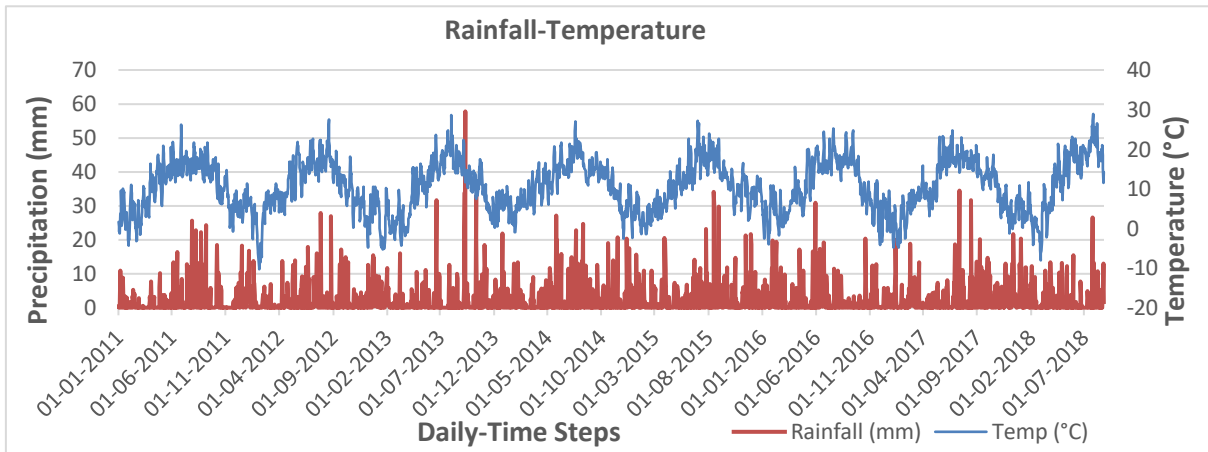


Figure 20: Rainfall and temperature of Aamsveen

#### 4.1.2. Reference evapotranspiration

The data was downloaded from [www.knmi.nl](http://www.knmi.nl). The data was homogenous for the entire study area hence no processing was required for the data.

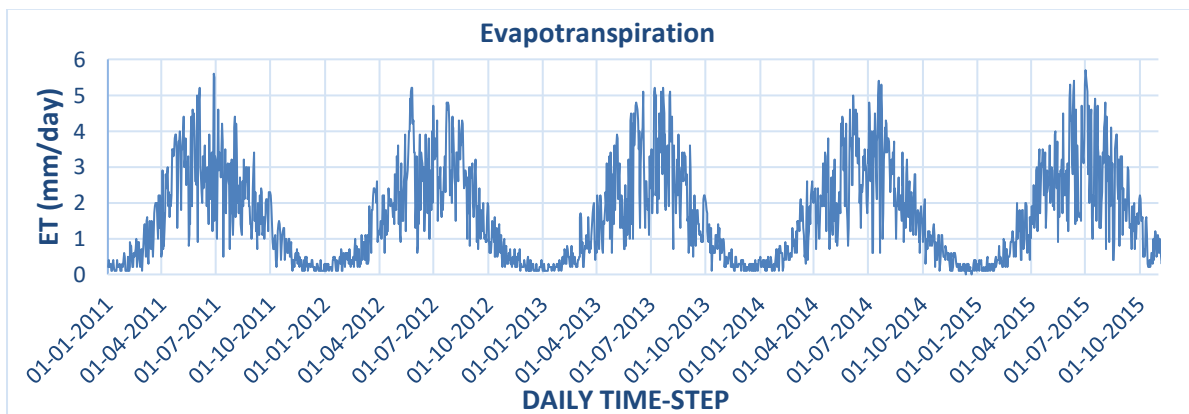


Figure 21: Daily reference evapotranspiration of the study area



#### 4.2. Interception and infiltration rates

One of the main objectives of land cover mapping was to assess the interception, including the leaves falling from deciduous trees during the winter season. The rest of the land cover was pretty much consistent since grass covers a major portion of the study area. The main changes in interception (due to agricultural crops and deciduous trees) have been addressed temporally by making 2 interception maps per year. Since the deciduous trees lose all their leaves in winter, the interception during winter when the precipitation is good, has been assigned as 0. It is assumed that all the precipitation, reaches the ground through stemflow and throughfall. The major differences are the change of agricultural crop from maize/corn to wheat and the dropping of leaves from the deciduous trees in winters.

The interception rates were calculated by subtracting the losses in interception from the precipitation. This was done by importing the interception maps presented below, into Modelmouse, as ASCII raster files and assigning the respective time series formulae in the UZF layer.

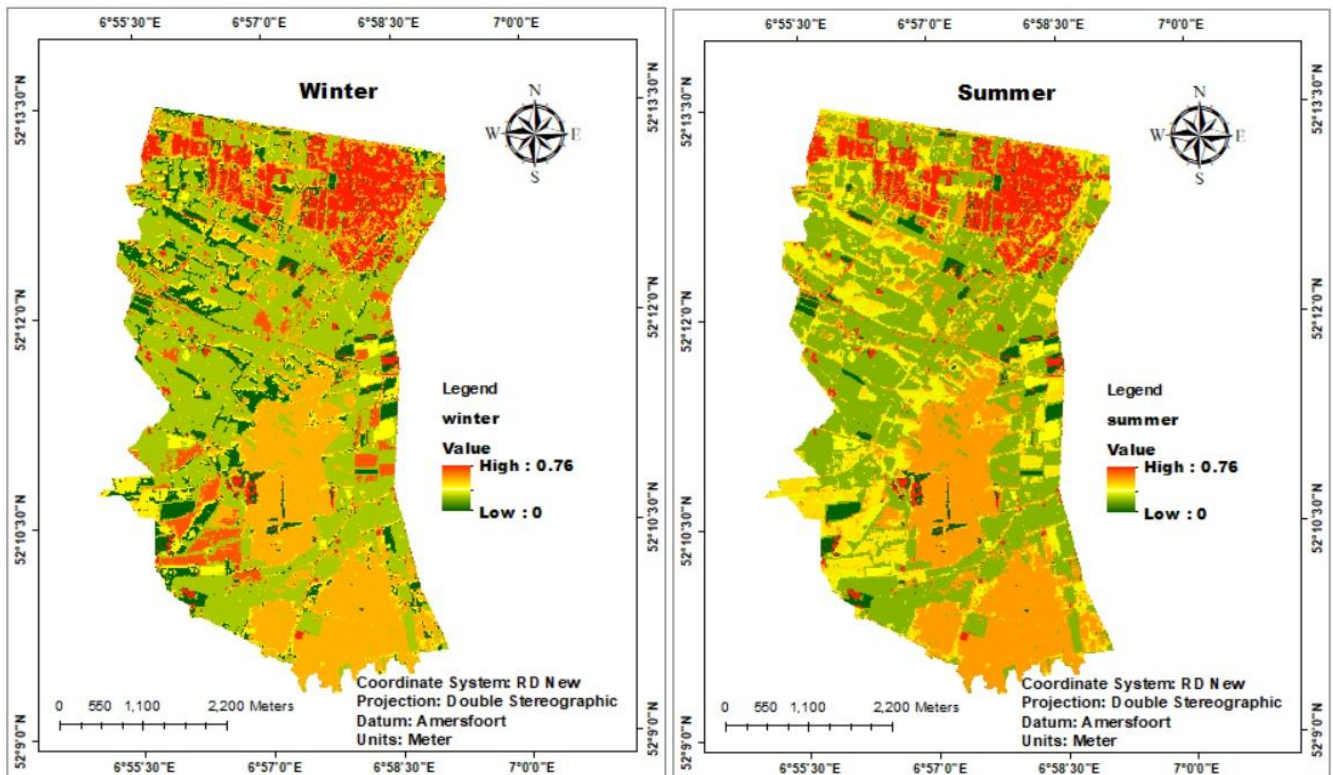
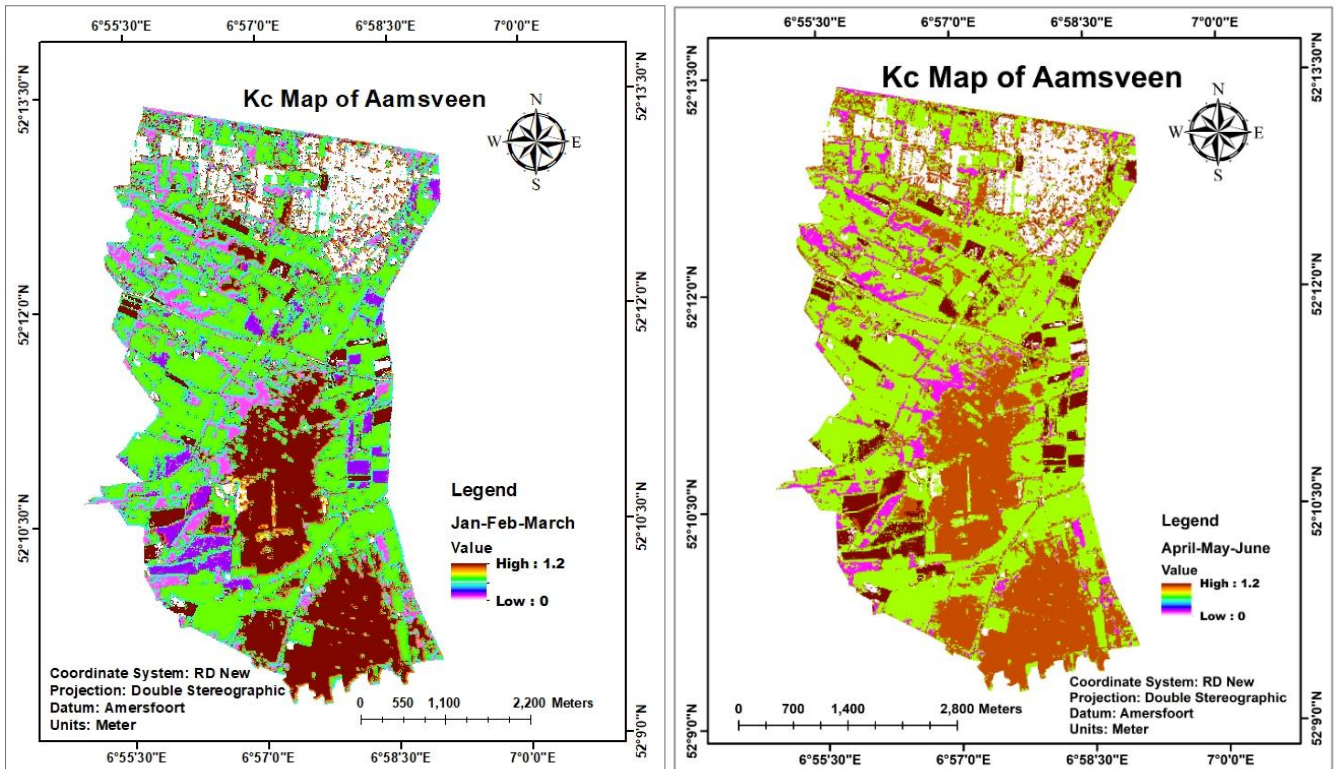


Figure 22: Interception maps for Summer and Winter in Aamsveen

### 4.3. Crop coefficients

The crop coefficient maps were prepared according to the land cover map and their values were taken from Allen et al. (1998). In order to keep the temporal consistency, importance was given to get information from the farmers about the seasonal land cover changes in and around the Aamsveen area. The major differences were again in the changes in the agricultural crop from maize/corn in summer to wheat in winter and the shedding of leaves from the deciduous trees in winter. Hence, 5 crop coefficient maps were created from the classified land cover map of Aamsveen. These maps consist of the Kc values taken from the single crop coefficient values for Kc initial, mid and end stage of the plant. Another more detailed approach would be to use the dual crop coefficient in which the Kc is split into Kcb, which is the basal crop coefficient and Ke which is the surface evaporation. In this study, the single crop coefficient was used, since the dual crop coefficient was beyond the scope of this thesis. A minimum of 5 maps were required to cover the temporal aspect of the crop coefficient per year and these were made by taking into consideration the land cover changes too. Hence, these 5 maps cover the spatial aspect, the temporal aspect, land cover changes and the growth stage aspects of the plants throughout the year.

For the leafless deciduous trees during winter (December to March), a Kc value of 0.19 was assigned, since according to Corbari et al. (2017), this value was measured by him using the eddy covariance method for deciduous trees in winter. The 5 crop coefficient maps that were created are presented below. The maps have been categorized separately for January-February-March, April-May-June, July-August-September, October-November and December. Categorizing of the maps was done according to the land cover type and the growing stages of the plants for every month and then the months with overall the same Kc values were made into a single map, which ensured that the temporal changes per year were covered.



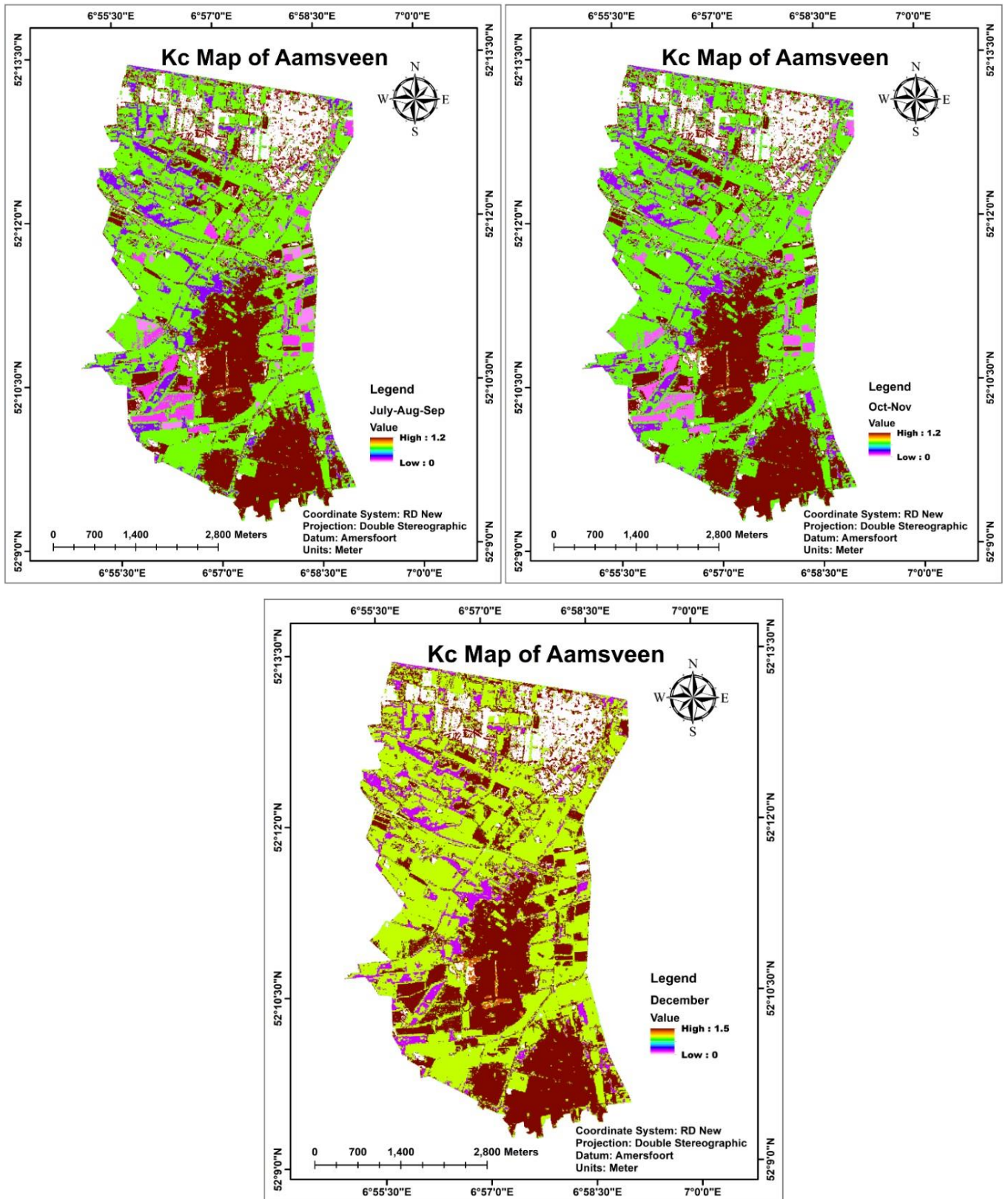


Figure 23: Yearly crop coefficient maps of Aamsveen



#### 4.4. Extinction depth

The UZF package requires the extinction depth of evapotranspiration for which the rooting depth map was used. Hence, a rooting depth map was created from the original classified land cover map of Aamsveen. The root depth values were taken from various literatures. The root depth map prepared for Aamsveen is shown in Figure 24. One map was sufficient since there were no major changes in terms of the root depths of the land cover in the different seasons.

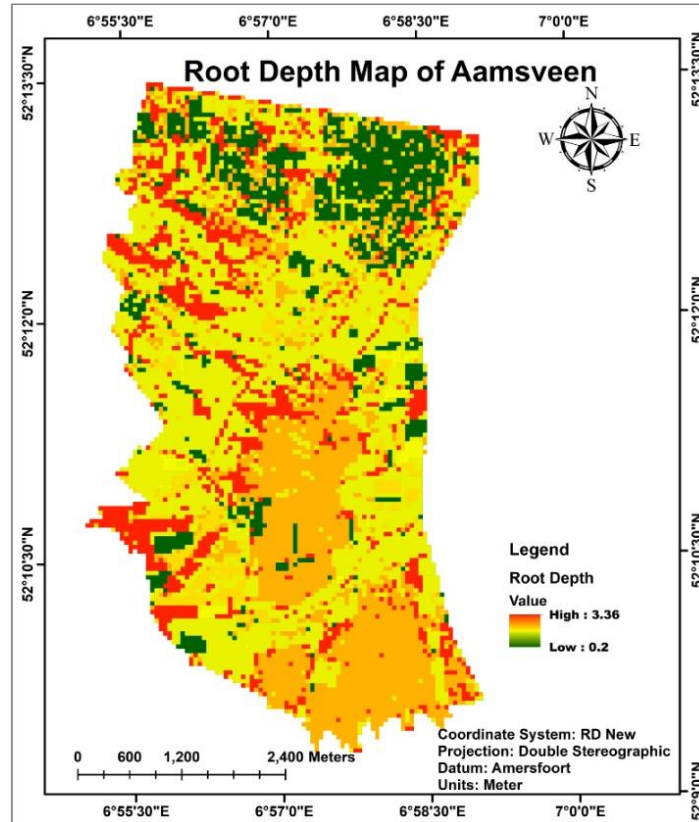


Figure 24: Extinction depth map of Aamsveen

#### 4.5. Hydraulic conductivity

The hydraulic conductivity zones were assigned based on values that were obtained from the laboratory particle size analysis. The layout of the hydraulic conductivity zones were altered during the calibration and also their values were changed. The study area consists of peat and fine sand and since it was not easy to assign the value of hydraulic conductivity for peat due to the fact that it was not feasible to find the hydraulic conductivity of the peat from laboratory work, certain relevant literatures were referred in-order to assign the hydraulic conductivity for peat. It was noticed that due to differences in the formation of peat, the hydraulic conductivities can have various values. The hydraulic conductivity of peatlands has been specified in the range of  $1 \times 10^{-8}$  [ $\text{m day}^{-1}$ ] to  $1.6 \times 10^{-2}$  [ $\text{m day}^{-1}$ ] by Lewis et al. (2012). The hydraulic conductivities in the present study ranged from 0.08 [ $\text{m day}^{-1}$ ] to 11 [ $\text{m day}^{-1}$ ]. The assigned hydraulic conductivities for both layers are represented in the Figure 25.

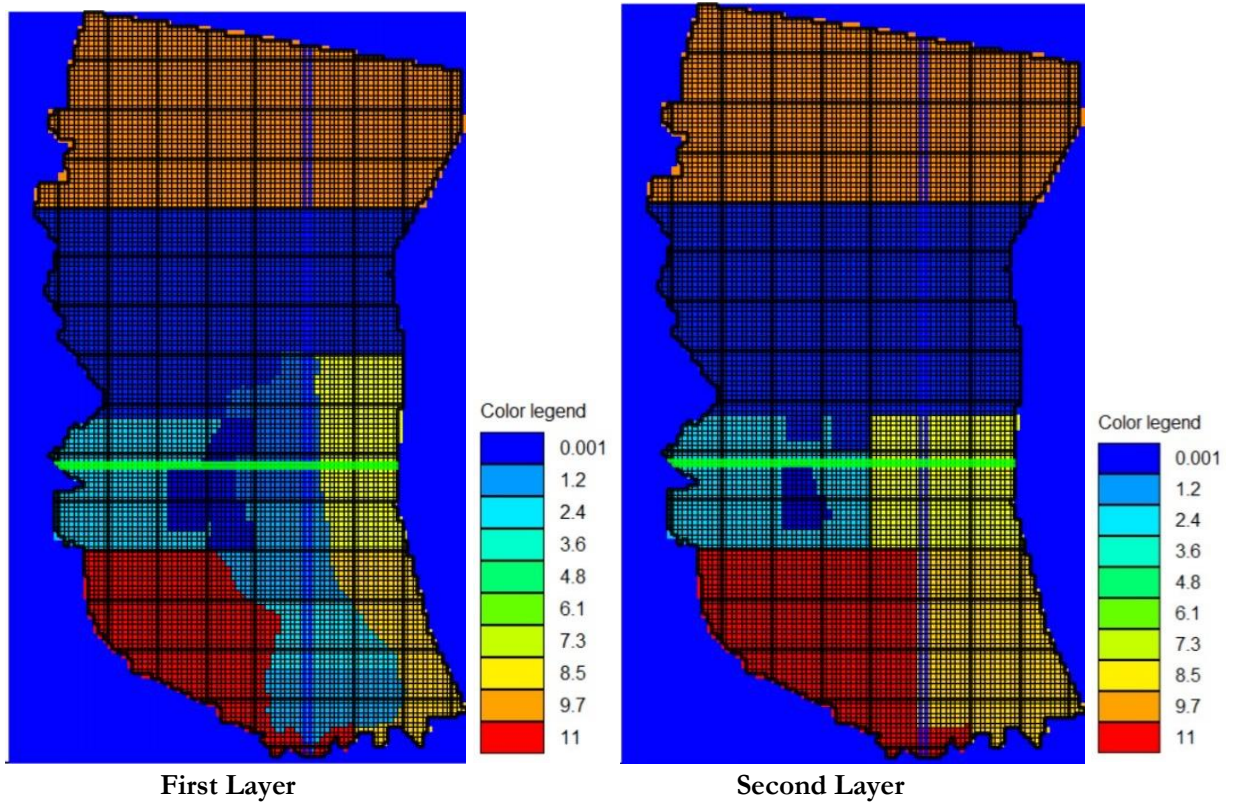


Figure 25: Hydraulic conductivities [m day<sup>-1</sup>] of the first layer and second layers.

#### 4.5.1. Calibrated stream flows

The study area had 2 stream gauges which measure the discharge every hour. However, the gauge present at Melodiestraat was not used for calibration due to unexplained rise and fall in its discharge values. The magnitude of highs and lows in the discharge were very high compared to the changes in the measured rainfall at Melodiestraat.

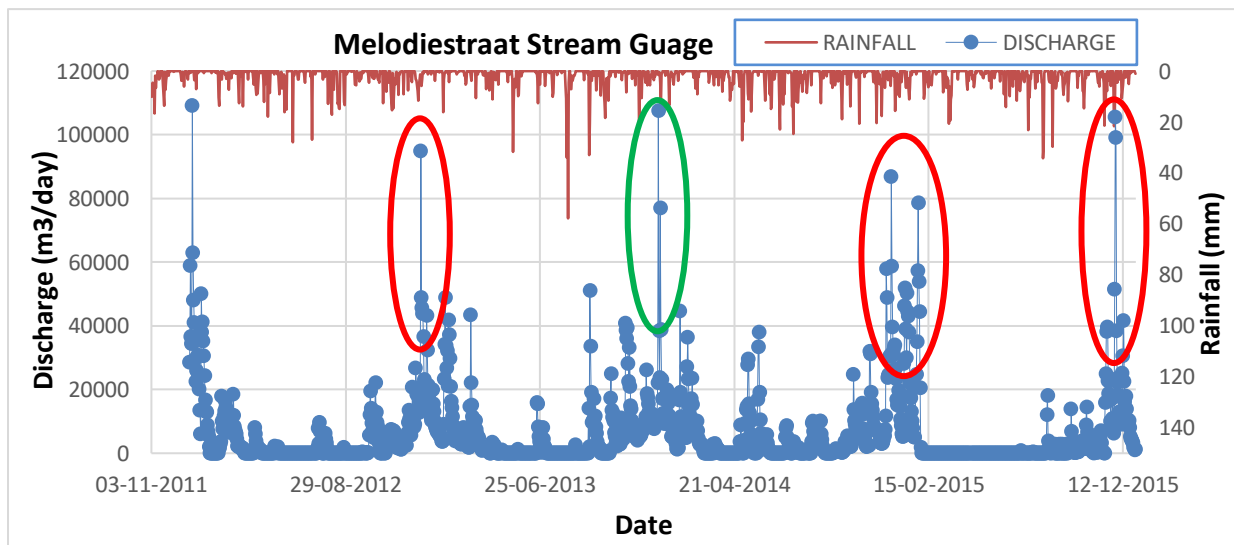


Figure 26: Discharge at Melodiestraat stream gauge

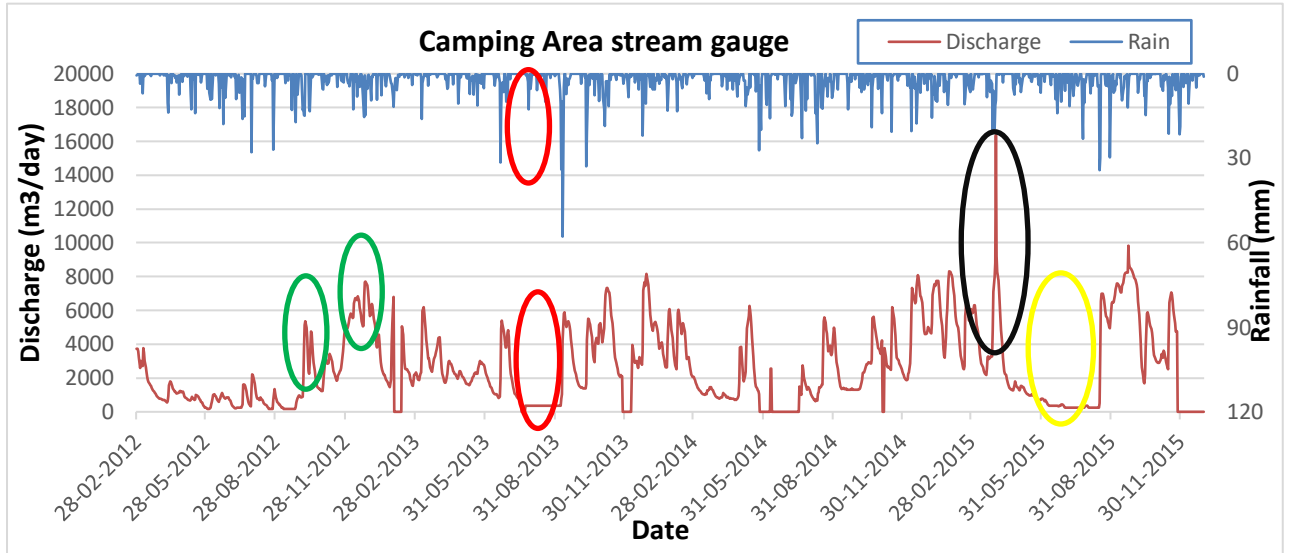


Figure 27: Discharge at Aamsveen stream gauge

The stream gauge at Melodiestraat was not used for calibration due to the fact that measured values of the discharge seemed to have high fluctuations which were not accounted for, during the study. The red and green ellipses in Figure 26, show very high value of discharges that have been measured when compared to the corresponding rainfall. Such high differences in discharge cannot be explained alone by the rainfall events hence, more accurate reasons are required for these high changes in the magnitudes of the discharge during a comparatively lower rainfall. It is also possible that these high discharges may arise when there was a consistent wet period of rainfall before, which is noticed in the rainfall events just before the high discharge which is indicated by the green ellipse in Figure 26. Yet, the magnitude of the discharge seemed to be much higher than what these reasonings can explain. It is also possible that the settlements in Glanerbrug, where this gauge is located may have had an influence in the measurement of the discharge. Hence, until reasonable causes are provided for these peculiar changes, calibration of the stream using these discharge values is not feasible. Hence, this gauge was discarded due to the unaccountability of the measured values.

The stream gauge at Aamsveen's Camping area had more reliable measured values of the discharge when compared to the rainfall. There were few delays that were noticed in the hydrograph. After consultation with the water board (Vechtstromen), it was concluded that these delays in the peaks of the hydrograph maybe be due to differences in the saturation capacity of the study area. Since a big part of the study area consists of a wetland, there is saturation in the place and usually the water level is very high. This fluctuates in different seasons with respect to the precipitation and evapotranspiration. Hence, these delays in the peaks can be accounted by the fact that when the wetland is saturated, the discharge is high whenever there is precipitation. During summers, when the evapotranspiration is high, the saturation of the wetland is not attained and water level is lower (buffer capacity is high) and the water first saturates the area during rains and when the area is saturated, runoff is measured higher and hence the hydrograph shows delays in the peaks. This can be accepted as a fair explanation of the delays that have been noticed in the hydrograph in comparison to the rains. Yet there are other unaccounted anomalies in the readings.

The green ellipses in Figure 27 show a delay in the peak of hydrograph of Aamsveen’s camping area’s stream gauge, which may have been due to the reasons that have been explained above. However, the red ellipses indicate that though there have been rainfall events, the discharge continues to remain constant which is very peculiar. This can only happen if an equilibrium has been attained, which means that either the quantity of the incoming recharge did not make any changes in the groundwater fluxes or it was lost through other groundwater fluxes apart from the runoff or baseflow. For this to happen, the quantity of the water leaving the system has to be in the same quantity as the incoming recharge without having any effect in the system. Before the discharge indicated by the black ellipse in Figure 27, there has been a continuous wet period in which higher discharges have been observed. Yet, the discharge shown by the black ellipse is very high when compared to the corresponding rainfall. Even though it is acceptable to say that there was a time of wet period before this discharge occurred and a higher measured value can be expected due to low buffer capacity, yet the magnitude of this high discharge value still remains peculiar and this reason cannot completely explain this high value.

The yellow ellipse shows a continuous decrease in the discharge that was measured during that period. However, there has been significant rainfall events which should create a higher discharge. It seems that the discharge was not at all sensitive to the rainfall which may be due to a higher buffer capacity (low saturation of the wetland) due to extremely high evapotranspiration. Yet, right after the yellow ellipse, a sudden high discharge has been measured. It may be due to the fact that the land was saturated from the rainfall events that happened before, which is an acceptable explanation yet, on carefully investigating the magnitudes of rainfall, that happened before the high discharge was measured, it was found that there weren’t very big differences in the magnitude of the rains. There was a higher rainfall observed during the high discharge yet, the magnitude of the change of discharge seemed to be much higher than what can be explained by these causes alone. So, unless and until, the management decided to cut down numerous trees on a single day, causing a sudden decrease in the evapotranspiration and subsequently increasing the saturation which increases runoff, this explanation is not adequate to provide the cause of this phenomenon.

When all the fluxes are quantified, the dynamics of the system can be explained properly. Human interventions may also have played a role in these unaccounted fluctuations of the discharge since Aamsveen has been subjected to many water management scenarios. The possible causes of human interventions are explained later in this chapter.

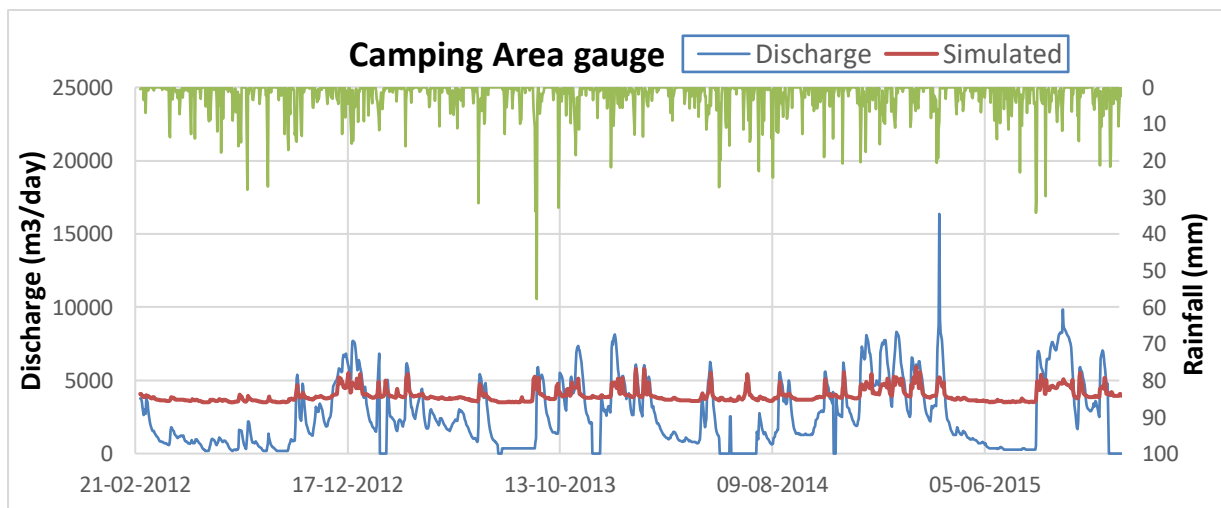


Figure 28: Observed vs simulated stream flow at Aamsveen’s camping area

As seen from the hydrograph in figure 28, the simulated flow has smaller peaks and higher baseflow and hence, it performs poorly in the magnitudes of the flows. However, on careful observation of the dynamics of the curve, it can be clearly seen that the simulated stream flow is following the changes in the observed stream flows. This shows that the model is sensitive to the changes in stress and is able to detect the dynamics of the flow of the stream. It performs poorly only when it comes to the magnitude of the flow of the stream when measured against the observed discharge. Whenever there is a rise in the peak of the observed discharge, there is also a rise in the simulated discharge. Therefore, it can be concluded that the simulated discharge from the model performs poorly in the magnitude of the flows but performs well in the temporal changes, since the observed and the simulated flows are coincidental. Few reasons for the non-performance of the simulated flow are discussed in sections 4.5.1.1. and 4.5.1.2.

#### **4.5.1.1. Use of LAK package for better simulation of the lake.**

The study area is drained by Glanerbeek which has a number of tributaries. However, a part of the flow in the Glanerbeek is from a lake located behind the camping ground near the wetland of the study area. This is also the place where the Aamsveen camping ground stream gauge is located. The gauge is actually located downstream from the lake. This means that the stream actually drains a large amount of water from the lake. This lake is fed by rains, possibly high groundwater and also from an incoming stream which drains its water into this lake. The package used in this model is the reservoir package which only simulates the interaction of the groundwater with the reservoir or surface water body. The reservoir package is not connected to the Stream Routing Package (SFR) according to Council (1997) which is necessary in this case since the lake is connected to the streams. Hence, the model is not able to simulate the magnitude of the flow which is contributed by the lake, Figure 28 shows lower simulated values when compared to the rises in discharge which is shown by the peaks.

In order to simulate the contribution of the lake to the stream, the LAK package of MODFLOW would provide a better hydrograph since it has been designed to simulate the lake-groundwater interaction and also the lake-stream interaction. As it was already discussed that the simulated hydrograph in Figure 28, performs well in the dynamics of the changes in the discharge in time but not the magnitude and this can be overcome by using the LAK package. However, using LAK package requires more time and more parameter input details for simulation of the interaction of the lake with the groundwater and stream flows which were not available. Hence, due to time constraints and the insufficiency of the data, LAK package was not used but it can be further recommended for the better performance of the model. The following Figure 29 shows the location of the stream gauge downstream from the lake.





Figure 29: Location of the Aamsven Camping area stream gauge downstream from the lake

#### 4.5.1.2. Possible human interventions for management of the wetland.

It is highly possible that numerous surface water management measures have interfered with the discharge at Aamsveen area. Though the simulation covered the period between 31<sup>st</sup> January 2011 to 31<sup>st</sup> December 2015, there are possibilities of the local changes in the wetland, done for its management. A similar intervention was also witnessed in which the discharge point of the lake into the stream had been blocked by a small bund and the excess water that was being stored was discharged into the stream using a pump. Hence, the natural flow of the water from the lake into the stream was hampered and this results in a sudden drop in the discharge measurement of the gauge even during a heavy rainfall. Removal of the bund that blocked the flow could also cause a large amount of water to suddenly rush into the stream thereby giving a higher measured discharge even though the rainfall was measured lower. The following Figure 30 shows the water management being carried out through the construction of a bund to block the flow of water and pumping of water into the stream using a pump. In Figure 30, the yellow circle shows the pipe through which the water is being pumped into the beginning of the stream by a pump shown by the red ellipse. The yellow arrow also shows that the natural flow of water has been blocked by a bund from where the water from the lake discharges into the stream. These human interventions can have a big influence in the measurement of the high and low discharge of the stream since the stream gage is located very close as seen in Figure 29.



Figure 30: Water Management in progress at Aamsveen's Camping area

Since the frequency of these human interventions is not known in this study and also the changes in the discharge due to these interventions is unknown, the best solution for this problem of the simulated flows can be solved by conducting analyses on these interventions and simulating them with the LAK (lake) package of MODFLOW in this model. Also, since the simulated flow was not fully reliable, equations 14 and 15, for NS and RVE, could not be used to assess the observed and simulated flow. It is evident from Figure 28, that the simulated heads are much lesser in magnitude and in this case only the sensitivities of the simulated flow can be studied by visual interpretation.

#### 4.5.2. Calibrated groundwater heads

The measured groundwater heads were not available for the entire simulation period from 1<sup>st</sup> January 2012 until 31<sup>st</sup> December 2015. There are data missing in boreholes B35A0836 (borehole A), B35A0837 (borehole B) and B35A0835 (borehole D) between 2<sup>nd</sup> November 2013 until 27<sup>th</sup> August 2014. The measurements in these boreholes started from 1<sup>st</sup> of June 2012. The other borehole (borehole C) had comparatively lesser measurements which only started from 10<sup>th</sup> December 2014 and continued for the rest of the simulation period. Only these 4 boreholes were active during the simulation period and these were mainly concentrated in the wetland. As discussed earlier, the model was not able to simulate the discharge from the lake to the stream and hence, the actual measured values of the stream gauge were “forced” into the upstream end of the stream into the model, where this gauge was located. This was done in order to attain a better simulation and hence a better model performance. On “forcing” these measured values, it was noticed that the groundwater heads gave better dynamics of the simulated heads when they were compared to the observed heads. It is important to note at this point that this method of “forcing” the measured flow into the stream is not an appropriate method, but this was only done because the reservoir package used in this model did not simulate the interaction of lake and stream, hence “forcing” these measured flow into that particular stream segment would provide the necessary flow that is required for a better simulation.

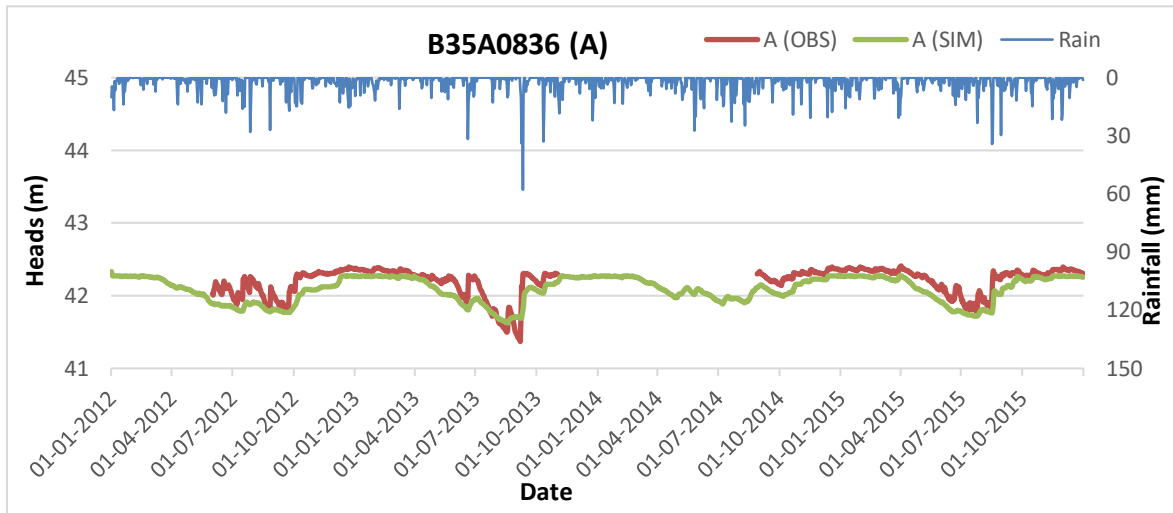


Figure 31: Observed vs simulated heads for B35A0836 (A)

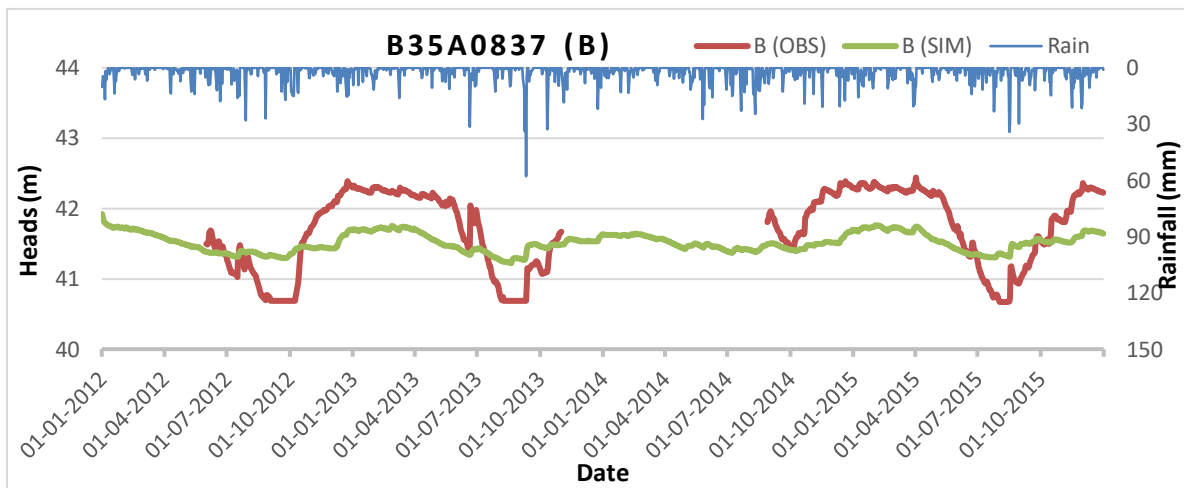


Figure 32: Observed vs simulated heads for B35A0837(B)

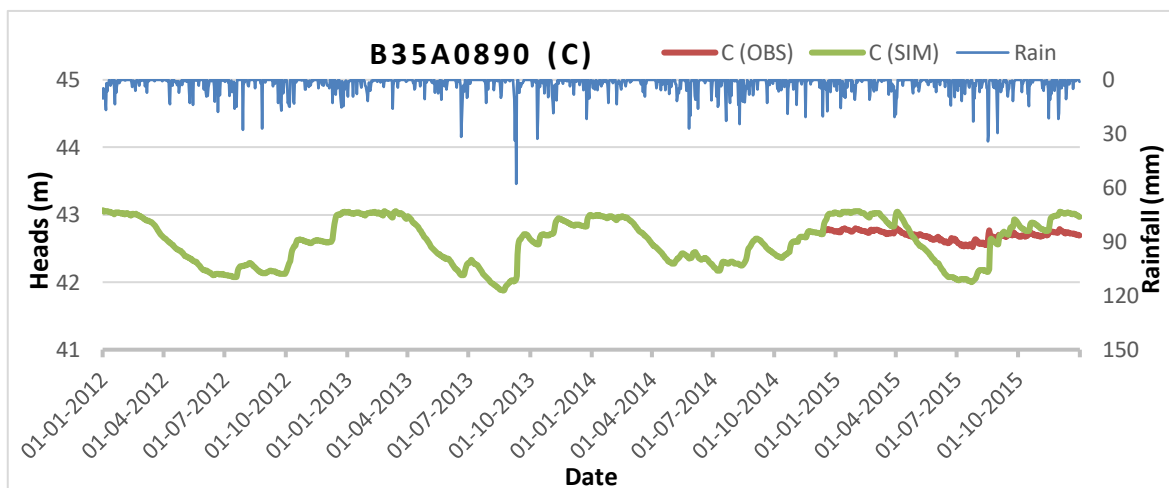


Figure 33: Observed vs simulated heads for B35A0890 (C)

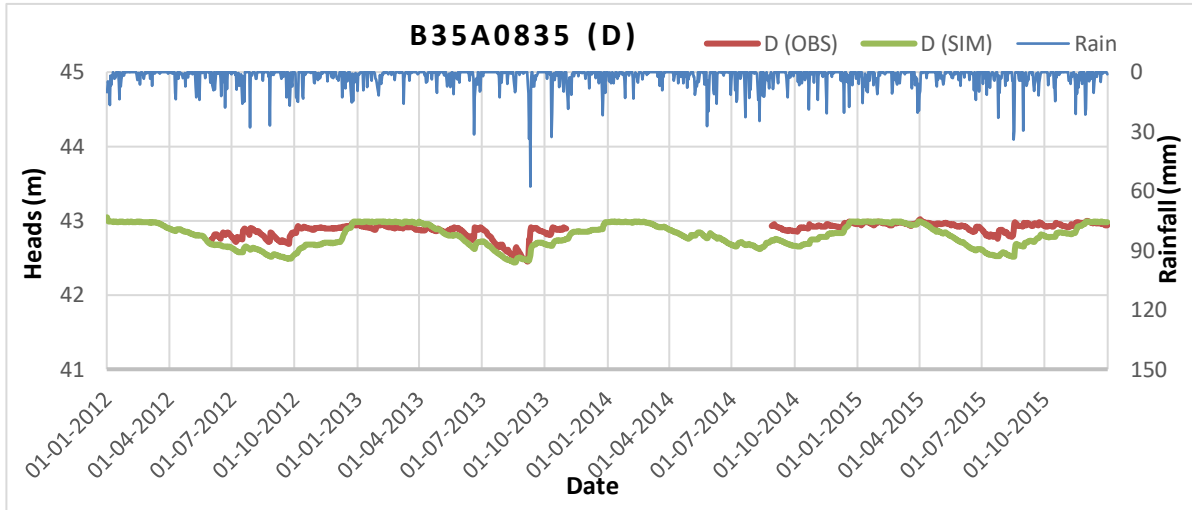


Figure 34: Observed vs simulated heads for B35A0835 (D)

Table 11: Error Analysis of Heads after Transient Calibration

Bore Hole	ME	MAE	RMSE
B35A0836 (A)	0.13	0.14	0.16
B35A0837 (B)	0.20	0.44	0.49
B35A0890 (C)	-0.01	0.25	0.29
B35A0835 (D)	0.11	0.25	0.29

Some discrepancies arise due to uncertainties like errors in the conceptualization of the study area, due to erroneous parameterization and uncertainties in the observations of the groundwater heads. Another type of error that can arise is due to the scale of the grids. Depending on the grid size, every single grid takes up a particular value of the elevation, and hence the altitude of the borehole in the field may actually not match the altitude of the simulated borehole in the model and this can be another cause of errors. A model which can produce a good match in terms of the dynamics of the groundwater heads and is able to reproduce the observed values of groundwater heads in its simulation, is a good model and it is able to provide better knowledge of the changes in fluxes.

The boreholes overall had a good match visually and were assessed to be sensitive to the changes in the flux. This shows that the calibrated heads responded very well to the groundwater conditions of Aamsveen.

### 4.5.3. Calibrated parameters

The final values of the calibrated parameters are shown in the Table 12.

Table 12: Final Calibrated Transient state model parameters: EXTDP-extinction depth; EXTWC-extinction water content; THTS- saturated volumetric water content; KVuz- unsaturated vertical hydraulic conductivity; STRHC1- stream bed vertical hydraulic conductivity; STRTOP- stream bed top; STRTHICK- stream bed thickness; Sy- specific yield; Ss- specific storage; Rbthck- reservoir bed thickness; Kx-horizontal hydraulic conductivity. C indicates all those parameters that have been adjusted during calibration. N indicates all the parameters that were not adjusted but were assumed to be true.

Vertical Zone	Parameter	Minimum Value	Maximum Value	Unit	Status
<b>Unsaturated Zone</b>	EXTDP	0.2	3.36	[m]	N
	EXTWC	0.1	0.1	[m <sup>3</sup> m <sup>-3</sup> ]	C
	THTS	0.45	0.45	[m <sup>3</sup> m <sup>-3</sup> ]	C
	KVuz	1	1	[m day <sup>-1</sup> ]	C
<b>Streams</b>	Width	0.8	6	[m]	C
	STRHC1	K <sub>x</sub> * 0.4	K <sub>x</sub> * 0.5	[m day <sup>-1</sup> ]	C
	STRTOP	1	2	[m]	C
	STRTHICK	0.011	0.1	[m]	C
	SLOPE	0.01	0.2	-----	C
	Roughness Coefficient	0.035	0.035	-----	N
<b>Saturated zone</b>	K (layer 1)	0.08	11	[m day <sup>-1</sup> ]	C
	K (Layer 2)	0.08	11	[m day <sup>-1</sup> ]	C
	Sy (Layer 1)	0.18	0.45		C
	Sy (layer 2)	0.36	0.4		C
	Ss (layer 2)	0.0001	0.0001		N
<b>Reservoir</b>	Rbthck	0.2	0.2		C
	K (reservoir)	0.8	0.8	[m day <sup>-1</sup> ]	C



#### 4.6. Sensitivity analysis on groundwater heads

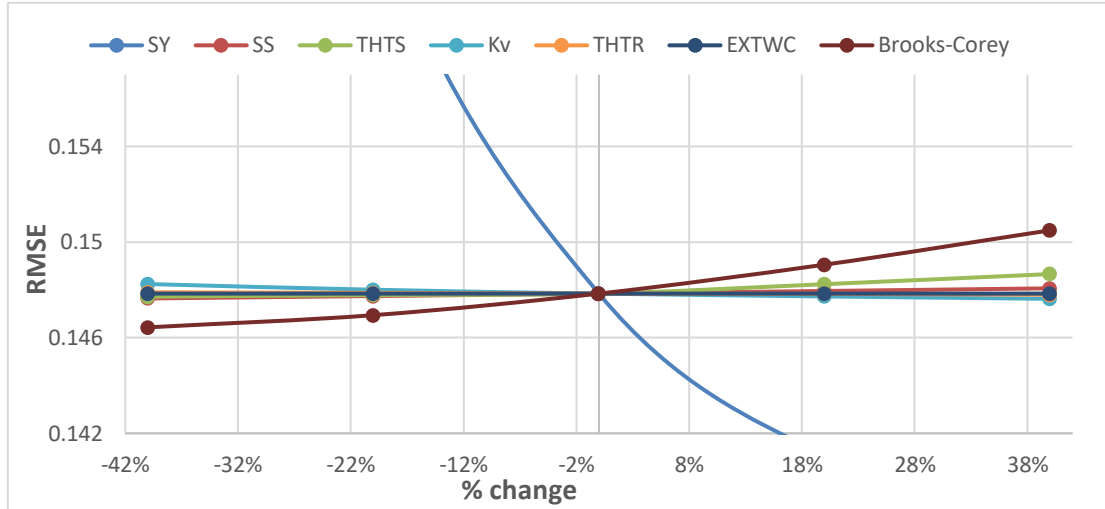


Figure 35: Sensitivity analysis of the groundwater heads

The sensitivity analysis was done for groundwater heads by changing few parameters that can be seen in Figure 35. The specific yield was the most sensitive to the groundwater heads as seen in Figure 35. This parameter was very essential during the calibration of the groundwater heads and the dynamics of the simulated curve were very sensitive to it. The other most sensitive parameter was the Brooks -Corey exponent. This is expected because in the UZF package, Brooks-Corey exponent is used for the calculation of the unsaturated hydraulic conductivity. The other parameters comparatively were not as sensitive as specific yield or Brooks-Corey exponent. Among the other remaining parameters, the saturated volumetric water content (THTS) was a bit more sensitive than Specific Storage (SS), Maximum Vertical hydraulic conductivity (Kv), Residual water content (THTR) and the extinction water content (EXTWC).

#### 4.7. Sensitivity analyses of the groundwater fluxes

The sensitivity analyses of the groundwater fluxes were done on the gross recharge ( $R_g$ ), groundwater evapotranspiration ( $ET_g$ ), groundwater exfiltration ( $Ex_f$ ) and the net recharge ( $R_n$ ). The parameters that were used to test the sensitivities of these water components were the horizontal hydraulic conductivity ( $K_h$ ), specific yield ( $S_y$ ), the extinction depth (EXTDP) and maximum unsaturated vertical hydraulic conductivity ( $K_v$ ).

As seen from the Figure 36, lower extinction depth gave higher gross recharge mainly in winter months since the evapotranspiration is lower especially because the deciduous trees shed their leaves in winter. Lower extinction depth decreased the evapotranspiration since the extinction depth defines the depth at which evapotranspiration ceases to extract water from the soil. Groundwater evapotranspiration was relatively more sensitive to the extinction depth as compared to the gross recharge. Also, groundwater exfiltration showed higher sensitivity to decrease in the extinction depth since  $ET_g$  decreases. Net recharge ( $R_n$ ) increased with a decrease in extinction depth since groundwater ET decreases with the decrease in the extinction depth.

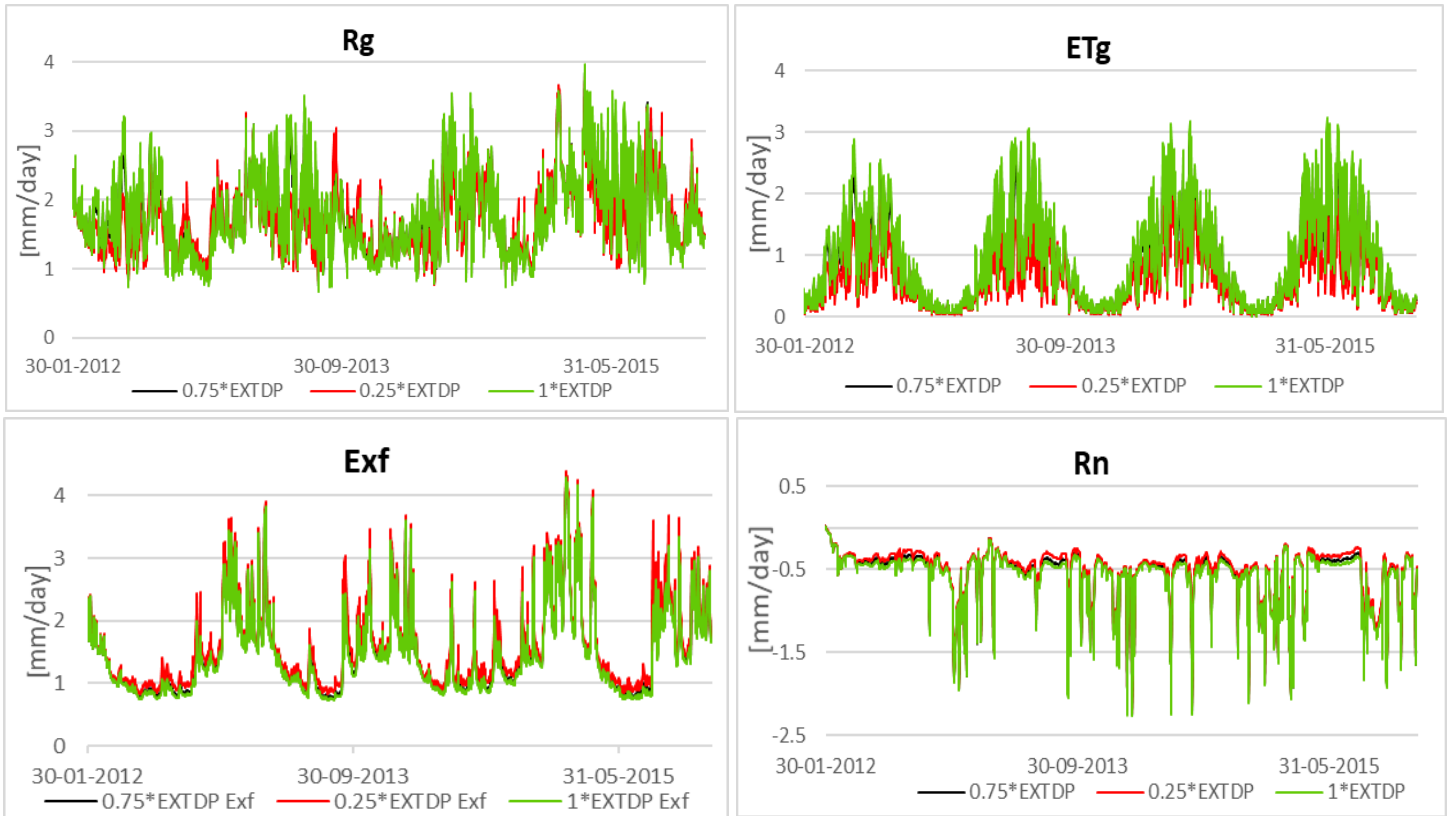


Figure 36: Sensitivity analysis of Extinction depth on groundwater fluxes

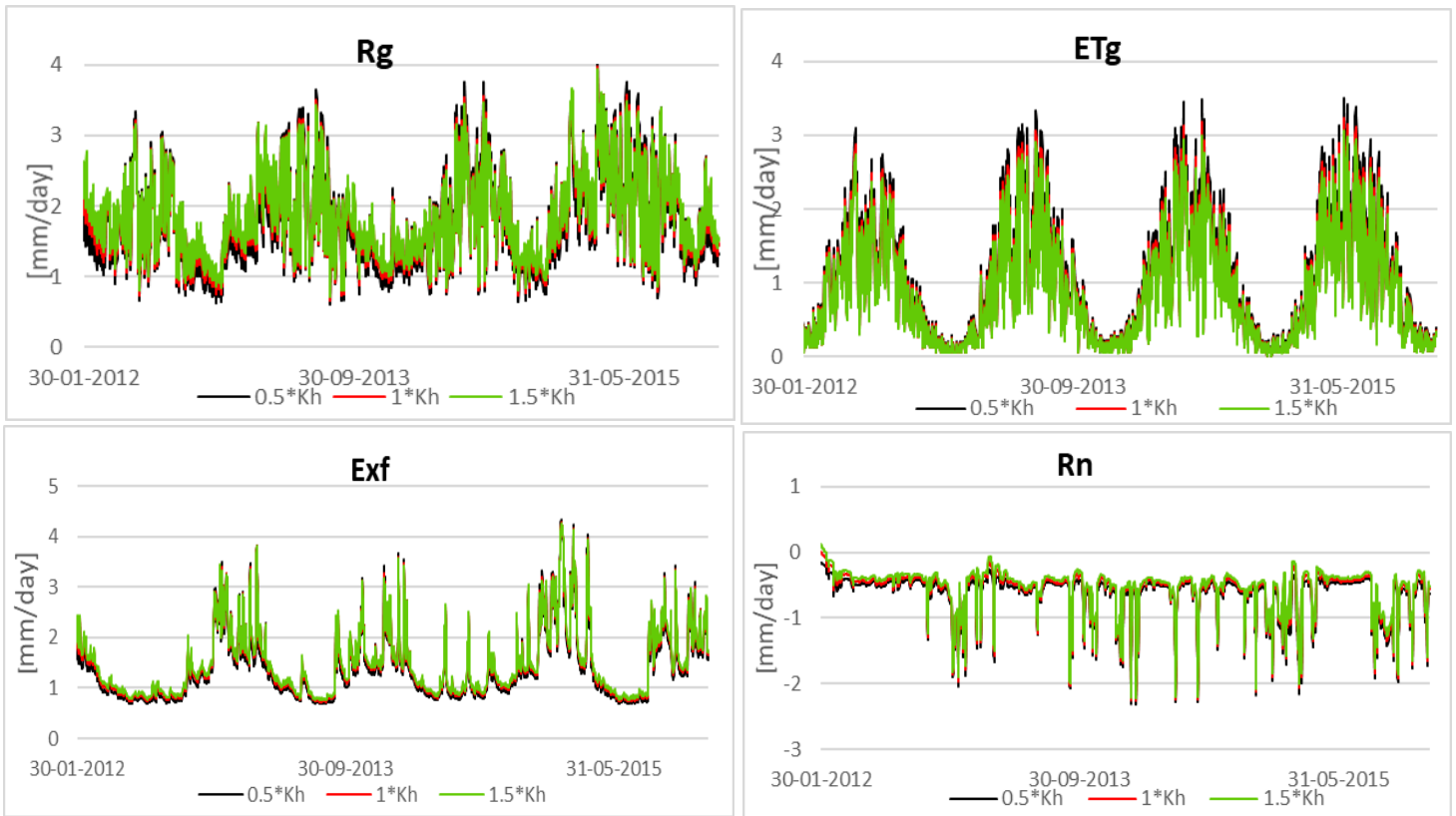


Figure 37: Sensitivity analysis of Hydraulic conductivity on groundwater fluxes

Figure 37 shows evapotranspiration to be higher with decrease in the hydraulic conductivity especially in summer when temperatures are high, and the ET demand is high. Small conductivity and large storage lead to an increase in the ETg. An increase in the groundwater exfiltration and gross recharge was also seen with a decrease in the hydraulic conductivity. Lower gross recharge was seen during the winter months. Exfiltration was seen to be higher during the winter months and lower during the summer months, which could be due to the fluctuations in evapotranspiration. The net recharge was consistently lower with lower hydraulic conductivity which may possibly be due to higher exfiltration.

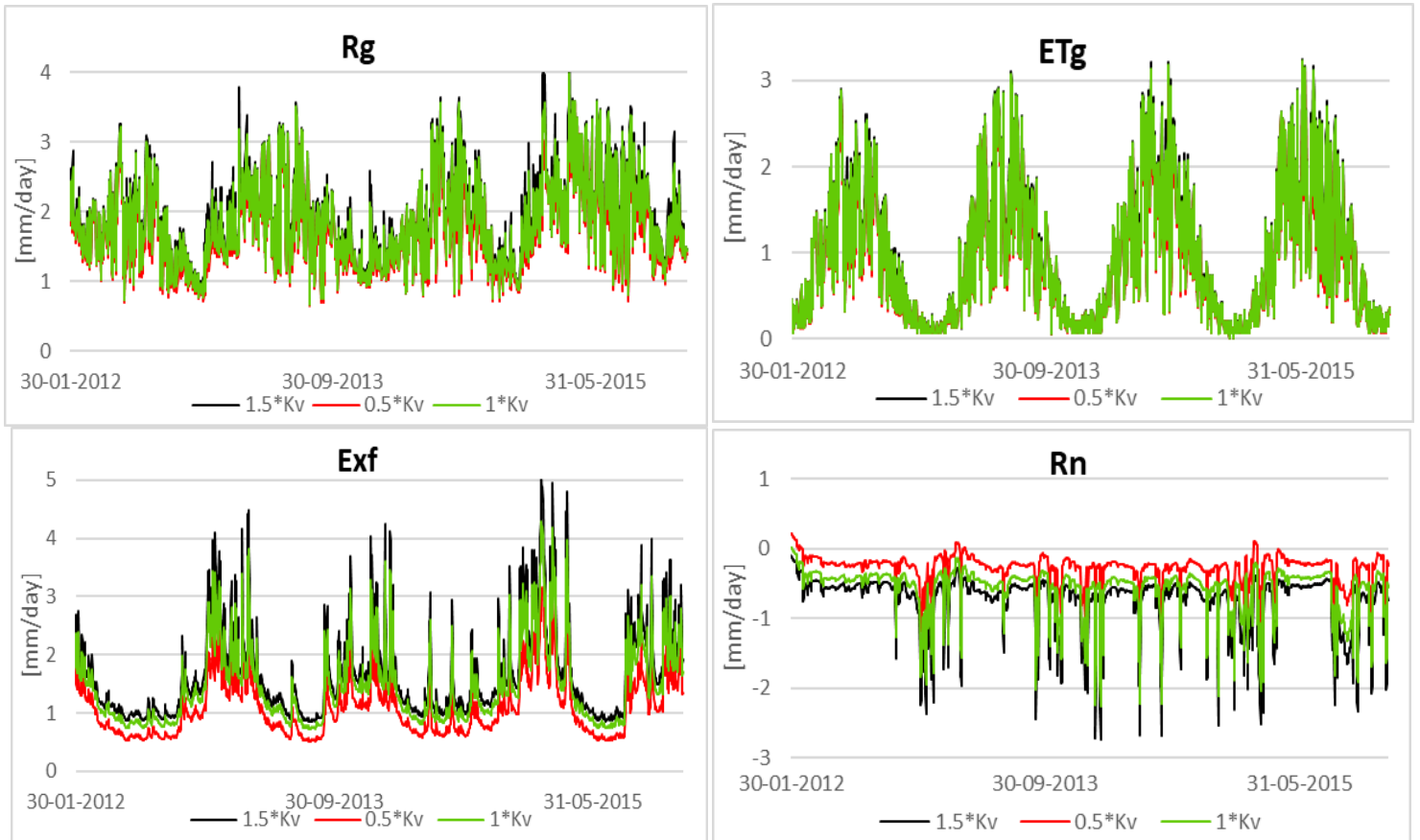


Figure 38: Sensitivity analysis of Maximum Unsaturated Vertical Conductivity on groundwater fluxes

Figure 38 shows the sensitivity analysis of the water balance components with the maximum unsaturated hydraulic conductivity ( $K_v$ ). Evapotranspiration showed minimal response to changes in  $K_v$  which may be due to the fact that it has more impact on the infiltration and exfiltration. As seen in Figure 38, exfiltration clearly increases with the increase in  $K_v$  and vice-versa. During calibration, the  $K_v$  was found to be an important parameter which influenced the exfiltration and reservoir leakage. The net recharge was higher with lower  $K_v$  since lower  $K_v$  limits exfiltration thus giving higher net recharge. Higher  $K_v$  is seen to lower the net recharge. Net recharge seemed to be quite sensitive to  $K_v$ . Gross recharge ( $R_g$ ) was seen to be higher with higher  $K_v$  during winter months only which maybe be due to higher exfiltration in the winter.



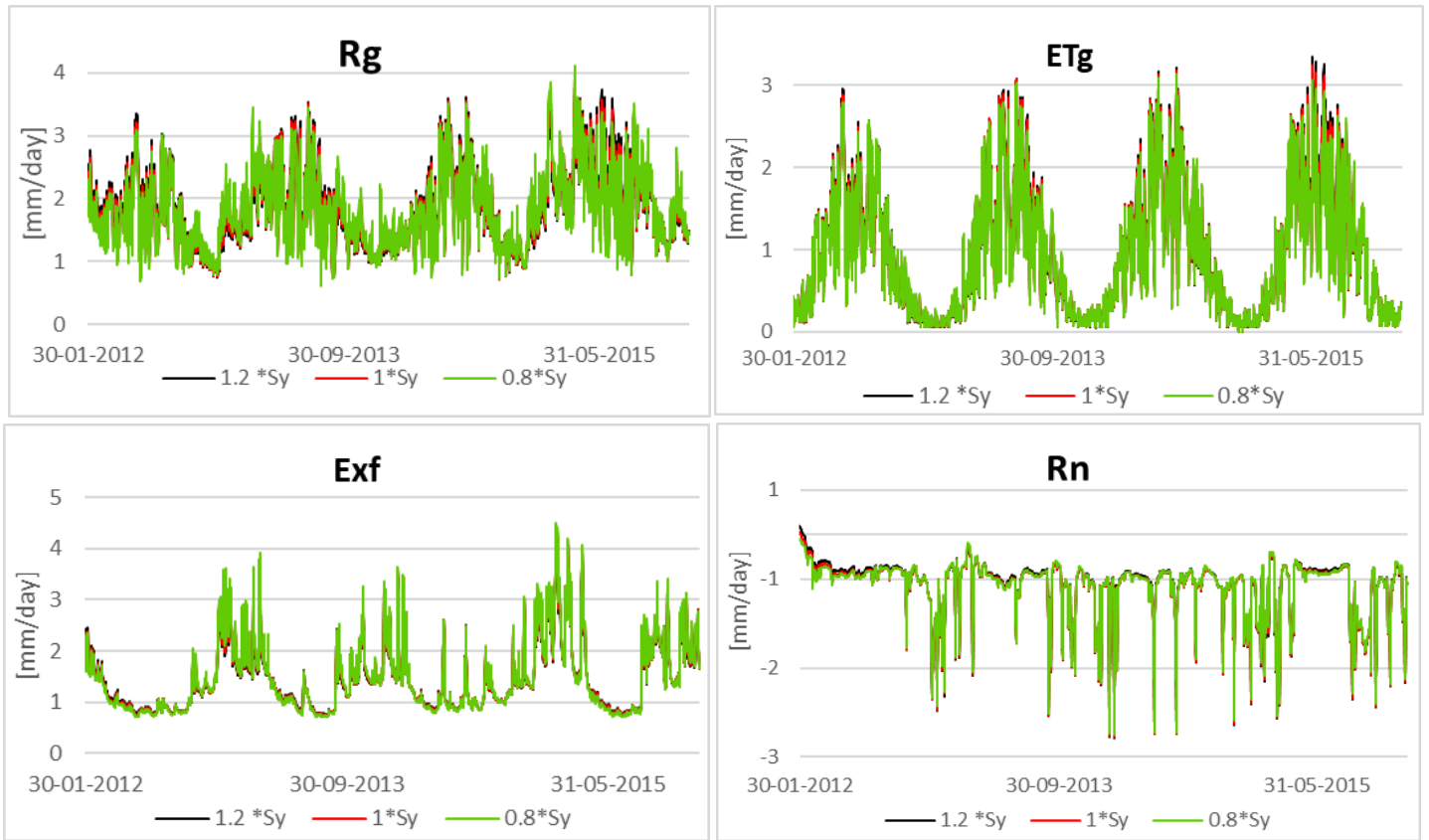


Figure 39: Sensitivity analysis of specific yield on groundwater fluxes

Figure 39 shows the sensitivity of the water fluxes to the specific yield. Evapotranspiration is seen to increase with an increase in specific yield (Sy) only during the summer months while the effect seems to be very less during the winter months. With higher Specific yield, gross recharge (Rg) was seen to be higher during the summer season and was lower during the winter season. Exfiltration is seen to decrease with a decrease in the specific yield though the changes do not seem to be very significant. Slightly higher values are seen during the winter months with a decrease in specific yield. Net recharge did not seem to vary much with changes in the specific yield though slightly lower values were seen with higher specific yield in the winter months but there are no significant changes seen.

#### 4.8. Volumetric Water budget

Table 13: Unsaturated zone package volumetric budget (2012 – 2015)

	IN [m <sup>3</sup> ]	OUT [m <sup>3</sup> ]
<b>INFILTRATION</b>	<b>64379496.3420</b>	<b>0</b>
<b>UZF ET</b>	<b>0</b>	<b>2224450.0417</b>
<b>UZF RECHARGE</b>	<b>0</b>	<b>64157975.5138</b>
<b>STORAGE CHANGE</b>	<b>-1939006.1877</b>	
<b>PERCENT DISCREPANCY</b>	<b>-0.02</b>	

Table 14: Volumetric budget of the entire model for the entire simulation.

	IN [m <sup>3</sup> ]	OUT [m <sup>3</sup> ]
<b>STORAGE</b>	<b>30562568</b>	<b>31832974</b>
<i>CONSTANT HEAD</i>	<i>0</i>	<i>0</i>
<b>DRAINS</b>	<b>0</b>	<b>17829</b>
<b>SPECIFIED FLOWS</b>	<b>7.0124</b>	<b>0</b>
<b>RESERV. LEAKAGE</b>	<b>30957842</b>	<b>263480.96</b>
<b>STREAM LEAKAGE</b>	<b>5152365</b>	<b>17191930</b>
<b>UZF RECHARGE</b>	<b>64157944</b>	<b>0</b>
<b>GW ET</b>	<b>0</b>	<b>31608978</b>
<b>SURFACE LEAKAGE</b>	<b>0</b>	<b>49891964</b>
<b>TOTAL IN</b>	<b>130830720</b>	<b>130807152</b>
<b>IN - OUT</b>		<b>23568.0000</b>
<b>PERCENT DISCREPANCY</b>	<b>0.02</b>	

Tables 13 and 14 show the volumetric water budget of the unsaturated zone and volumetric budget for the entire domain respectively for the entire simulation period of 4 years.

#### 4.9. Water balance

The water balance of the study area is given in Table 15. Since the simulation period was for 4 years from 1<sup>st</sup> January 2012 to 31<sup>st</sup> January 2015, the yearly water budget of the distribution of the fluxes is described along with the water budget of the entire simulation period.

#### 4.10. Yearly variations in the water balance components

Table 15 shows the relationship between P (Precipitation), I (infiltration), Pe (Effective precipitation), ET (potential evapotranspiration),  $Q_{H+D}$  (Hortonian and Durnian runoff),  $Q_s$  (outflow through streams),  $Q_D$  (flow through drains),  $Q_{st}$  (in) and  $Q_{st}$  (out) are the flow from stream to groundwater and vice-versa,  $Q_B$  (baseflow),  $Q_{res}$  (in) and  $Q_{res}$  (out) are the flow from reservoir to groundwater and vice-versa,  $R_g$  (gross recharge),  $R_n$  (net recharge),  $ET_g$  (groundwater evapotranspiration),  $ET_{uz}$  (unsaturated zone evapotranspiration),  $Exf$  (exfiltration),  $\Delta S_g$  (change in storage of groundwater),  $\Delta S_{uz}$  (change in storage of unsaturated zone) and SF (specified flow). All values are in [mm year<sup>-1</sup>].

Table 15: Yearly water balances of the entire simulation period starting from 1<sup>st</sup> January 2012 to 31<sup>st</sup> December 2015 in [mm year<sup>-1</sup>]

Year	P	I	Pe	ET	$Q_{H+D}$	$Q_s$	$Q_D$	$Q_{st}$ (in)	$Q_{st}$ (out)	$Q_B$	$Q_{res}$ (in)	$Q_{res}$ (out)	$R_g$	$R_n$	$ET_g$	$ET_{uz}$	Exf	$\Delta S_g$	$\Delta S_{uz}$	SF
2012	859.3	218.6	573.8	552.5	99.6	249.7	0.2	53.8	203.9	150.1	292.8	8.4	616.4	-192.4	310.8	23.2	498.1	-18.0	-65.8	0.0
2013	980.8	249.5	692.8	601.6	156.5	282.8	0.2	56.4	182.7	126.3	329.6	6.1	679.8	-188.8	333.4	18.8	535.2	-11.4	-5.7	0.0
2014	875.4	222.7	725.2	608.9	94.7	199.4	0.2	58.9	163.5	104.6	338.2	3.1	692.4	-160.4	356.7	29.5	496.1	-8.2	3.3	0.0
2015	1178.6	299.8	828.1	698.5	220.3	362.8	0.2	54.9	197.4	142.4	385.5	3.0	818.9	-194.3	373.5	25.2	639.8	-17.7	-16.1	0.0
<b>Total</b>	3894.1	990.5	2820	2461.6	571.2	1094.7	0.8	224.0	747.5	523.5	1346.0	17.7	2807.5	-736.0	1374.3	96.7	2169.2	-55.2	-55.2	0.0
<b>Mean</b>	973.5	247.6	705	615.4	142.8	273.7	0.2	56.0	186.9	130.9	336.5	4.4	701.9	-184	343.6	24.2	542.3	-13.8	-84.3	0.0
<b>% of P</b>		25.4%	72.4%	63.2%	14.7%	28.1%	0.0	5.8%	19.2%	13.4%	34.6%	0.3%	72.1%	18.9%	35.3%	2.5%	55.7%			

According to the water budget provided in Table 15 for Aamsveen, the highest outflow flux was evapotranspiration which accounted for 63.2 % of the total precipitation. Evapotranspiration is generally high in the region because of the presence of many trees and plants which are concentrated especially in the wetland area. Big trees are also found throughout the study area. It should be noted that this 63.2 % also includes the canopy interception. The precise evapotranspiration of the groundwater is 37.8 % excluding the canopy interception. Exfiltration was found to be 55.7 % which can be accounted by the fact that the wetland covers a considerable area inside the study area. The movement of groundwater to the streams was only 13.4 % which suggest that the streams are mainly fed by the rains and very little is contributed by the groundwater. The gross recharge accounted for 72.1 % of the inflow into the saturated zone and the net recharge accounted for 18.9 % of the total precipitation. Specified flow was negligible hence it did not add much towards the inflow of water into the system. The reservoir had a major role since it contributed 35.9 % of the water to groundwater. The amount of water added to the groundwater by stream was much lesser compared to the water that was gained by the stream from the groundwater. This means that the streams gained water during the entire simulation, from the groundwater. The Hortonian and Durnian runoff accounted for 14.7% which is estimated to be mainly during the winter seasons when groundwater is higher.

4.11. Temporal variability of the water fluxes

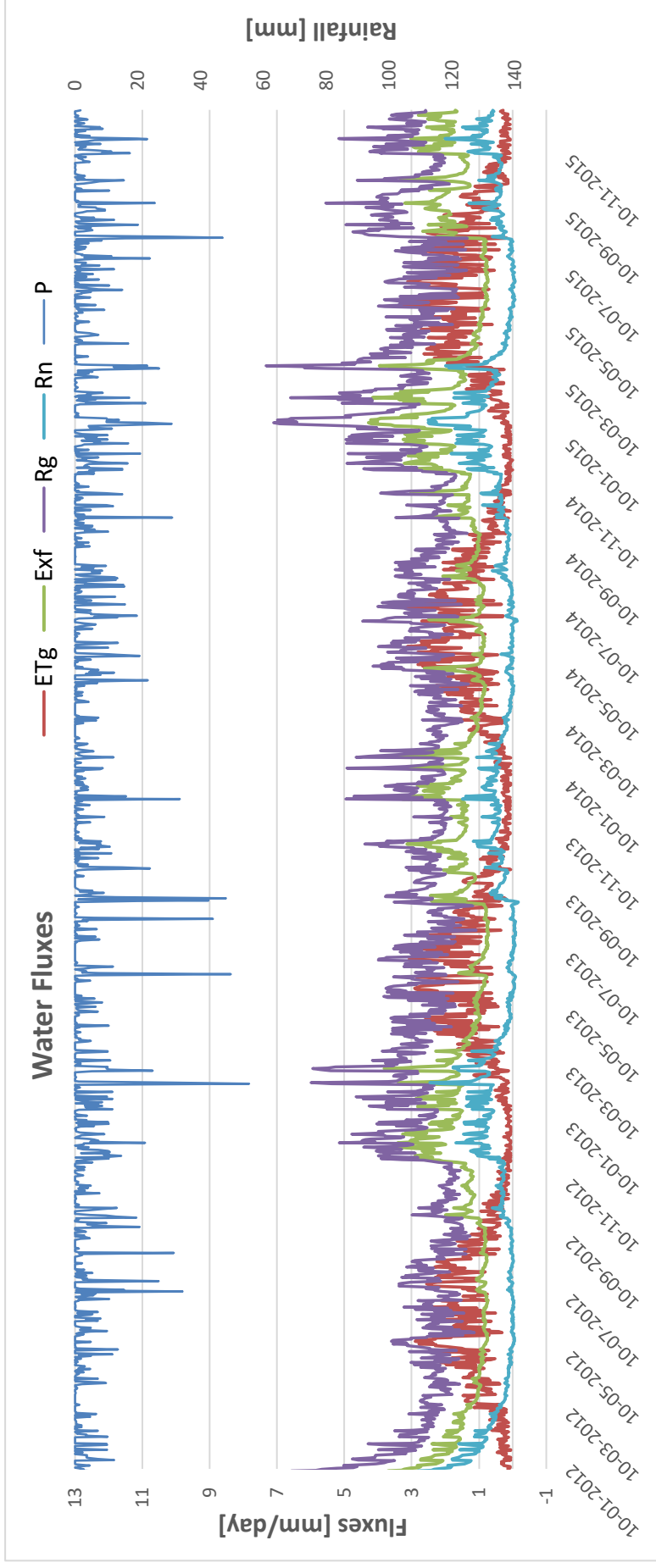


Figure 40: Daily variability of groundwater fluxes for the whole simulation period starting 1st January 2012 to 31st December 2015

The analysis of the temporal variability of the water fluxes were done daily and also yearly. Figure 40 shows an increase in the exfiltration whenever there is a decrease in the evapotranspiration. The net recharge also increased with the decrease in the evapotranspiration. This was noticed especially during the winter months. As seen from Figure 40, it is estimated that evapotranspiration plays a great role in the dynamics of the fluxes at Aamsveen since the gross recharge increases with the decrease in evapotranspiration and this can very well mean that exfiltration increases to such an extent due to the decrease in evapotranspiration that the values for gross recharge are higher in winter than in summer, even though evapotranspiration is one of the component for the calculation of the gross recharge. The yearly variations of the water components are presented in the Figure 41.

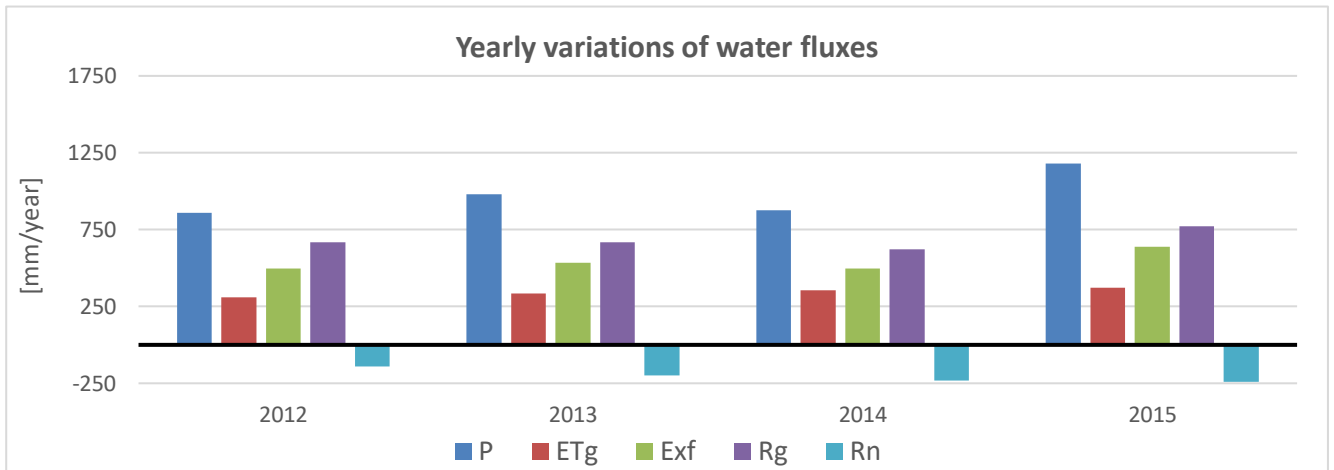


Figure 41: Yearly variations in the water fluxes

The dynamics of the groundwater fluxes are temporally and spatially very high. This can be justified by the fact that Aamsveen is located in a region which receives continuous precipitation throughout the year in the form of rain, hail and snow. Presence of a wetland with thick vegetation is expected to influence the dynamics of the study area a lot. During the winters, the exfiltration was noticed to be much higher than the summers. Since the wetland is mainly composed of peat soil, it is estimated that this can cause significant changes in the hydraulic properties, which affects the amount of infiltration, the hydraulic conductivity and water retention etc. Since peat swells, it does not really have fixed dimensions which makes many things uncertain in terms of quantifying the fluxes. Its hydraulic conductivity depends on whether it is an amorphous peat or fibrous peat. Compared to inorganic soil, peat can exhibit hydraulic conductivities which can range from high to moderate. It has also been studied to have a rapid primary consolidation and can also exhibit large secondary consolidation (Wong et al. 2009). Figure 42 shows the distribution of fluxes in the study area from 2012-2015.

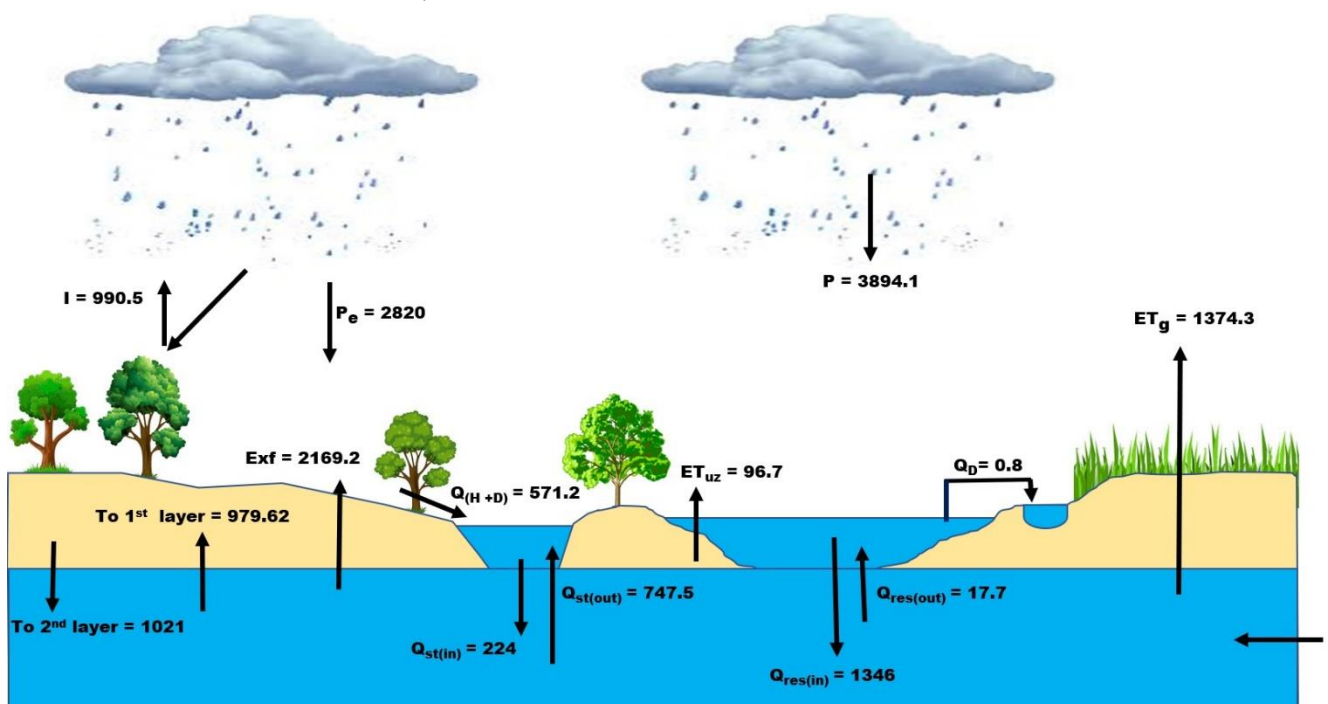


Figure 42: Schematic of the distribution of fluxes in the study area from 2012-2015 in [mm]

## 5. CONCLUSION AND RECOMMENDATIONS

### 5.1. Conclusion

The main objective was to assess the surface-groundwater interactions in Aamsveen. This was achieved by simulating the model in transient conditions for 4 years beginning from 1<sup>st</sup> January 2012 until 31<sup>st</sup> December 2015. MODFLOW NWT coupled with UZF1, SFR2, FHB, Drain and Reservoir packages was used for simulation. The study area was spatially discretized into grid sizes of 50 x 50 metres each. Time discretization of daily time steps with each time step representing a stress period was assigned.

Hence, after the analyses of the present model, it was found that the model does not run dry neither does it flood but is able to simulate the important dynamics. The simulated groundwater heads have a good match with the observed groundwater heads. The stream flows showed high sensitivity to the changes in the flows which corresponded with changes in the observed discharges. With respect to the specific objectives and the research questions of this present study, it is concluded that:

#### 5.1.1.1. With reference to the research objectives in section 1.4:

- i) The conceptual model of the study area was updated, and a specified flow boundary was used across the eastern boundary while the rest of the boundary was a no-flow boundary. The previous studies had a no-flow boundary on all sides.
- ii) The land cover changes were modelled by making a more detailed land cover map of the area which included the further categorization of trees into deciduous and evergreen trees which affect evapotranspiration and infiltration during winter seasons.
- iii) Exfiltration was recorded to be the highest flux that had a major influence on the groundwater system which is confirmed by the presence of a wetland which occupies a large area in the present study area. Recharge was the main inflow into the groundwater system with negligible contributions from the inflow of groundwater from the eastern boundary of the study area. The reservoir contributes significantly to the groundwater whereas the streams gain more water from the groundwater than they contribute. Groundwater evapotranspiration was the highest flux which removes the groundwater out of the system. It was modelled to be highest during the summer seasons
- iv) The assessment of the results from the old models and the present models are described under section 5.1.2.

#### 5.1.1.2. With reference to the specific research questions in the section 1.4.1.2:

- i) The eastern boundary had flux entering inside the study area and in the present study a specified flux was applied, but the data from the German side was not adequate for a proper quantification of the flux. To get a better estimate of the flux entering inside the area from the eastern boundary, adequate data is required.

- ii) The land cover of the study area was used to generate the root depth map which was used for the extinction depth of the evapotranspiration. The changes in the extinction depth showed high sensitivity to the water balance components which can be seen from the sensitivity analysis in Figure 36.
- iii) Exfiltration and evapotranspiration were seen to highly affect each other since Figure 40 showed a considerable increase in one quantity when the other showed a decrease and vice-versa. In the winters, exfiltration was higher but in summer, evapotranspiration was higher than exfiltration. The loss of groundwater through the streams was very less as compared to the evapotranspiration which suggests that evapotranspiration has a very high influence in the groundwater dynamics of Aamsveen. The streams gained more water while their contribution to groundwater was comparatively lesser. Delays in the discharges were observed in summer even during a relatively high rainfall which is due to the fact that evapotranspiration decreases the groundwater due to which, the soil is first saturated during rains and then higher discharges are observed later. This confirms the conclusion that evapotranspiration is significantly high during summers and hence has a very high influence on the fluctuation of the groundwater.
- iv) In 2011, major significant changes were done in Aamsveen which are explained in Table 1. Since then, it is estimated that the human interventions that have been carried out, have created uncertainties in the measurement of the discharges of the streams. The reservoir was made to hold the water back and the interventions done to control the reservoir affects the stream flows since the discharge is sometimes measured over controlled outflows. Since, in this study, the effects of these interventions have not been modelled, reliable conclusions cannot be made without a proper investigation of these interventions.

### **5.1.2. Comparison of results of the present study with previous studies**

#### **5.1.2.1. Comparison of results from steady state model proposed by Bakhtiyari (2017).**

Bakhtiyari (2017) concluded that the gross recharge contributed 76.7 % of total inflow towards the aquifer systems which is close to 72.1 % gross recharge in the present study, but she reported a higher contribution of streams to groundwater and lower contribution of reservoir leakage which is just the opposite to the present study. She reported that in the outflow components, stream leakage was the highest which was 73.67%, followed by 13.47% from the evapotranspiration and 12.86% from surface drain which is opposed to this study since this study concludes that evapotranspiration is the major flux of the outflow components with a total evapotranspiration of 63.2 %, of which the groundwater loses 37.8 %. The contribution of groundwater to the outflow through stream was measured as only 28.1 % which makes the conclusion of this present study to be the opposite of the conclusion given by Bakhtiyari (2017).

#### **5.1.2.2. Comparison of results from steady state model proposed by Nyarugwe (2016)**

Nyarugwe (2016) concluded that the leakage from the stream was the major outflow component in Aamsveen with 68.77 % outflow and 15.69 % and 15.14% outflow was through the drain and evapotranspiration. It is important to note that the extent of his study area is different from the present study. Though there is a difference in the extent of the area, he concludes that the wetland contributes a total of 42% of all the evapotranspiration in his study area. The reason for this conclusion given by him was the presence of high groundwater level in the wetland and also high vegetation cover. A solid comparison cannot be made of this present study and Nyaruwe's study due to the differences in the spatial coverage of the study area, however it can be said that the conclusions of the present model and Nyarugwe (2016) model do not agree.

## 5.2. Model failures

As discussed in the earlier chapter, a well calibrated model for transient simulation of Aamsveen can only be achieved if the discharge measured in the stream gauges can have the accountability of the anomalies that were discussed earlier. Since that was not available, the model could not be properly calibrated with respect to the stream flows. Another reason for this can be attributed towards the use of a better package which would be able to connect the streams with the surface water/lake and provide better simulated results, since this was also not achieved in this present study due to lack of data and the time constraints. Due to this problem, the measured discharge readings were “forced” into the particular stream where the gauge was located but again the flow could not be validated since no stream gauge was available downstream, but “forcing” the observed discharge provided better simulation of the hydraulic heads. Hence, due to the above stated conditions, it was not feasible to assess the complete calibration of the present model with respect to the stream flows.

Since, the transient calibration requires temporal initial and final stages of the reservoir heads, due to the non-availability of the data, the reservoirs heads were assigned with respect to the water level in the stream where the Aamsveen camping ground’s gauge was installed. Due to the location of this gauge being very close to the reservoir, it was assumed that heads of the water in the stream are linear to the head of the water in the reservoir. The location of the gauge near the reservoir can be seen in Figure 29. This may also account for the reservoir leakage being too high into the groundwater which can be seen from the water balance which was 34.6% of the entire recharge to the aquifer.

These reasons may be attributed for the under-performance of the model in certain areas and further recommendations can be made for a better performance of the model if it needs to be used for decision making. It is also important to note that the entire study area has a large network of streams covering almost the entire study area and this also makes the proper calibration of the model with respect to the stream gauges of critical importance.

## 5.3. Recommendations.

The distribution of the groundwater monitoring points was not good in the study area since all the piezometers were located only in the wetland area and were very close to each other. Moreover, there were only 4 piezometers which provided data for most part of the simulation. Other piezometers had data which did not match with the duration of the simulation period. Hence, for a better simulation of heads, the management needs to install functional piezometers that would be well distributed throughout the entire study area. The German side did not have even a single piezometer data and a major part of the wetland is located in Germany.

It was analysed that the study area has a no-flow boundary on all the sides except the eastern side which had an inflow of flux and hence a constant flux was specified. Yet the data available was too scarce to make a better conceptual model of the study area hence, piezometers should also be installed outside the wetland which will enable a better conceptualization of the model boundaries. The study area consists of many streams which form a complex network that covers almost the entire study area, yet only 3 gauges are available, 2 of which are located inside the study area. For such a vast network of streams, the number of gauges is too little. Also, the discharges measured in these gauges are not entirely reliable especially in the gauge at Melodiestraat.



Hence, a well distributed network of gauges should be installed which would be able to aptly cover the stream network. Also, an audit of the gauge at Melodiestraat should be done to assess if it receives water from any other unaccounted sources apart from the Glanerbeek itself. The proper functioning of this gauge should also be analysed. All the human interventions done in the wetland should be accounted for and should be considered for the observed values of the discharge in the stream gauge, especially the gauge near the Aamsveen camping ground.

The reservoir package which was used in the present model simulates only the reservoir-groundwater interactions. In the study area, there is a major interaction of the reservoir with the stream network which could not be simulated using the reservoir package. Hence, LAK package should be used to obtain a better simulation of the fluxes provided that the bathymetry of all the lake is available in the study area.

Since, the overall performance of the model was reasonable, given the fact that sufficient data could not be made available regarding the spatial distribution and temporal measurements of the piezometers and uncertainties in the stream flows, this model could be updated with the needed information and data and can be used to analyse surface-groundwater system of the study area.

## LIST OF REFERENCES

- Allen, R.G., Pereira, L.S., Raes, D., Smith, M. (1998). Crop Evapotranspiration (guidelines for computing crop water requirements)-FAO Irrigation and drainage paper 56, 1-15
- Anderson, M.P., Woessner, W.W., Hunt, R.J. (2015). Applied Groundwater Modeling: simulation of flow and advective transport (2<sup>nd</sup> ed.). San Diego: Elsevier Science
- Anderson, M.P. and Woessner, W.W. (1992). Applied Groundwater Modeling— Simulation of Flow and Advective Transport. Academic Press, Inc., San Diego, CA, 381 p.
- Armandine, Les Landes A., Aquilina, L., De Ridder, J. (2014). Investigating the respective impacts of groundwater exploitation and climate change on wetland extension over 150 years. *J Hydrol* 509:367–378. doi: 10.1016/j.jhydrol.2013.11.039
- Bakar, O.M. (2015). Integrated hydrologic model for the assessment of surface-groundwater interactions: The case of Ziębice Basin. Faculty of Geo-Information Science and Earth Observation, University of Twente, Netherlands (master's thesis) 63. Retrieved from [https://library.itc.utwente.nl/papers\\_2015/msc/wrem/bakar.pdf](https://library.itc.utwente.nl/papers_2015/msc/wrem/bakar.pdf)
- Bakhtiyari, S.G. (2017). Analysis and modeling of groundwater system for wetland management. Faculty of Geo-Information Science and Earth Observation, University of Twente. Retrieved from <https://library.itc.utwente.nl/login/2017/msc/wrem/ghasemi.pdf>
- Barthel, R., Banzhaf, S. (2016). Groundwater and Surface Water Interaction at the Regional-scale – A Review with Focus on Regional Integrated Models. *Water Resour Manag* 30:1–32. doi: 10.1007/s11269-015-1163-z
- Bear, J. (1972). Dynamics of fluids in porous media. New York : American Elsevier
- Bell, J., Hullenaar van 't, J.W., Jansen, A.J. (2018). Ecohydrologische systeemanalyse Aamsveen. Bell Hullenaar Ecohydrol Adviesbur 1–118
- Bell, J.S., Hullenaar van 't, J.W., Jansen, A.J. (2015). Ecohydrologische systeemanalyse dal van de Glanerbeek, Zwolle
- Boonstra, J. & de Ridder, N. (1981). Numerical modelling of groundwater basins: A user-oriented manual. Wageningen: International Institute for Land Reclamation and Improvement
- Brenot, A., Petelet-Giraud, E., Gourcy, L. (2015). Insight from Surface Water-groundwater Interactions in an Alluvial Aquifer: Contributions of  $\delta^2\text{H}$  and  $\delta^{18}\text{O}$  of Water,  $\delta^{34}\text{S}\text{SO}_4$  and  $\delta^{18}\text{O}\text{SO}_4$  of Sulfates,  $^{87}\text{Sr}/^{86}\text{Sr}$  Ratio. *Procedia Earth Planet Sci* 13:84–87. doi: 10.1016/j.proeps.2015.07.020
- Brown, G.O. (2002). Henry Darcy and the making of a law. *Water Resour Res* 38:11-1-11–12. doi: 10.1029/2001WR000727
- Brown, R.J. (1976). A Study of the Impact of the Wetlands Easement Program on Agricultural Land Values. *Land Econ* 52:509. doi: 10.2307/3145193
- Brunner, P., Simmons, C.T., Cook, P.G., Therrien, R. (2010). Modeling surface water-groundwater interaction with MODFLOW: Some considerations. *Ground Water* 48:174–180. doi: 10.1111/j.1745-6584.2009.00644.x
- Bullock, A & M, Acreman. (2003). The role of wetlands in the hydrological cycle. *Hydrology and Earth System Sciences Discussions, European Geosciences Union*, 2003, 7 (3), pp.358-389.
- Carman, P.C. (1937) Fluid flow through granular beds. *Chem Eng Res Des* 150–156. doi: 10.1016/S0263-8762(97)80003-2
- Clarkson, B.R., Ausseil, A.E., Gerbeaux, P. (2013). Wetland Ecosystem Services. *Ecosyst Serv New Zeal – Cond trends* 192–202. doi: 10.1139/f95-059
- Corbari, C., Ravazzani, G., Galvagno, M. (2017). Assessing crop coefficients for natural vegetated areas using satellite data and eddy covariance stations. *Sensors (Switzerland)* 17:. doi: 10.3390/s17112664
- Corbett & Crouse. (1968). Rainfall Interception By Annual Grass and Chaparral. USDA For Serv Res Pap PSW-48: doi: 10.1080/00382167.1962.9629728
- Cosby, B. J., Hornberger, G. M., Clapp, R. B., & Ginn, T. R. (1984). A statistical exploration of the relationships of soil moisture characteristics to the physical properties of soils. *Water Resources Research*, 20(6), 682–690. <https://doi.org/10.1029/WR020i006p00682>
- Council, G.W. (1997). Simulating Lake-Groundwater interaction with MODFLOW, presented at Proceedings of the 1997 Georgia Water Resour Conference, at The University of Georgia, Athens, held March 20-22, 457–462
- Drastig, K., Suárez, Quiñones, Zare, M., Dammer K., Pronchow, A. (2019). Rainfall interception by winter rapeseed in Brandenburg (Germany) under various nitrogen fertilization treatments. *Agric For Meteorol* 268:308–317. doi: 10.1016/j.agrformet.2019.01.027
- El-Zehairy, A.A., Lubczynski, M.W., Gurwin, J. (2018) Interactions of artificial lakes with groundwater applying an integrated modflow solution. *Hydrogeol J* 26:109–132. doi: 10.1007/s10040-017-1641-x

- Fenske, JP., Leake, SA., Prudic, DE. (1996). Documentation of a Computer Program (RES1) to Simulate Leakage from Reservoirs Using the Modular Finite-Difference Ground-Water Flow Model (MODFLOW). US Geological Survey Open-File Report 96-364, 51p. doi: 10.3133/ofr96364
- Foxx, TS., Tierney, GD., Williams, JM. (1984). Rooting depths of plants relative to biological and environmental factors. Los Alamos National Lab NM, United States. doi:10.2172/6215530.
- Harbaugh, A.W. (2005). MODFLOW-2005, The U.S. Geological Survey modular ground-water model—the Ground-Water Flow Process: U.S. Geological Survey Techniques and Methods 6-A16, variously p. Retrieved from <https://doi.org/10.3133/tm6A16>
- Harbaugh, AW & Hill, MC. (2013). Observations in modflow-2005,1–32 Retrieved 10 February, 2019 from <https://water.usgs.gov/ogw/modflow/MODFLOW-2005-Guide/index.html?gbob.htm>
- Hassan, SMT., Lubczynski, MW., Niswonger RG., Su, Z. (2014). Surface–groundwater interactions in hard rocks in Sardon Catchment of western Spain: An integrated modeling approach. *Journal of Hydrology* 517:390–410. doi: 10.1016/j.jhydrol.2014.05.026
- Hunt, RJ., Prudic, DE., Walker, JF., Anderson, MP. (2008). Importance of unsaturated zone flow for simulating recharge in a humid climate. *Ground Water* 46:551–560. doi: 10.1111/j.1745-6584.2007.00427.x
- Hwang, HT., Jeon, SW., Suleiman, AA., Lee, KK. (2017). Comparison of saturated hydraulic conductivity estimated by three different methods. *Water (Switzerland)* 9:1–15. doi: 10.3390/w9120942
- Jafari, N. (2009). Ecological integrity of wetland, their functions and sustainable use. *Journal of Ecology and Natural Environment* 1:45–54. Retrieved from <https://pdfs.semanticscholar.org/f0cf/fd7ddb9087526c7d4af00608d4081b6a8673.pdf>
- Jetten, VG. (1996). Interception of tropical rain forest: performance of a canopy water balance model. *Hydrological Processes* 10: 671–685. Retrieved from [https://doi.org/10.1002/\(SICI\)1099-1085\(199605\)10:5%3C671::AID-HYP310%3E3.0.CO;2-A](https://doi.org/10.1002/(SICI)1099-1085(199605)10:5%3C671::AID-HYP310%3E3.0.CO;2-A)
- Jiang, Y., G.H, Somers., J, Mutch. (2004). Application of numerical modeling to groundwater assessment and manage-ment in Prince Edward Island. In *Proceedings of the 57th Canadian Geotechnical Conference and the 5th CGS/IAH-CNC Conference, Quebec City, October 2004*
- John, Manning & Colin, Paterson-Jones. (2007). *Field Guide to Fynbos, Cape Town: Struik*, 507 p. (p. 298).
- Jong, SM & Jetten, VG. (2007). Estimating spatial patterns of rainfall interception from remotely sensed vegetation indices and spectral mixture analysis. *Int J Geogr Inf Sci* 21:529–545. doi: 10.1080/13658810601064884
- Kinoti, IK. (2018). Integrated hydrological modeling of surface and groundwater interactions in Heuningnes catchment (South Africa). Faculty of Geo-Information Science and Earth Observation, University of Twente. Retrieved from [https://library.itc.utwente.nl/papers\\_2018/msc/wrem/kinoti.pdf](https://library.itc.utwente.nl/papers_2018/msc/wrem/kinoti.pdf)
- Kozak, JA., Ahuja, LR., Green, TR., Ma, Liwang. (2007). Modelling crop canopy and residue rainfall interception effects on soil hydrological components for semi-arid agriculture. *Hydrol Process* 21:229–241. doi: 10.1002/hyp.6235
- Kozeny, J. (1927). Ueber kapillare Leitung des Wassers im Boden. *Sitzungsber Akad. Wiss., Wien*, 136(2a), pp 271-306. Retrieved from [https://www.zobodat.at/pdf/SBAWW\\_136\\_2a\\_0271-0306.pdf](https://www.zobodat.at/pdf/SBAWW_136_2a_0271-0306.pdf)
- Kuhry, P. (1985). Transgression of a raised bog across a coversand ridge originally covered with an oak-lime forest. Palaeoecological study of a Middle Holocene local vegetational succession in the Amtsven (northwest Germany). *Review of Palaeobot Palynol* 44:303–353. doi: 10.1016/0034-6667(85)90023-5
- Kumar, CP & Singh, S. (2015). Concepts and Modeling of Groundwater System, *Int. J. . Innov. Res. Sci. Engg. Technol.* 2 (2), 262-271. Retrieved from <http://citeseerx.ist.psu.edu/viewdoc/download?doi=10.1.1.706.7101&rep=rep1&type=pdf>
- Kumar, R., Horwitz, P., Milton, GR., Sellamuttu, SS., Buckton, ST., Davidson, NC., Pattnaik, AK., Zavagli M. (2011). Assessing wetland ecosystem services and poverty interlinkages: a general framework and case study. *Hydrol Sci J* 56:1602–1621. doi: 10.1080/02626667.2011.631496
- Leake, SA., Lilly, MR., Johns, ST. (1997). Documentation of a Computer Program (FHB1) for Assignment of Transient Specified-Flow and Specified-Head Boundaries in Applications of the Modular Finite-Difference Ground-Water Flow Model (MODFLOW). Open-File Report 97-571 .50p. doi: 10.3133/ofr97571
- Lewis, C., Albertson, J., Xu, X., Kiely ,G. (2012). Spatial variability of hydraulic conductivity and bulk density along a blanket peatland hillslope. *Hydrol Process* 26:1527–1537. doi: 10.1002/hyp.8252
- Lianghui, X.(2015). Wetland reconstruction by controlling water level in Aamsveen: the effects on variation of vegetation and nutrients. Faculty of Geo-Information Science and Earth Observation, University of Twente. Retrieved from <https://library.itc.utwente.nl/login/2015/msc/wrem/xing.pdf>

- Lin, T., Xue, XZ., Lu, CY. (2007). Analysis of Coastal Wetland Changes Using the “DPSIR” Model: A Case Study in Xiamen, China. *Coast Manag* 35:289–303. doi: 10.1080/08920750601169592
- Linden, W. (2010) Rainfall interception by buildings for urban hydrology modeling. 104. Eindhoven University of Technology, Eindhoven, The Netherlands. Retrieved from <https://pure.tue.nl/ws/portalfiles/portal/46984283/685278-1.pdf>
- Maltby, E. (1991.) *The World’s Wetlands under Threat*. In: *Environmental Concerns*. Springer Netherlands, Dordrecht, pp 109–136. doi: 10.1007/978-94-011-2904-6\_8
- Meriam, RA. (1960). A Note on the Interception Loss Equation. *J Geophys Res* 65(11):3850–3851. doi: 10.1029/JZ065i011p03850
- Nash, J.E. & Sutcliffe, J.V. (1970). River Flow Forecasting through Conceptual Models Part I—A Discussion of Principles. *Journal of Hydrology*, 10, 282-290. doi: 10.1016/0022-1694(70)90255-6
- Niswonger, RG., Panday, S., Motomu, I. (2011). MODFLOW-NWT, A Newton Formulation for MODFLOW-2005. USGS reports 44. doi: 10.3133/tm6A37
- Niswonger, RG., Prudic, DE. (2010). Documentation of the Streamflow-Routing (SFR2) Package to Include Unsaturated Flow Beneath Streams—A Modification to SFR1: U.S. Geological Survey Techniques and Methods 6-A13, 50p. Retrieved from <https://pubs.usgs.gov/tm/2006/tm6A13/pdf/tm6a13.pdf>
- Niswonger RG., Prudic, DE., Regan, SR. (2006.) Documentation of the Unsaturated-Zone Flow (UZFI) Package for Modeling Unsaturated Flow Between the Land Surface and the Water Table with MODFLOW-2005. US Geol Surv Tech Methods 6-A19,62p. Retrieved from <https://pubs.usgs.gov/tm/2006/tm6a19/pdf/tm6a19.pdf>
- Nyarugwe, K. (2016). Effect of surface water management measures on a groundwater fed wetland. Faculty of Geo-Information Science and Earth Observation, University of Twente. Retrieved from [https://library.itc.utwente.nl/papers\\_2016/msc/wrem/nyarugwe.pdf](https://library.itc.utwente.nl/papers_2016/msc/wrem/nyarugwe.pdf)
- Reilly, T.E., & Harbaugh, A.W. (2004). Guidelines for evaluating ground-water flow models: U.S. Geological Survey Scientific Investigations Report 2004-5038, 30 p. doi: 10.3133/sir20045038
- Rientjes T (2015) Hydrologic modelling for Intergated Water Resource. Lect notes Modul 9-10 Surface water stream. Faculty of Geo-Information Science and Earth Observation, University of Twente, Enschede, The Netherlands.
- Rijtema, PE. (1959). Calculation methods of potential evapotranspiration. 1–10. Wageningen, The Netherlands: Institute for Agriculture and Water Managenemt. Retrieved from <http://edepot.wur.nl/394529>
- Schwartz, F.W. & Zhang, H. (2003). *Fundamentals of Groundwater*. New York: John Wiley & Sons.
- Shah, N., Nachabe, M. & Ross, M. 2007. Extinction depth and evapotranspiration from ground water under selected land covers. *Ground Water* 45 (3): 329–338. doi: 10.1111/j.1745-6584.2007.00302.x
- Tanner, JL & D.A, Hughes. (2015). Understanding and modelling surface water-groundwater interactions. WRC Report No. 2056/2/14. Water Research Comission
- Todd, David.(1959). *Groundwater Hydrology*. New York: John Wiley and sons
- Urumović, K. (2016). The referential grain size and effective porosity in the Kozeny-Carman model. *Hydrol Earth Syst Sci* 20:1669–1680. doi: 10.5194/hess-20-1669-2016
- Veer, G. (2006). *Geochemical Soil Survey of the Netherlands – Atlas of Major and Trace Elements in Topsoil and Parent Material; Assessment of Natural and Anthropogenic Enrichment Factors*. (Published Ph.D. thesis) Universiteit Utrecht, The Netherlands, Netherlands Geographical Studies, 347, 245 pp. Retrieved from <https://dspace.library.uu.nl/bitstream/handle/1874/13275/full.pdf>
- Winston, R.B., 2009, ModelMuse—A graphical user interface for MODFLOW–2005 and PHAST: U.S. Geological Survey Techniques and Methods 6–A29, 52 p. doi: 10.13140/RG.2.1.1411.4402
- Wong, LS., R, Hashim., F.H, Ali. (2009). A Review on Hydraulic Conductivity and Compressibility of Peat. *Journal of Applied Sciences*, 9(18): 3207-3218. doi: 10.3923/jas.2009.3207.3218
- Wong, T.E., Batjes, D.A.J., De Jager, J. [eds.] (2007). *Geology of the Netherlands*. Royal Netherlands Academy of Arts and Sciences, Amsterdam, 354 p.
- Xu, CY & Chen D. (2005). Comparison of seven models for estimation of evapotranspiration and groundwater recharge using lysimeter measurement data in Germany. *Process* 19:3717–3734. doi: 10.1002/hyp.5853
- Zhang, J., Ross, MA., Geurink, J. (2012). Discretization approach in integrated Hydrologic Model for surface and groundwater interaction. *Chinese Geogr Sci* 22:659–672. doi: 10.1007/s11769-012-0566-5